Dissecting the role of Phospholipase A_2 in the late stages of regulated exocytosis

Deepti Dabral, Student ID 18398276

Molecular Medicine Research Group

School of Medicine

Western Sydney University

A thesis presented to Western Sydney University in partial fulfilment of the requirements for the degree of Doctorate of Philosophy

Statement of Authenticity

The work presented in this thesis is, to the best of my knowledge, original except as acknowledged in the text. I hereby declare that I have not previously submitted this material, either in whole or in part, for a degree at this or any other institution.

Deepti Dabral

25-05-2019

Publications

1. **Dabral Deepti**, Coorssen, Jens R. (**2017**), Phospholipase A_2: Potential roles in native membrane fusion, **The International Journal of Biochemistry & Cell Biology** https://doi.org/10.1016/j.biocel.2017.01.011
2. **Dabral Deepti**, Coorssen, Jens R. (**2019**), Combined targeted Omic and Functional Assays Identify Phospholipases A_2 that Regulate Docking/Priming in Calcium-Triggered Exocytosis, **Cells** https://doi.org/10.3390/cells8040303
3. **Dabral Deepti**, Coorssen, Jens R. (**2019**), Arachidonic acid and lysophosphatidylcholine inhibit multiple late steps of regulated exocytosis, **Biochem. Biophys. Res. Commun,** https://doi.org/10.1016/j.bbrc.2019.05.106
4. **Dabral Deepti**, Qinghua Fang, Manfred Lindau, Jens R Coorssen (**Manuscript in preparation**), Phospholipase A_2 activating peptide disturbs native membrane lipid homeostasis, affecting terminal steps of Ca^{2+} triggered exocytosis.

Conference presentations

1. Prabhodh S. Abbineni, **Deepti Dabral**, and Jens R. Coorssen **(2015)** Dissecting phosphoregulation of exocytosis: assessing the roles of kinases in late steps of the exocytotic pathway. **18th International Symposium on Chromaffin Cell Biology**. (Cairns, Australia).
2. **Deepti Dabral**, Jens R. Coorssen **(2018)** Cortical vesicle-associated PLA_2: Identification and characterization. **Health Beyond Research & Innovation Showcase** (Sydney, Australia)
3. **Deepti Dabral**, Jens R. Coorssen **(2019)** Vesicle-associated Phospholipase A_2: Identification, characterization, and effects on native membrane fusion. **63rd Annual Meeting of the Biophysical Society** (Baltimore, Maryland, US).

Publications (other than Ph.D. project)

1. Subasa C. Bishwal, Mrinal K. Das, Vinod K. Badireddy, **Deepti Dabral**, Aleena Das, Alok R. Mohapatra, Sukanya Sahu, Dipankar Malakar, I. Ibungo Singh, Himanghsu Mazumdar, Saurav J. Patgiri, Trinayan Deka, Wetetsho Kapfo, Kevideme Liegise, Rukuwe-u Kupa,Sanjita Debnath, Rajesh Bhowmik, Rahul Debnath, Rajendra K. Behera, Manoj G. Pillai, Pranjal Deuri, Reema Nath, K. Pewezo Khalo, W. Asoka Sing, Bhaswati Pandit, Anjan Das, Sibabrata Bhattacharya, Digamber Behera, Lahari Saikia, Vinotsole Khamo, and Ranjan K. Nanda **(2019)** Sputum Proteomics Reveals a Shift in Vitamin D-binding Protein and Antimicrobial Protein Axis in Tuberculosis Patients. **Scientific Reports** http://doi.org/10.1038/s41598-018-37662-9
2. Rakesh Arya, **Deepti Dabral**, Himanghsu Mazumdar, Saurav Jyoti Patgiri, Trinayan Deka, Rumi Basumatary, Wetetsho Kapfo, Kevideme Liegise, Rukuwe-u Kupa, Chayale Semy, Rajendra Kumar Behera, Pranjal Deori, K. Pewezo Khalo, Lahari Saikia, Vinotsole Khamo, Ranjan Kumar Nanda **(accepted in Proteomics clinical applications)** Serum Small Extracellular Vesicles Proteome of Tuberculosis Patients Demonstrated Deregulated Immune Response.
3. Mrinal Kumar Das, Subasa Chandra Bishwal, Aleena Das, **Deepti Dabral**, Vinod Kumar Badireddy, Bhaswati Pandit, George M. Varghese, and Ranjan Kumar Nanda **(2015)** Deregulated Tyrosine−Phenylalanine Metabolism in Pulmonary Tuberculosis Patients. **Journal of Proteome Research** http://doi.org/10.1021/acs.jproteome.5b00016
4. Mrinal Kumar Das, Subasa Chandra Bishwal, Aleena Das, **Deepti Dabral**, Ankur Varshney, Vinod Kumar Badireddy, and Ranjan Kumar Nanda **(2013)** Investigation of gender-specific exhaled breath volatome in humans by GCxGC-TOF-MS. **Analytical Chemistry** http://pubs.acs.org/doi/abs/10.1021/ac403541a

Conference presentation (other than Ph.D. project)

1. Rakesh Arya, **Deepti Dabral**, Himanghsu Mazumdar, Saurav Jyoti Patgiri, Trinayan Deka, Rumi Basumatary, Wetetsho Kapfo, Kevideme Liegise, Rukuwe-u Kupa, Chayale Semy, Rajendra Kumar Behera, Pranjal Deori, K. Pewezo Khalo, Lahari Saikia, Vinotsole Khamo, Ranjan Kumar Nanda (2017) Identification of exosomal based novel protein biomarkers in TB patients. Presented at **Computational Mass-spectrometry Based Proteomics, 9th Max Quant Summer School, Berlin, Germany**
2. Mrinal Kumar Das, Rakesh Arya, Subasa C. Bishwal, Aleena Das, **Deepti Dabral**, Vinod Kumar Badireddy, Bhaswati Pandit, George M. Varghese, and Ranjan Kumar Nanda (2015) Deregulated fatty acid profile in pulmonary tuberculosis patients. Presented at **11th Annual Conference of the Metabolomics Society, San Francisco, USA**

Acknowledgments

I would like to express my sincere gratitude to my advisor Prof. Jens R. Coorssen, for his guidance, rigorous training, patience, and continuous support during my candidature. I sincerely thank him for insightful comments and also for the hard questions which had inspired me to widen my research throughout my candidature. I am eternally indebted to him for this enriched experience. I would also like to thank Dr. David Mahns for providing moral support, in times of need, facilitating urchin collection and proper maintenance of the aquatic facility. I am also grateful to Dr. Ranjan Nanda, Translational Health Research Group, International Centre for Genetic Engineering and Biotechnology, New Delhi, for early guidance in my research career and his continued support.

I greatly appreciate Prof. Manfred Lindau, Max Planck Institute for Biophysical Chemistry, Göttingen, for inviting me to his laboratory on a Deutscher Akademischer Austauschdienst (DAAD) exchange program. Here, I carried out whole-cell voltage clamp capacitance measurement on mouse chromaffin cells. I also thank Drs. Qinghua Fang and Ying Zhao, Max Planck Institute for Biophysical Chemistry, Göttingen, for their training in mouse handling, chromaffin cell culture, and whole-cell capacitance measurements.

Thank you, Ashleigh Claire Deschamps and Nikola Mills, Western Sydney University, School of Medicine for urchin collection and aquatic facility maintenance and; David Massih and Lana Kajlich, Underwater Research Group of New South Wales, for additional urchin collection.

Special thanks to dear ones, Praapti, Chitra, and Szeifoul from neighbouring laboratories for much needed CHEER.

Last but not least, I thank all my laboratory colleagues in helping me grow as a person and Prabhodh S. Abbineni for initial laboratory training.

This thesis is dedicated to beloved, Rudra Mani Dabral, and Kamla Dabral.

Wouldn’t be possible without you, Nikhil Singh!

Preface

This thesis is divided into five chapters. The overarching working hypothesis is published as a 'perspective' article in **International Journal of Biochemistry and Cell biology, 2017** https://doi.org/10.1016/j.biocel.2017.01.011 and is also discussed in the last section of **Chapter - 1.** Hence, there are similarities in the published article and sections of Chapter - 1. The working hypothesis states that endogenous PLA_2 near docking/ fusion sites provide basal levels of LPC that acts as a 'molecular brake' against spontaneous fusion, and FFA that aids in *trans*-SNARE complex formation to ensure efficient docking of secretory vesicles to the plasma membrane (PM) prior to triggering. The data in **Chapters - 2 and - 3** then test the working hypothesis and are also published as original articles in **cells, 2019** https://doi.org/10.3390/cells8040303 and **Biochemical and Biophysical Research Communications, 2019** https://doi.org/10.1016/j.bbrc.2019.05.106, respectively. The data presented in **Chapter - 2**, indicate that vesicle-associated endogenous PLA_2 isozymes – $sPLA_2$ in the CV lumen and $iPLA_2$ on the CV surface – maintain docking/priming steps in regulated exocytosis. The specific CV localization of $sPLA_2$ and $iPLA_2$ is also shown, using highly sensitive two-dimensional gel electrophoresis (2DE) immuno-blotting with selective antibodies on separated luminal and membrane fractions. Biochemical assays confirmed that these isozymes are catalytically active; $sPLA_2$ showed higher efficiency in catalyzing PE than PC, while $iPLA_2$ showed no such preference. Notably, a significant increase in the *de novo* metabolite TAG upon $iPLA_2$ inhibition confirmed the role of this isozyme in maintaining membrane lipid homeostasis. Removal of CV surface proteins by treatment with trypsin, coupled with the use of a selective PLA_2 substrate (PED6) also confirmed the presence of an active PLA_2 isozyme in the outer CV membrane. Overall, the data presented in **Chapter - 2**, provide evidence in support of the working hypothesis. To test the hypothesis further, in **Chapter - 3**, exogenous arachidonic acid (ARA) and lysophosphatidylcholine (LPC),

canonical PLA_2 metabolites, are shown to impair docking/priming and actual membrane merger steps, respectively. The observed decrease in docking/priming induced by exogenous ARA is contradictory to part of the working hypothesis that was put forth based on existing literature. That exogenous LPC and ARA were to a significant extent converted into endogenous PC and FFA, respectively, indicated that endogenous enzymes maintain lipid homeostasis in the native vesicle membrane. With the intension of activating CV luminal $sPLA_2$, Phospholipase A_2 activating peptide (PLAP) - a melittin homolog, was used in **Chapter – 4.** The data presented indicates that PLAP inhibited CSC, and CV fusion by impairing docking/priming and also altered endogenous PE and FFA levels in the CV membrane. This suggests that PLAP caused no change in the CV luminal $sPLA_2$ activity; an observation contrary to the earlier *in vitro* studies. To test further, PLAP was delivered to mouse chromaffin cells and was seen to reduce membrane capacitance and readily releasable pool (RRP) size, when triggered with depolarizing pulses. This substantiate that the PLAP blocked a common underlying mechanism associated with the late stages of Ca^{2+} triggered exocytosis. **The Chapter - 4 is another manuscript in preparation and will be submitted to an appropriate journal.** Finally, in **Chapter - 5,** the Discussion and Future Directions, all key finding in this thesis are reviewed and integrated with a critical evaluation of the existing literature, and prospective future experiments are outlined.

TABLE OF CONTENTS

(Manuscript in preparation)

CHAPTER - 5

CHAPTER – 1

Introduction

In the late 1950s during the investigation of secretory processes in the pancreatic cell, secretory vesicles were observed near the plasma membrane (PM), apparently in preparation to release their content [3]. As we understand today, this was amongst the last steps of regulated exocytosis (also see below), that prepares vesicles to release their content into the extracellular space. In eukaryotes, the cell undergoes constitutive exocytosis (e.g., the fusion of vesicles budding off from trans-Golgi network to the PM) without apparent stimulation as a well-defined trigger is yet unknown, as well as regulated exocytosis, which is usually triggered by an elevation of the intracellular calcium concentration ($[Ca^{2+}]_{free}$). Regulated exocytosis proceeds through multiple steps including (i) biogenesis and release of vesicles from the trans-Golgi network; (ii) their translocation to the PM; (iii) initial contact and 'tethering' with the PM [4]; (iv) stabilised contact or 'docking' on the PM; (iv) ATP-dependent and independent priming reactions to become release-ready [5,6] - notably, there would seem to be priming reactions that occur both before and after docking [4,7-9]. Therefore, before triggering, vesicles remain in close apposition (~3-8 nm, predicted by course-grain model [10] and [11]), with the PM and; (v) upon elevation in $[Ca^{2+}]_{free}$, fully primed vesicles fuse with the PM, releasing membrane impermeable cargo stored in the vesicle lumen into the extracellular space (**Figure - 1**). Interestingly, the late steps, i.e., Ca^{2+} sensing, docking, priming, and actual membrane merger, appear to be highly conserved across all cell types [1,12-20]. Therefore, to better define these steps, the (lipidic or proteinic) components that carry out these functions are described as belonging to the fundamental fusion mechanism (FFM) and/or the physiological fusion machine (PFM)[1,21-23]. The components associated with FFM constitute the minimum essential machinery that induces the actual membrane merger steps and; PFM defines the efficiency of membrane merger, via 'accessory' components that regulate mechanisms such as Ca^{2+} sensing, docking, priming, and perhaps even fusion pore.

1. Rationale: CV isolated from unfertilized sea urchin eggs are an excellent model for studying the late steps of regulated exocytosis

Sea urchins belong to the class Echinoidea, that diverged in the phylogenetic tree before the two whole-genome duplication events that occurred in the Chordate lineage [24]. Notably, Echinoidea is closer to the phylum Chordata to which all vertebrates belong, relative to other phyla. Furthermore, the size of the urchin genome is about one-quarter that of the human genome (i.e., 814 megabase pairs (Mbp), relative to 3100 Mbp) [25-27]. Despite this, urchins possess genes representing all vertebrate gene families, including humans [27]. Therefore, in many instances, the urchin genome carries a single 'original' copy of the later vertebrate genes, hence proteins to regulate all fundamental processes, including fertilization. The fertilization of a sea urchin eggs occur externally, with the assistance of chemoattractants (e.g., peptides and cyclic nucleotides) that escort movement of sperms toward unfertilized eggs [28]. Upon fertilization, a transient, 'fast block' to polyspermy occurs in a fertilized egg, that changes the membrane potential from -70 mV to + 20 mV within 1-3 secs [29]; the positive membrane potential does not favor subsequent sperm attachment [29]. Then, to cause a permanent or 'slow block' to polyspermy, another mechanism initiates in ~20 s after sperm attachment and usually completes within ~1 min. This occurs due to increase in subplasmalemmal $[Ca^{2+}]_{free}$ from ~0.1 to 1 mM at the sperm attachment site, that triggers fusion of ~15,000 fully docked cortical secretory vesicles (CV) to the PM. Thus, releasing the luminal cargo into the extracellular space between the PM and vitelline layer. Released proteases cleave proteins that bind the vitelline layer to the PM and mucopolysaccharides induce an osmotic gradient causing movement of water into the space between PM and the vitelline layer. This expands the vitelline layer forming the fertilization envelope [30-32].

Interestingly, CV remain fully prime, retain the ability to dock, sense increase in $[Ca^{2+}]$ and undergo homotypic as well as heterotypic fusion (e.g., CV-PM) even after isolation from

the eggs. The steps mentioned above are essentially the late steps of regulated exocytosis and are described by a characteristic sigmoidal Ca^{2+} activity curve [33-39]. That, increase in $[Ca^{2+}]_{free}$ triggers fusion of the secretory vesicles to the PM is consistent across cell types [20,38-42], indicating a conserved underlying mechanism that drives membrane merger (and the steps immediate preceding it). Hence, information learned about the late steps of regulated exocytosis using CV-CV, or CV-PM fusion has proven to be consistent across other secretory model systems [16,43]. To better understand FFM, the fusion of secretory vesicles to the PM was suggested to be triggered by a hypothetical entity or activatable fusion complexes, which were estimated to be randomly distributed on a CV with an average of 5-9 such complexes per CV. Nevertheless, molecular components of the active fusion complex remain unknown, activation of a single fusion complex appeared sufficient for triggering the membrane merger [35,44-46]. Importantly, the mechanisms that precede membrane merger also seem to require calcium sensors operating at basal i$[Ca^{2+}]_{free}$. Indeed, studies have also suggested that docking and priming occur at different $[Ca^{2+}]_{free}$, with docking potentially occurring at lower nanomolar (nM) levels than priming [47-49] and membrane merger require increased Ca^{2+} levels [38,40,45]. Therefore, local changes in $[Ca^{2+}]_{free}$ near fusion and docking sites even before triggering is crucial for several underlying processes, such as docking and priming.

There are several advantages associated with studying the late steps of regulated exocytosis using CV-CV and CV-PM fusion; foremost is that a single gravid female urchin releases gram quantities of eggs, and each carries ~15,000 stage-specific, release-ready CV. Thus, such high egg yields enable a variety of straightforward manipulations (*ex-vivo* treatments) that are impossible with isolated mammalian secretory vesicles that de-prime during isolation. Additionally, endogenously docked CV on PM fragments (e.g., cell surface complexes (CSC) which are essentially cell ghosts) remain stably docked even hours after isolation [18] or can be detachment from the PM to isolate high purity CV. Thus, homotypic

CV or heterotypic CV-PM fusion enabled highly focussed investigations to dissect molecular mechanisms associated with the late steps of regulated exocytosis. Critically, this also enables tight coupling of the functional assays (standard and settle fusion assays) with parallel molecular analyses to directly relate specific molecules with the underlying mechanism(s) [22,23,37,44,50]. The CV-CV fusion using the standard fusion assay measures the fundamental ability of CV to fuse while the settle fusion assay assesses the capacity of the endogenous machinery to support docking/priming [23,37]. Studies using homotypic CV fusion also reduce the large 'molecular background' imposed by components in the PM. Thus providing better focus to identify endogenous components in the native membrane that play direct roles in the late steps of regulated exocytosis [44,51,52].

2. Lipid classes and their effect on native membrane fusion

Major lipidic components of the native membrane include, cholesterol (CHOL), sphingomyelin (SM), phosphatidyl-choline, -inositol, -ethanolamine, -serine (PC/PI/PE/PS) and phosphatidic acid (PA) [53-56]. These lipids are asymmetrically distributed in the inner and outer membrane monolayers, and their levels are tightly regulated enzymatically [2,57-64]. The distribution of PE, PS, PI dominates in the cytoplasmic monolayer, and PC and CHOL are approximately equally distributed in both monolayers [63,65,66]. Unfertilized sea urchin eggs contain ~54% triglycerides, ~33% phospholipids, and ~9% cholesterol [67]; in terms of per 100 μg protein, PE, PI, PC and cholesterol levels are 86.0 nmol, 61.0 nmol, 25.3 nmol, and 16.2 nmol, respectively while PS, SM, PA are < 2.5 nmol [56]. However, in isolated CV, PE, PI, PC, PS, SM and CHOL constitute 10.2%, 5.1%, 36.9 %, 5.9%, <0.4% and 23.6%, respectively and; of all lipids ~15% are anionic under physiological conditions [68]. PS and PA fall under the category of anionic lipids as attain a deprotonated negative charge and bind to di- and trivalent cations, such as Ca^{2+} [69-71]. Perhaps, due to this Ca^{2+} binding capacity, PS can sense Ca^{2+} at the triggering steps [22]. While PA can also bind to Ca^{2+}, no change in Ca^{2+} sensitivity occurred

due to the incorporation of PA into the CV membrane [36]. Instead, PLD-derived endogenous PA was seen to mediate docking/ priming [23,72].

The incorporated lipids in the membrane either lowers or increases the energy required to bend, rearrange, and merge the membrane bilayers [15,16,55,73-75], due to their spontaneous curvature. Lipids, such as lysophosphatidylcholine (LPC), have a large polar head group and relatively 'slim' hydrocarbon tail. Such lipids are defined as having positive spontaneous curvature. While arachidonic acid (ARA) and CHOL carry a small head group and proportionally 'bulkier' tails. These lipids are defined as having spontaneous negative curvature [1,74]. According to the Stalk-pore hypothesis, membrane merger proceeds through transient steps, that include (i) merging of the proximal monolayers (i.e., merging of the outer vesicle monolayer with the inner PM monolayer, in case of heterotypic fusion and; outer monolayers of contacting vesicles, in case of homotypic fusion). This follows (ii) merging of the distal monolayers (i.e., merging of the inner vesicle monolayer with the outer PM monolayer, in case of heterotypic fusion and; inner monolayers of contacting vesicles, in case of homotypic fusion) [15,16,55,74]. The entire fusion process proceeds from the point of contact between merging bilayers, followed by the formation of a stalk and hemifusion diaphragm (HD), and then to formation, opening, and expansion of a fusion pore (**Figure - 2**). Notably, merging of proximal monolayers is promoted on introducing negative curvature lipids to these monolayers; this supports stalk formation. However, merging of these monolayers is inhibited on introducing positive curvature lipids [2,55]. In contrast, merging of distal monolayers is promoted and inhibited, respectively, upon introducing positive and negative curvature lipids [2,55], thus directly affecting the formation, opening, and expansion of the fusion pore. Hence, upon Ca^{2+} triggering, membrane merger proceeds through high curvature lipid intermediates at exocytotic sites that are likely to be localized in CHOL and sphingolipid (SL) microdomains [1,76]. In addition to maintaining the integrity of exocytotic sites, CHOL

also facilitates membrane merger by lowering the energy barrier for the initial fusion step [1,34], and SL regulate the efficiency of the native Ca^{2+} triggered membrane fusion mechanism, presumably by localizing and maintaining other critical components to enable rapid response upon triggering [37,50].

3. Phospholipase A_2 isozymes and their suggested roles

Mammalian phospholipase A_2 (PLA_2) belong to a diverse enzyme family, that is sub-divided into 15 Groups (IXV) [77-80]; nevertheless, all hydrolyze membrane phospholipids at the sn-2 position producing lysophospholipids (LPL) and free fatty acids (FFA) (**Figure - 3**). However, a broader classification, based on their subcellular localization and Ca^{2+} requirement, categorizes these into (i) Ca^{2+}-dependent secretory or $sPLA_2$; (ii) Ca^{2+}-dependent cytoplasmic or $cPLA_2$ and; (iii) Ca^{2+} independent cytoplasmic or $iPLA_2$ (also see **Chapter - 2** and [81]).

$sPLA_2$ are 12-19 kDa secretory proteins that have 5-7 conserved disulfide bonds that contribute to their high stability. Once secreted, their Ca^{2+} requirement for catalysis is in the low millimolar (mM) range with no strict fatty acid selectivity, although most target PE, PG, PI, and PS [78,82]. In contrast, $cPLA_2$ isozymes have a molecular weight ranging from 61-114 kDa [78,80] and are generally found in the cytosol. These enzymes require micromolar (μM) Ca^{2+} for membrane binding, via conserved lipase consensus sequences - GXSXG, GXSGS or GXSXV in the C2 domain at the N-terminal [77,78,83]. Mammalian $cPLA_2$ has six isoforms, designated as α, β, γ, δ, ε, ζ, of them, only α and β have N terminal C2 domain [77,78,83]. Similarly, $iPLA_2$ are intracellular enzymes that do not require Ca^{2+} beyond basal cytosolic levels for activity and carry a GXSXG lipase and GXGXXG nucleotide consensus sequences. Mammalian $iPLA_2$ has six isoforms, designated as β, γ, δ, ε, ζ, and η and their molecular weights range from 27 to 146 kDa [2,84,85]. (Note: sequence alignment with percent identity and similarity between characterized human, murine and putative PLA_2 isozymes is shown **Chapter - 2** and [81]). While secreted $sPLA_2$ is associated with inflammation, as these clear

variety of non-cellular targets (e.g., virus, bacteria, exosomes, etc.) by cleaving the membrane phospholipids from outside of the cell [86]. A well-established function of iPLA$_2$β is membrane phospholipid remodelling via the Lands cycle [2,84,85]. At steady state, the molecular species composition in the membrane is regulated by *de novo* biosynthesis (or the Kennedy cycle) [58,87] and acyl chain remodelling (or the Lands cycle) [57] (**Figure - 4**), the latter mediated by phospholipases and acyltransferases or transacylases [61,88-91]. The levels of phospholipids are thus maintained via Lands cycle due to the basal activities of enzymes, including iPLA$_2$ that metabolize membrane phospholipids to generate lysophospholipids, and a FFA is also liberated. Released FFA rapidly converts to fatty acyl-CoA and incorporate back into the membrane phospholipids via *de novo* pathway [2,88,89] (also see **Chapter - 3**).

1.4 SNAREs, PLA$_2$, and native membrane merger

The *Clostridium botulinum* (BotX) and *Clostridium tetani* (TetX) toxins were early tools to study neurotransmission, which cleaved synaptosome-associated protein-25 (SNAP-25), vesicle-associated membrane protein-2 (VAMP-2), and single-pass transmembrane proteins (syntaxin) and also blocked regulated secretion [92-94]. VAMP-2 and syntaxin carry a trans membrane-domains (TMD) that associate with membrane [95,96] while the association of SNAP-25 to the membrane occurs via its palmitoylated residues [97]. All these proteins also carry a cytoplasmic domain that interacts to form stable SDS-resistant heterotrimeric *trans or cis* SNARE complexes; docking and priming are believed to be the functional consequence of *trans* SNARE complex formation. As toxins cleaved SNAP-25, VAMP-2, and syntaxin (collectively termed as SNAREs) and caused a parallel block in regulated secretion, an oversimplified interpretation led to the suggestion that perhaps SNAREs also catalyze actual membrane merger, in addition to mediating the upstream docking and priming steps. Therefore, to understand the underlying mechanism, the original SNARE hypothesis suggested that N-ethylmaleimide-sensitive factor (NFS), an ATPase, disrupt *trans* SNARE complexes that drive

membrane merger [98]; nevertheless, it has also been long known that actual membrane merger is independent of ATP [5,46,99,100]. Therefore, the 'modified' SNAREpin hypothesis suggested that NSF disassembles *cis* SNARE complexes, after fusion, to recover monomeric SNAREs for further rounds of fusion [13]. Thus emphasizing that SNARE assembly play a central role in membrane merger. According to the SNAREpin hypothesis, membrane merger is driven by the NH_2 terminus-to-COOH terminus 'zippering' of the parallel coiled-coil SNARE domains, that pulls two apposed membranes together [101], also purportedly providing sufficient free energy to overcome inter-membrane repulsive forces [102]. However, SNARE-driven membrane merger still fails to explain homotypic and heterotypic CV fusion [33,35,103] and homotypic yeast vacuole fusion [104]. These studies instead suggested the role of SNAREs in targeting, docking, and priming [33,35,81,103] (also see **Chapter - 3** and Discussion and future direction).

On average, a CV contains ~5500, ~700, and ~300 copies of VAMP, SNAP-25, and syntaxin, respectively [33,35,103]. All these proteins carry a substantial number of trypsin, chymotrypsin, papain, and clostripain cleavage sites in their cytoplasmic domains that interact to form *trans* SNARE complexes [35]. Notably, Ca^{2+}-triggered CV fusion occurred despite the proteolytic removal of the SNAREs using trypsin, papain, and clostripain [35]. In contrast, fusion reduced significantly in CV that were treated with chymotrypsin without substantial removal of the SNAREs [105]. Also, CV lost their fusion competence when treated with chaotropic buffer, without affecting Ca^{2+} induced disruption of SNARE complexes [44]. Furthermore, disruption of SNARE complexes using saturating levels of Ca^{2+} (i.e., $\geq$ 100 µM) triggered homotypic CV fusion [33], while triggering with Sr^{2+} and Ba^{2+} did not disrupted SNARE complexes, but triggered homotypic CV fusion [44]. Therefore, based on these studies, the actual membrane merger step appears to be independent of inter-membrane SNARE complex formation.

Notably, BotX decreased ARA levels in addition to blocking acetylcholine release [106], suggesting possible action against PLA_2, in addition, to SNAP 25 cleavage [107]; nevertheless, this has never been shown or perhaps explored (also see [108] for other potential targets of BotX). Also, based on *in vitro* studies, exogenous ARA is thought to enhance SNARE complex formation by releasing syntaxin from syntaxin/Munc18 complexes [109,110] and also suggested to restrict the lateral motion of secretory vesicles that are closer to the PM [111]. However, whether ARA acted as 'active' species is unknown, as supplemented ARA can also convert to other FFA species (see **Chapter - 3** and [112]**)**. Overall, the current interpretation in the field is that PLA_2 or its metabolites may directly or indirectly promote SNARE complex formation, hence promoting regulated exocytosis.

In this thesis, the role of PLA_2 in the late steps of regulated exocytosis is thus investigated. Firstly, a working hypothesis was proposed [2], based on already existing information relating to the spontaneous curvature of the canonical PLA_2 metabolites, LPC and ARA [16,55,73-75], their effects on SNARE complex formation *in vitro* [110,113,114] and membrane merger steps [16,55,73,74]. The working hypothesis stated that the localized endogenous PLA_2 supply basal level of LPL and FFA near fusion sites to maintain docking/priming steps; LPC acts as molecular fusion 'brake' to block membrane merger before Ca^{2+} triggering while ARA promotes SNARE complexes formation, thus supporting docking/priming steps (**Figure - 5**). Notably, estimated levels of LPC and ARA on the PM and vesicle membrane in an unstimulated state appear to be extremely low [2,115] and both these metabolites can also rapidly metabolize [2] (also see **Chapter - 3** and [112]). Therefore, if ARA would have to support *trans* SNARE complex *in vivo*, a localized PLA_2 near docking or fusion sites in the PM or associated with vesicle would be needed to generate sufficient levels of ARA to carry out such roles. This has been depicted in the working hypothesis [2]. Using targeted omics, the vesicle-associated PLA_2 isozymes – CV luminal $sPLA_2$, and surface $iPLA_2$

– were identified and characterized [81] and were seen to regulate docking/priming steps of regulated exocytosis **(Chapter - 2)** and **[81]**. This substantiated the working hypothesis. To confirm, canonical PLA_2 metabolites, LPC and ARA were supplemented to CV suspension, and treatment effects confirmed that LPC acted as molecular fusion 'clamp' **(Chapter - 3)**. However, in contrast, to the suggested role in the working hypothesis, ARA impaired docking/priming. On further attempts to manipulate CV luminal $sPLA_2$ using phospholipase A_2 activating peptide (PLAP) suggested that docking/priming steps, the endogenous lipid composition and SNARE complex formation or 'zippering' could be inter-related. (**Chapter - 4**). Importantly, PLAP also reduced membrane capacitance and readily releasable pool (RRP) size in the chromaffin cells, thus highlighting the similarity in the molecular state of RRP secretory vesicles in the chromaffin cell and fully primed release-ready CV.

Figure (s)

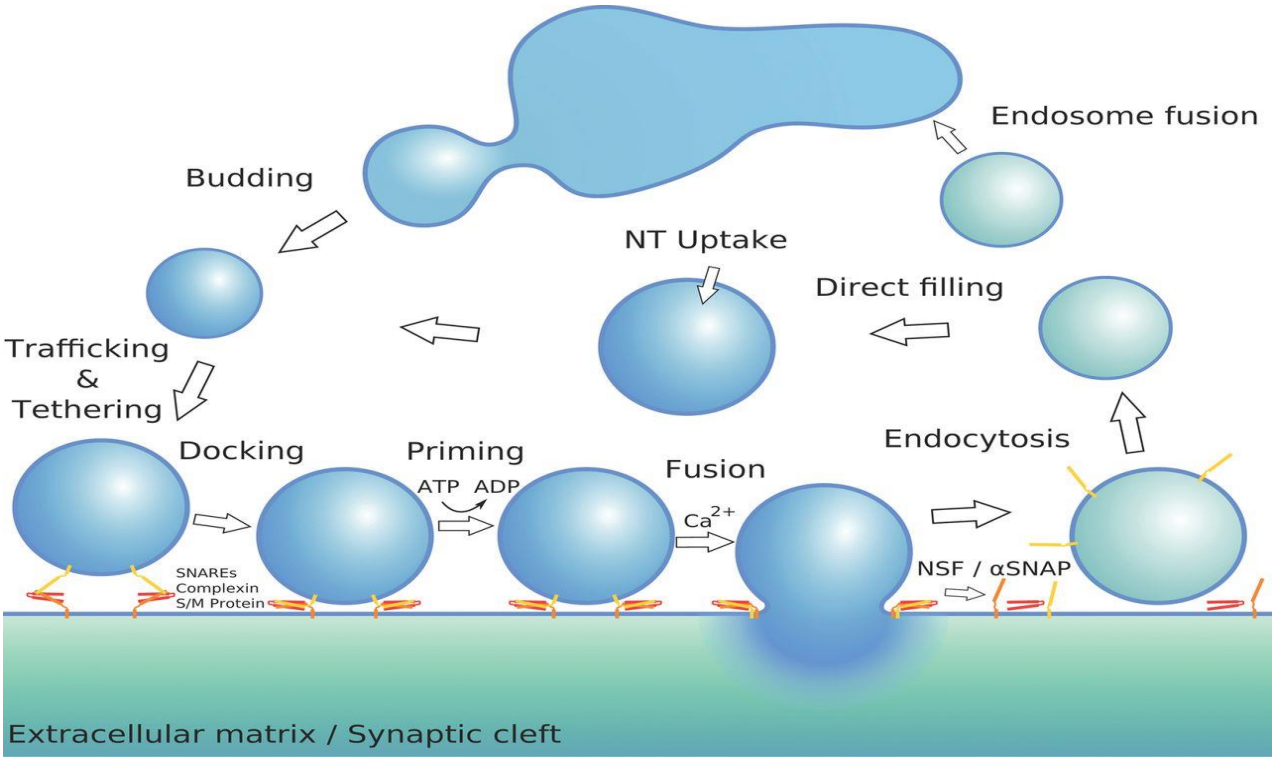

Figure 1. Schematic diagram of exocytosis in the presynaptic terminal [1].

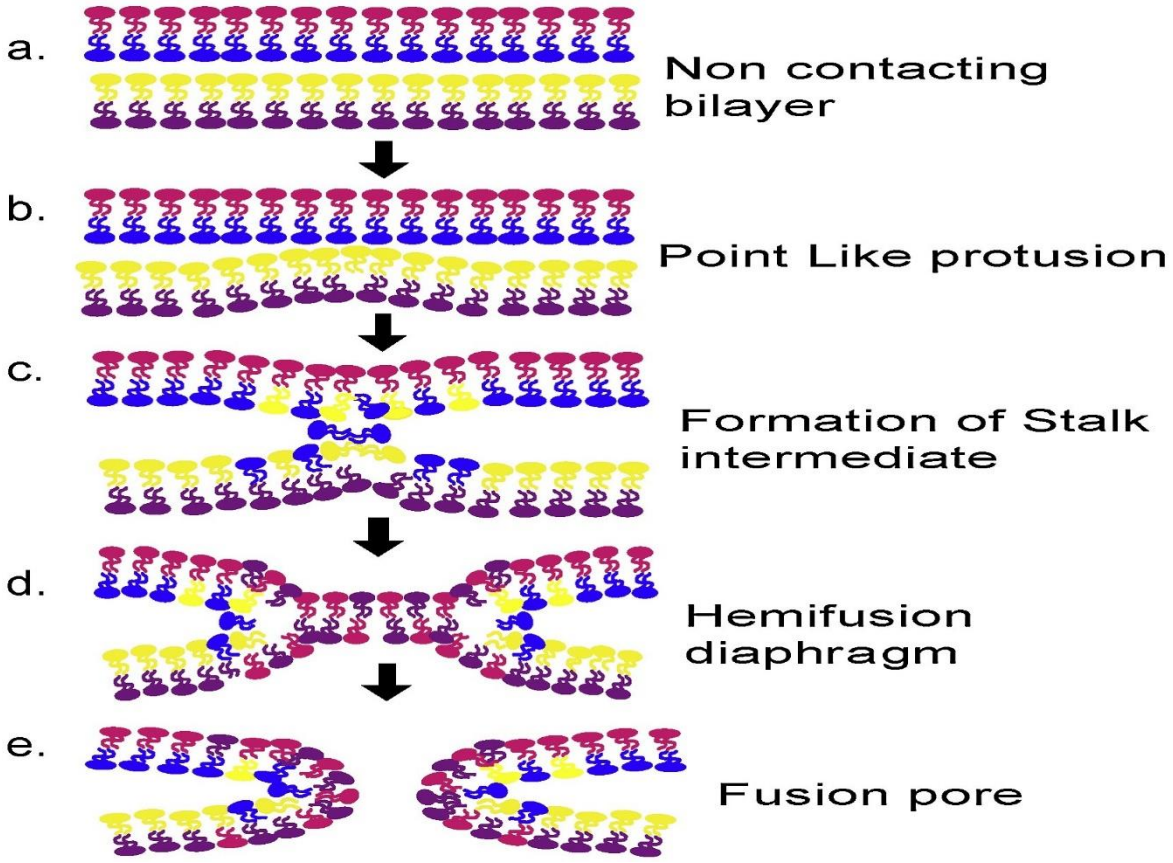

Figure 2. Stalk-pore hypothesis: membrane fusion proceeds from point of contact through to opening of a fusion pore via high curvature intermediates [2].

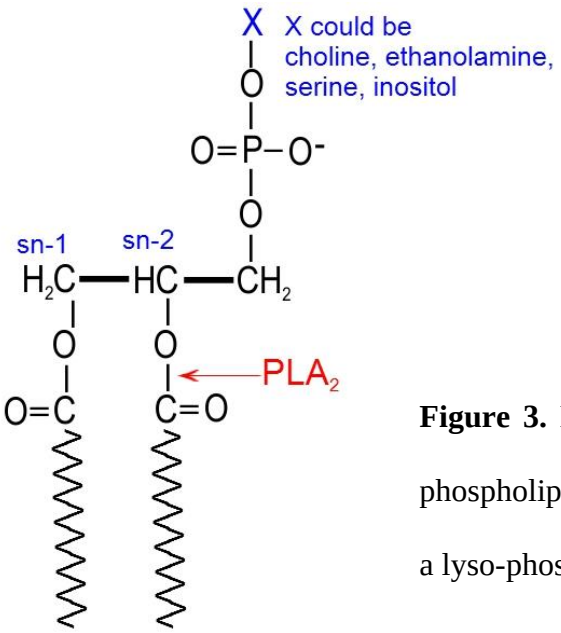

Figure 3. Hydrolytic site of phospholipases A_2 on a glycerol phospholipid. PLA_2 enzymes cleave at sn-2 positions to generate a lyso-phospholipid and a free fatty acid.

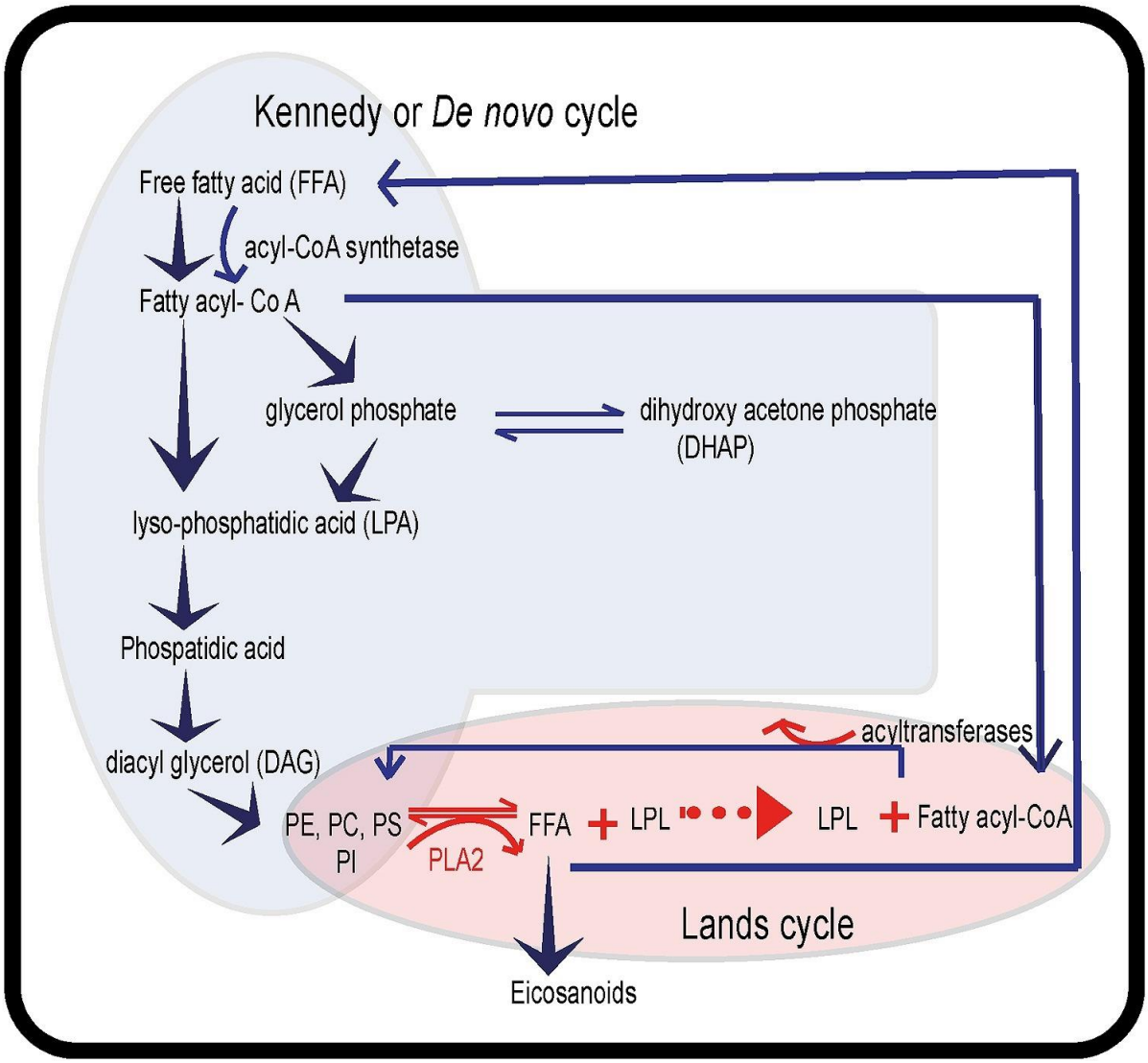

Figure 4. Membrane remodelling via Kennedy and Lands cycles: In the Kennedy pathway, FFA is progressively converted to finally yield PE, PC, PS, and PI. In contrast, in Lands cycle, existing PE, PC, PS, and PI are metabolized by PLA_2, resulting in the formation of LPL and FFA. The released FFA is converted either to eicosanoids or into fatty acyl-CoA; the LPL is acylated by acyltransferases using fatty acyl-CoA [2].

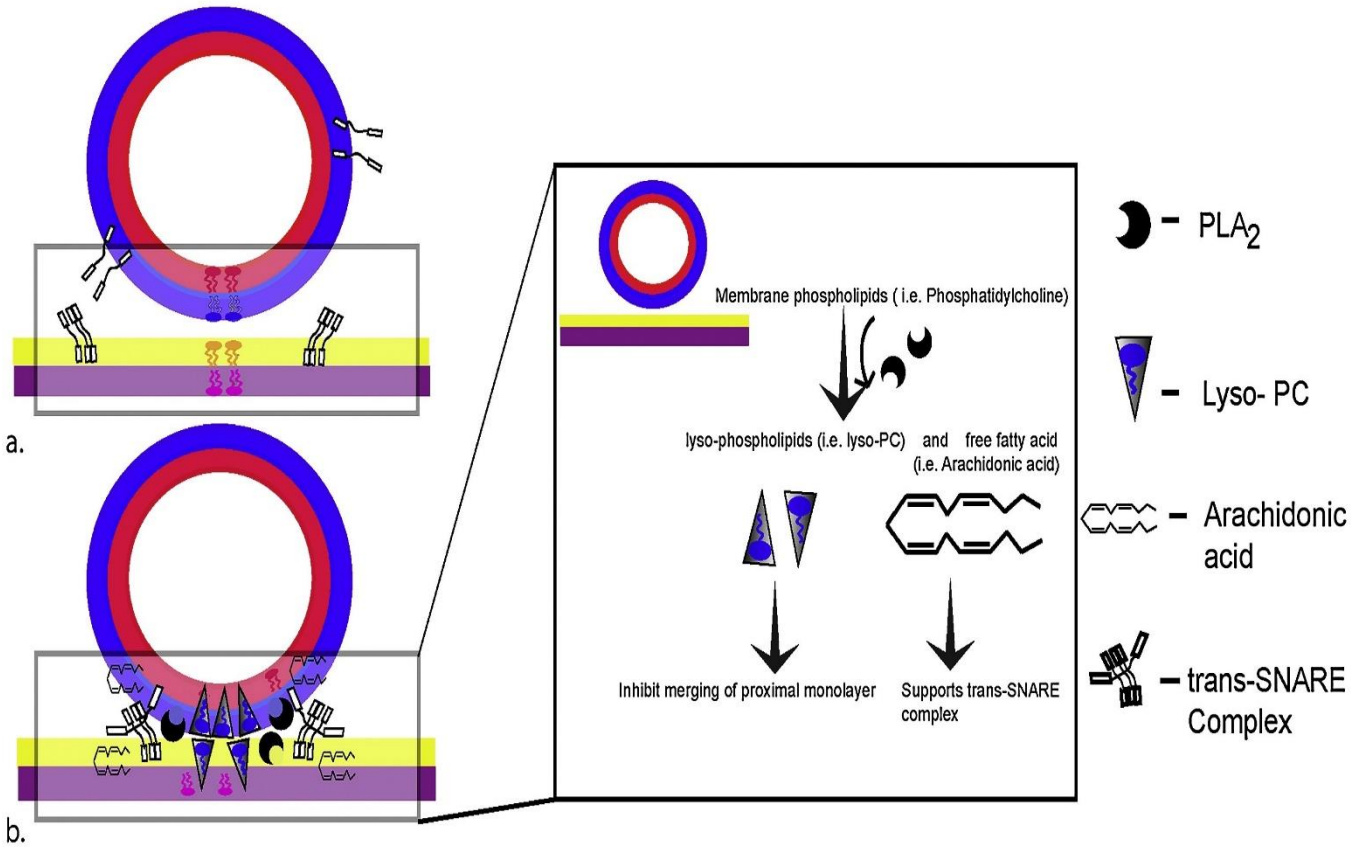

Figure 5. a. Non-contacting membranes; b. membranes in close proximity. Working hypothesis: a fusion ready state is maintained by localized PLA_2 that produces LPL and ARA; LPL acts as a local 'fusion block' inhibiting the premature (i.e. pre-stimulus) merger of the proximal membranes while ARA supports the *trans* SNARE complex(es) in maintaining the fully primed, fusion-ready state [2].

References

1. Churchward, Matthew A.; Coorssen, Jens R. Cholesterol, regulated exocytosis and the physiological fusion machine. *Biochemical Journal* **2009**, *423*, 1-14.
2. Dabral, D.; Coorssen, J.R. Phospholipase A2: Potential roles in native membrane fusion. *The International Journal of Biochemistry & Cell Biology* **2017**, *85*, 1-5.
3. Palade, G. Intracellular aspects of the process of protein synthesis. *Science (New York, N.Y.)* **1975**, *189*, 347-358.
4. Kato, M.; Wickner, W. Vam10p defines a Sec18p-independent step of priming that allows yeast vacuole tethering. *Proceedings of the National Academy of Sciences of the United States of America* **2003**, *100*, 6398-6403.
5. Heidelberger, R.; Sterling, P.; Matthews, G. Roles of ATP in depletion and replenishment of the releasable pool of synaptic vesicles. *Journal of neurophysiology* **2002**, *88*, 98-106.
6. Becherer, U.; Rettig, J. Vesicle pools, docking, priming, and release. *Cell and Tissue Research* **2006**, *326*, 393-407.
7. Lumpert, C.J.; Kersken, H.; Plattner, H. Cell surface complexes ('cortices') isolated from Paramecium tetraurelia cells as a model system for analysing exocytosis in vitro in conjunction with microinjection studies. *The Biochemical journal* **1990**, *269*, 639-645.
8. Meunier, F.A.; Osborne, S.L.; Hammond, G.R.V.; Cooke, F.T.; Parker, P.J.; Domin, J.; Schiavo, G. Phosphatidylinositol 3-Kinase C2α Is Essential for ATP-dependent Priming of Neurosecretory Granule Exocytosis. *Molecular Biology of the Cell* **2005**, *16*, 4841-4851.

9. Morimoto, T.; Ogihara, S. ATP is required in platelet serotonin exocytosis for protein phosphorylation and priming of secretory vesicles docked on the plasma membrane. *Journal of Cell Science* **1996**, *109*, 113-118.

10. Fortoul, N.; Singh, P.; Hui, C.Y.; Bykhovskaia, M.; Jagota, A. Coarse-Grained Model of SNARE-Mediated Docking. *Biophysical journal* **2015**, *108*, 2258-2269.

11. Imig, C.; Min, S.-W.; Krinner, S.; Arancillo, M.; Rosenmund, C.; Südhof, Thomas C.; Rhee, J.; Brose, N.; Cooper, Benjamin H. The Morphological and Molecular Nature of Synaptic Vesicle Priming at Presynaptic Active Zones. *Neuron* **2014**, *84*, 416-431.

12. Wickner, W. Yeast vacuoles and membrane fusion pathways. *The EMBO Journal* **2002**, *21*, 1241-1247.

13. Weber, T.; Zemelman, B.V.; McNew, J.A.; Westermann, B.; Gmachl, M.; Parlati, F.; Sollner, T.H.; Rothman, J.E. SNAREpins: minimal machinery for membrane fusion. *Cell* **1998**, *92*, 759-772.

14. Richmond, J.E.; Broadie, K.S. The synaptic vesicle cycle: exocytosis and endocytosis in Drosophila and C. elegans. *Current Opinion in Neurobiology* **2002**, *12*, 499-507.

15. Kozlovsky, Y.; Kozlov, M.M. Stalk Model of Membrane Fusion: Solution of Energy Crisis. *Biophysical journal* **2002**, *82*, 882-895.

16. Chernomordik, L.V.; Kozlov, M.M. Mechanics of membrane fusion. *Nat Struct Mol Biol* **2008**, *15*, 675-683.

17. Kozlov, M.M.; Leikin, S.L.; Chernomordik, L.V.; Markin, V.S.; Chizmadzhev, Y.A. Stalk mechanism of vesicle fusion. *European Biophysics Journal* **1989**, *17*, 121-129.

18. Szule, J.A.; Coorssen, J.R. Revisiting the role of SNAREs in exocytosis and membrane fusion. *Biochimica et Biophysica Acta (BBA) - Molecular Cell Research* **2003**, *1641*, 121-135.

19. Knight, D.E.; von Grafenstein, H.; Athayde, C.M. Calcium-dependent and calcium-independent exocytosis. *Trends in Neurosciences* **1989**, *12*, 451-458.

20. Abbineni, P.S.; Hibbert, J.E.; Coorssen, J.R. Critical Role of Cortical Vesicles in Dissecting Regulated Exocytosis: Overview of Insights Into Fundamental Molecular Mechanisms. *The Biological Bulletin* **2013**, *224*, 200-217.

21. Rogasevskaia, T.P.; Coorssen, J.R. A new approach to the molecular analysis of docking, priming, and regulated membrane fusion. *Journal of Chemical Biology* **2011**, *4*, 117-136.

22. Rogasevskaia, T.P.; Churchward, M.A.; Coorssen, J.R. Anionic lipids in Ca(2+)-triggered fusion. *Cell Calcium* **2012**, *52*, 259-269.

23. Rogasevskaia, T.P.; Coorssen, J.R. The role of phospholipase D in regulated exocytosis. *Journal of Biological Chemistry* **2015**, http://10.1074/jbc.M115.681429.

24. Abbineni, P.S.; Wright, E.P.; Rogasevskaia, T.P.; Killingsworth, M.C.; Malladi, C.S.; Coorssen, J.R. The Sea Urchin Egg and Cortical Vesicles as Model Systems to Dissect the Fast, Ca2+-Triggered Steps of Regulated Exocytosis. In *Exocytosis Methods*, Thorn, P., Ed. Humana Press: Totowa, NJ, 2014; pp. 221-241.

25. Bradham, C.A.; Foltz, K.R.; Beane, W.S.; Arnone, M.I.; Rizzo, F.; Coffman, J.A.; Mushegian, A.; Goel, M.; Morales, J.; Geneviere, A.-M., et al. The sea urchin kinome: A first look. *Developmental biology* **2006**, *300*, 180-193.

26. Cameron, R.A. Comparing the Human and Sea Urchin Genomes. In *eLS*, 2013; http://doi:10.1002/9780470015902.a0020745.pub2.

27. Sodergren, E.; Weinstock, G.M.; Davidson, E.H.; Cameron, R.A.; Gibbs, R.A.; Angerer, R.C.; Angerer, L.M.; Arnone, M.I.; Burgess, D.R.; Burke, R.D., et al. The genome of the sea urchin Strongylocentrotus purpuratus. *Science (New York, N.Y.)* **2006**, *314*, 941-952.

28. Kaupp, U.B.; Solzin, J.; Hildebrand, E.; Brown, J.E.; Helbig, A.; Hagen, V.; Beyermann, M.; Pampaloni, F.; Weyand, I. The signal flow and motor response controling chemotaxis of sea urchin sperm. *Nature Cell Biology* **2003**, *5*, 109.

29. Jaffe, L.A. Fast block to polyspermy in sea urchin eggs is electrically mediated. *Nature* **1976**, *261*, 68-71.

30. Nakamura, M.; Yasumasu, I. Mechanism for increase in intracellular concentration of free calcium in fertilized sea urchin egg. A method for estimating intracellular concentration of free calcium. *The Journal of general physiology* **1974**, *63*, 374-388.

31. Vacquier, V.D.; Tegner, M.J.; Epel, D. Protease released from sea urchin eggs at fertilization alters the vitelline layer and aids in preventing polyspermy. *Experimental cell research* **1973**, *80*, 111-119.

32. Schuel, H.; Kelly, J.W.; Berger, E.R.; Wilson, W.L. Sulfated acid mucopolysaccharides in the cortical granules of eggs: Effects of quaternary ammonium salts on fertilization. *Experimental cell research* **1974**, *88*, 24-30.

33. Tahara, M.; Coorssen, J.R.; Timmers, K.; Blank, P.S.; Whalley, T.; Scheller, R.; Zimmerberg, J. Calcium Can Disrupt the SNARE Protein Complex on Sea Urchin Egg Secretory Vesicles without Irreversibly Blocking Fusion. *Journal of Biological Chemistry* **1998**, *273*, 33667-33673.

34. Churchward, M.A.; Rogasevskaia, T.; Höfgen, J.; Bau, J.; Coorssen, J.R. Cholesterol facilitates the native mechanism of Ca2+-triggered membrane fusion. *Journal of Cell Science* **2005**, *118*, 4833-4848.

35. Coorssen, J.R.; Blank, P.S.; Albertorio, F.; Bezrukov, L.; Kolosova, I.; Chen, X.; Backlund, P.S.; Zimmerberg, J. Regulated secretion: SNARE density, vesicle fusion and calcium dependence. *Journal of Cell Science* **2003**, *116*, 2087-2097.

36. Churchward, M.A.; Rogasevskaia, T.; Brandman, D.M.; Khosravani, H.; Nava, P.; Atkinson, J.K.; Coorssen, J.R. Specific Lipids Supply Critical Negative Spontaneous Curvature—An Essential Component of Native Ca2+-Triggered Membrane Fusion. *Biophysical journal* **2008**, *94*, 3976-3986.

37. Abbineni, P.S.; Coorssen, J.R. Sphingolipids modulate docking, Ca2+ sensitivity and membrane fusion of native cortical vesicles. *The International Journal of Biochemistry & Cell Biology* **2018**, *104*, 43-54.

38. Blank, P.S.; Cho, M.-S.; Vogel, S.S.; Kaplan, D.; Kang, A.; Malley, J.; Zimmerberg, J. Submaximal Responses in Calcium-triggered Exocytosis Are Explained by Differences in the Calcium Sensitivity of Individual Secretory Vesicles. *The Journal of General Physiology* **1998**, *112*, 559-567.

39. Blank, P.S.; Vogel, S.S.; Malley, J.D.; Zimmerberg, J. A kinetic analysis of calcium-triggered exocytosis. *J Gen Physiol* **2001**, *118*, 145-156.

40. Heinemann, C.; von Rüden, L.; Chow, R.H.; Neher, E. A two-step model of secretion control in neuroendocrine cells. *Pflügers Archiv* **1993**, *424*, 105-112.

41. Smith, S.J.; Augustine, G.J. Calcium ions, active zones and synaptic transmitter release. *Trends in Neurosciences* **1988**, *11*, 458-464.

42. Becherer, U.; Moser, T.; Stühmer, W.; Oheim, M. Calcium regulates exocytosis at the level of single vesicles. *Nature Neuroscience* **2003**, *6*, 846-853.

43. Burgoyne, R.D.; Morgan, A. Secretory granule exocytosis. *Physiological reviews* **2003**, *83*, 581-632.

44. Coorssen, J.R.; Blank, P.S.; Tahara, M.; Zimmerberg, J. Biochemical and Functional Studies of Cortical Vesicle Fusion: The SNARE Complex and Ca2+ Sensitivity. *The Journal of cell biology* **1998**, *143*, 1845-1857.

45. Vogel, S.S.; Blank, P.S.; Zimmerberg, J. Poisson-distributed active fusion complexes underlie the control of the rate and extent of exocytosis by calcium. *The Journal of Cell Biology* **1996**, *134*, 329-338.

46. Vacquier, V.D. The isolation of intact cortical granules from sea urchin eggs: calcium lons trigger granule discharge. *Developmental biology* **1975**, *43*, 62-74.

47. Neher, E.; Sakaba, T. Multiple roles of calcium ions in the regulation of neurotransmitter release. *Neuron* **2008**, *59*, 861-872.

48. Neher, E.; Zucker, R.S. Multiple calcium-dependent processes related to secretion in bovine chromaffin cells. *Neuron* **1993**, *10*, 21-30.

49. Pasche, M.; Matti, U.; Hof, D.; Rettig, J.; Becherer, U. Docking of LDCVs Is Modulated by Lower Intracellular [Ca2+] than Priming. *PLOS ONE* **2012**, *7*, e36416.

50. Rogasevskaia, T.; Coorssen, J.R. Sphingomyelin-enriched microdomains define the efficiency of native Ca^{2+}-triggered membrane fusion. *Journal of Cell Science* **2006**, *119*, 2688-2694.

51. Holthuis, J.C.; Pomorski, T.; Raggers, R.J.; Sprong, H.; Van Meer, G. The organizing potential of sphingolipids in intracellular membrane transport. *Physiological reviews* **2001**, *81*, 1689-1723.

52. Hibbert, J.E.; Butt, R.H.; Coorssen, J.R. Actin is not an essential component in the mechanism of calcium-triggered vesicle fusion. *The International Journal of Biochemistry & Cell Biology* **2006**, *38*, 461-471.

53. Milne, S.; Ivanova, P.; Forrester, J.; Alex Brown, H. Lipidomics: an analysis of cellular lipids by ESI-MS. *Methods (San Diego, Calif.)* **2006**, *39*, 92-103.

54. van Meer, G.; Voelker, D.R.; Feigenson, G.W. Membrane lipids: where they are and how they behave. *Nature Reviews Molecular Cell Biology* **2008**, *9*, 112.

55. Chernomordik, L.; Kozlov, M.M.; Zimmerberg, J. Lipids in biological membrane fusion. *J. Membarin Biol.* **1995**, *146*, 1-14.

56. Kozhina, V.P.; Terekhova, T.A.; Svetashev, V.I. Lipid composition of gametes and embryos of the sea urchin Strongylocentrotus intermedius at early stages of development. *Dev Biol* **1978**, *62*, 512-517.

57. Lands, W.E. Metabolism of glycerolipides; a comparison of lecithin and triglyceride synthesis. *The Journal of biological chemistry* **1958**, *231*, 883-888.

58. Kennedy, E.P.; Weiss, S.B. The function of cytidine coenzymes in the biosynthesis of phospholipides. *The Journal of biological chemistry* **1956**, *222*, 193-214.

59. Kreutzberger, A.J.B.; Kiessling, V.; Liang, B.; Yang, S.-T.; Castle, J.D.; Tamm, L.K. Asymmetric Phosphatidylethanolamine Distribution Controls Fusion Pore Lifetime and Probability. *Biophysical journal* **2017**, *113*, 1912-1915.

60. Alder-Baerens, N.; Lisman, Q.; Luong, L.; Pomorski, T.; Holthuis, J.C.M. Loss of P4 ATPases Drs2p and Dnf3p Disrupts Aminophospholipid Transport and Asymmetry in Yeast Post-Golgi Secretory Vesicles. *Molecular Biology of the Cell* **2006**, *17*, 1632-1642.

61. Hishikawa, D.; Shindou, H.; Kobayashi, S.; Nakanishi, H.; Taguchi, R.; Shimizu, T. Discovery of a lysophospholipid acyltransferase family essential for membrane asymmetry and diversity. *Proceedings of the National Academy of Sciences* **2008**, *105*, 2830-2835.

62. Zachowski, A.; Henry, J.-P.; Devaux, P.F. Control of transmembrane lipid asymmetry in chromaffin granules by an ATP-dependent protein. *Nature* **1989**, *340*, 75.

63. Devaux, P.F.; Zachowski, A. Maintenance and consequences of membrane phospholipid asymmetry. *Chemistry and Physics of Lipids* **1994**, *73*, 107-120.

64. Contreras, F.X.; Sanchez-Magraner, L.; Alonso, A.; Goni, F.M. Transbilayer (flip-flop) lipid motion and lipid scrambling in membranes. *FEBS letters* **2010**, *584*, 1779-1786.

65. Quinn, P.J.; Kagan, V.E. *Phospholipid Metabolism in Apoptosis*; Springer US: 2013.

66. Kalra, V.K.; Gupta, C.M.; Zachowski, A.; Pomorski, T. Lipid Asymmetry of Membranes. In *Manual on Membrane Lipids*, Prasad, R., Ed. Springer Berlin Heidelberg: Berlin, Heidelberg, 1996; 10.1007/978-3-642-79837-5_6pp. 112-143.

67. Kinsey, W.H.; Decker, G.L.; Lennarz, W.J. Isolation and partial characterization of the plasma membrane of the sea urchin egg. *The Journal of Cell Biology* **1980**, *87*, 248-254.

68. Churchward, M.A.; Brandman, D.M.; Rogasevskaia, T.; Coorssen, J.R. Copper (II) sulfate charring for high sensitivity on-plate fluorescent detection of lipids and sterols: quantitative analyses of the composition of functional secretory vesicles. *Journal of Chemical Biology* **2008**, *1*, 79-87.

69. Duzgunes, N. Membrane fusion. *Sub-cellular biochemistry* **1985**, *11*, 195-286.

70. Melcrová, A.; Pokorna, S.; Pullanchery, S.; Kohagen, M.; Jurkiewicz, P.; Hof, M.; Jungwirth, P.; Cremer, P.S.; Cwiklik, L. The complex nature of calcium cation interactions with phospholipid bilayers. *Scientific Reports* **2016**, *6*, 38035.

71. Sinn, C.G.; Antonietti, M.; Dimova, R. Binding of calcium to phosphatidylcholine–phosphatidylserine membranes. *Colloids and Surfaces A: Physicochemical and Engineering Aspects* **2006**, *282-283*, 410-419.

72. Starr, M.L.; Sparks, R.A.; Hurst, L.R.; Zhao, Z.; Arango, A.; Lihan, M.; Jenkins, J.L.; Tajkhorshid, E.; Fratti, R.A. Phosphatidic acid inhibits SNARE priming by inducing conformational changes in Sec18 protomers. *bioRxiv* **2018**, 10.1101/365775, 365775.

73. Chernomordik, L. Non-bilayer lipids and biological fusion intermediates. *Chemistry and physics of lipids* **1996**, *81*, 203-213.

74. Chernomordik, L.; Chanturiya, A.; Green, J.; Zimmerberg, J. The hemifusion intermediate and its conversion to complete fusion: regulation by membrane composition. *Biophysical journal* **1995**, *69*, 922-929.

75. Fuller, N.; Rand, R.P. The influence of lysolipids on the spontaneous curvature and bending elasticity of phospholipid membranes. *Biophysical journal* **2001**, *81*, 243-254.

76. Chasserot-Golaz, S.; Vitale, N.; Umbrecht-Jenck, E.; Knight, D.; Gerke, V.; Bader, M.F. Annexin 2 promotes the formation of lipid microdomains required for calcium-regulated exocytosis of dense-core vesicles. *Mol Biol Cell* **2005**, *16*, 1108-1119.

77. Dennis, E.A. The growing phospholipase A2 superfamily of signal transduction enzymes. *Trends in biochemical sciences* **1997**, *22*, 1-2.

78. Farooqui, A.A.; Yang, H.C.; Rosenberger, T.A.; Horrocks, L.A. Phospholipase A2 and its role in brain tissue. *Journal of neurochemistry* **1997**, *69*, 889-901.

79. Diez, E.; Chilton, F.H.; Stroup, G.; Mayer, R.J.; Winkler, J.D.; Fonteh, A.N. Fatty acid and phospholipid selectivity of different phospholipase A2 enzymes studied by using a mammalian membrane as substrate. *The Biochemical journal* **1994**, *301 (Pt 3)*, 721-726.

80. Brown, W.J.; Chambers, K.; Doody, A. Phospholipase A2 (PLA2) enzymes in membrane trafficking: mediators of membrane shape and function. *Traffic (Copenhagen, Denmark)* **2003**, *4*, 214-221.

81. Dabral, D.; Coorssen, J.R. Combined Targeted Omic and Functional Assays Identify Phospholipases A2 that Regulate Docking/Priming in Calcium-Triggered Exocytosis. *Cells* **2019**, *8*, 303.

82. Kudo, I.; Murakami, M.; Hara, S.; Inoue, K. Mammalian non-pancreatic phospholipases A2. *Biochimica et Biophysica Acta (BBA) - Lipids and Lipid Metabolism* **1993**, *1170*, 217-231.

83. Clark, J.D.; Lin, L.L.; Kriz, R.W.; Ramesha, C.S.; Sultzman, L.A.; Lin, A.Y.; Milona, N.; Knopf, J.L. A novel arachidonic acid-selective cytosolic PLA2 contains a Ca(2+)-dependent translocation domain with homology to PKC and GAP. *Cell* **1991**, *65*, 1043-1051.

84. Balsinde, J.; Balboa, M.A.; Dennis, E.A. Antisense inhibition of group VI Ca2+-independent phospholipase A2 blocks phospholipid fatty acid remodeling in murine P388D1 macrophages. *The Journal of biological chemistry* **1997**, *272*, 29317-29321.

85. Ramanadham, S.; Ali, T.; Ashley, J.W.; Bone, R.N.; Hancock, W.D.; Lei, X. Calcium-independent phospholipases A2 and their roles in biological processes and diseases. *Journal of Lipid Research* **2015**, *56*, 1643-1668.

86. Murakami, M.; Taketomi, Y.; Girard, C.; Yamamoto, K.; Lambeau, G. Emerging roles of secreted phospholipase A2 enzymes: Lessons from transgenic and knockout mice. *Biochimie* **2010**, *92*, 561-582.

87. Gibellini, F.; Smith, T.K. The Kennedy pathway--De novo synthesis of phosphatidylethanolamine and phosphatidylcholine. *IUBMB life* **2010**, *62*, 414-428.

88. Balsinde, J.; Bianco, I.D.; Ackermann, E.J.; Conde-Frieboes, K.; Dennis, E.A. Inhibition of calcium-independent phospholipase A2 prevents arachidonic acid incorporation and phospholipid remodeling in P388D1 macrophages. *Proceedings of the National Academy of Sciences of the United States of America* **1995**, *92*, 8527-8531.

89. Balsinde, J.; Winstead, M.V.; Dennis, E.A. Phospholipase A2 regulation of arachidonic acid mobilization. *FEBS Letters* **2002**, *531*, 2-6.

90. de Kroon, A.I.P.M.; Rijken, P.J.; De Smet, C.H. Checks and balances in membrane phospholipid class and acyl chain homeostasis, the yeast perspective. *Progress in Lipid Research* **2013**, *52*, 374-394.

91. Lager, I.; Yilmaz, J.L.; Zhou, X.-R.; Jasieniecka, K.; Kazachkov, M.; Wang, P.; Zou, J.; Weselake, R.; Smith, M.A.; Bayon, S., et al. Plant Acyl-CoA:Lysophosphatidylcholine Acyltransferases (LPCATs) Have Different Specificities in Their Forward and Reverse Reactions. *Journal of Biological Chemistry* **2013**, *288*, 36902-36914.

92. Blasi, J.; Chapman, E.R.; Link, E.; Binz, T.; Yamasaki, S.; De Camilli, P.; Sudhof, T.C.; Niemann, H.; Jahn, R. Botulinum neurotoxin A selectively cleaves the synaptic protein SNAP-25. *Nature* **1993**, *365*, 160-163.

93. Marsal, J.; Ruiz-Montasell, B.; Blasi, J.; Moreira, J.E.; Contreras, D.; Sugimori, M.; Llinás, R. Block of transmitter release by botulinum C1 action on syntaxin at the squid giant synapse. *Proceedings of the National Academy of Sciences of the United States of America* **1997**, *94*, 14871-14876.

94. Hayashi, T.; McMahon, H.; Yamasaki, S.; Binz, T.; Hata, Y.; Sudhof, T.C.; Niemann, H. Synaptic vesicle membrane fusion complex: action of clostridial neurotoxins on assembly. *Embo j* **1994**, *13*, 5051-5061.

95. Teng, F.Y.H.; Wang, Y.; Tang, B.L. The syntaxins. *Genome Biology* **2001**, *2*, reviews3012.3011.

96. Bowen, M.; Brunger, A.T. Conformation of the synaptobrevin transmembrane domain. *Proc Natl Acad Sci U S A* **2006**, *103*, 8378-8383.

97. Gonzalo, S.; Linder, M.E. SNAP-25 palmitoylation and plasma membrane targeting require a functional secretory pathway. *Molecular biology of the cell* **1998**, *9*, 585-597.

98. Sollner, T.; Bennett, M.K.; Whiteheart, S.W.; Scheller, R.H.; Rothman, J.E. A protein assembly-disassembly pathway in vitro that may correspond to sequential steps of synaptic vesicle docking, activation, and fusion. *Cell* **1993**, *75*, 409-418.

99. Parsons, T.D.; Coorssen, J.R.; Horstmann, H.; Almers, W. Docked granules, the exocytic burst, and the need for ATP hydrolysis in endocrine cells. *Neuron* **1995**, *15*, 1085-1096.

100. Berglund, E.; Berglund, D.; Akcakaya, P.; Ghaderi, M.; Daré, E.; Berggren, P.-O.; Köhler, M.; Aspinwall, C.A.; Lui, W.-O.; Zedenius, J., et al. Evidence for Ca2+-regulated ATP release in gastrointestinal stromal tumors. *Experimental cell research* **2013**, *319*, 1229-1238.

101. Fasshauer, D.; Otto, H.; Eliason, W.K.; Jahn, R.; Brunger, A.T. Structural changes are associated with soluble N-ethylmaleimide-sensitive fusion protein attachment protein receptor complex formation. *The Journal of biological chemistry* **1997**, *272*, 28036-28041.

102. Melia, T.J.; Weber, T.; McNew, J.A.; Fisher, L.E.; Johnston, R.J.; Parlati, F.; Mahal, L.K.; Sollner, T.H.; Rothman, J.E. Regulation of membrane fusion by the membrane-proximal coil of the t-SNARE during zippering of SNAREpins. *J Cell Biol* **2002**, *158*, 929-940.

103. Coorssen, J.R.; Blank, P.S.; Albertorio, F.; Bezrukov, L.; Kolosova, I.; Backlund, P.S., Jr.; Zimmerberg, J. Quantitative femto- to attomole immunodetection of regulated secretory vesicle proteins critical to exocytosis. *Analytical biochemistry* **2002**, *307*, 54-62.

104. Ungermann, C.; Sato, K.; Wickner, W. Defining the functions of trans-SNARE pairs. *Nature* **1998**, *396*, 543-548.

105. Szule, J.A.; Jarvis, S.E.; Hibbert, J.E.; Spafford, J.D.; Braun, J.E.A.; Zamponi, G.W.; Wessel, G.M.; Coorssen, J.R. Calcium-triggered Membrane Fusion Proceeds Independently of Specific Presynaptic Proteins. *Journal of Biological Chemistry* **2003**, *278*, 24251-24254.

106. Ray, P.; Berman, J.D.; Middleton, W.; Brendle, J. Botulinum toxin inhibits arachidonic acid release associated with acetylcholine release from PC12 cells. *The Journal of biological chemistry* **1993**, *268*, 11057-11064.

107. Ray, P.; Ishida, H.; Millard, C.B.; Petrali, J.P.; Ray, R. Phospholipaise A2 and arachidonic acid-mediated mechanism of neuroexocytosis: a possible target of botidinum neurotoxin A other then SNAP-25. *Journal of Applied Toxicology* **1999**, *19*, S27-S28.

108. Matak, I.; Lackovic, Z. Botulinum neurotoxin type A: Actions beyond SNAP-25? *Toxicology* **2015**, *335*, 79-84.

109. Rickman, C.; Davletov, B. Arachidonic acid allows SNARE complex formation in the presence of Munc18. *Chemistry & biology* **2005**, *12*, 545-553.

110. Latham, C.F.; Osborne, S.L.; Cryle, M.J.; Meunier, F.A. Arachidonic acid potentiates exocytosis and allows neuronal SNARE complex to interact with Munc18a. *Journal of neurochemistry* **2007**, *100*, 1543-1554.

111. García-Martínez, V.; Villanueva, J.; Torregrosa-Hetland, C.J.; Bittman, R.; Higdon, A.; Darley-Usmar, V.M.; Davletov, B.; Gutiérrez, L.M. Lipid Metabolites Enhance Secretion Acting on SNARE Microdomains and Altering the Extent and Kinetics of Single Release Events in Bovine Adrenal Chromaffin Cells. *PLOS ONE* **2013**, *8*, e75845.

112. Dabral, D.; Coorssen, J.R. Arachidonic acid and lysophosphatidylcholine inhibit multiple late steps of regulated exocytosis. *Biochemical and Biophysical Research Communications* **2019**, https://doi.org/10.1016/j.bbrc.2019.05.106.

113. Darios, F.; Davletov, B. Omega-3 and omega-6 fatty acids stimulate cell membrane expansion by acting on syntaxin 3. *Nature* **2006**, *440*, 813-817.

114. Dulubova, I.; Sugita, S.; Hill, S.; Hosaka, M.; Fernandez, I.; Sudhof, T.C.; Rizo, J. A conformational switch in syntaxin during exocytosis: role of munc18. *The EMBO journal* **1999**, *18*, 4372-4382.

115. Narayana, Vinod K.; Tomatis, V.M.; Wang, T.; Kvaskoff, D.; Meunier, Frederic A. Profiling of Free Fatty Acids Using Stable Isotope Tagging Uncovers a Role for Saturated Fatty Acids in Neuroexocytosis. *Chemistry & biology* **2015**, *22*, 1552-1561.

The International Journal of Biochemistry & Cell Biology 85 (2017) 1–5

Contents lists available at ScienceDirect

The International Journal of Biochemistry & Cell Biology

journal homepage: www.elsevier.com/locate/biocel

Molecules in focus

Phospholipase A_2: Potential roles in native membrane fusion

Deepti Dabral[a], Jens R. Coorssen[b,*]

[a] Molecular Physiology, and Molecular Medicine Research Group, School of Medicine, Western Sydney University, Campbelltown Campus, Penrith, NSW 2751, Australia
[b] Faculty of Graduate Studies and the Departments of Health Sciences and Biological Sciences, Brock University,St. Catharines, ON L2S 3A1, Canada

ARTICLE INFO

Article history:
Received 9 October 2016
Received in revised form
29 December 2016
Accepted 22 January 2017
Available online 25 January 2017

Keywords:
Membrane fusion
Phospholipase A_2
Lyso-phosphatidylcholine
Arachidonic acid

ABSTRACT

Membrane fusion is a fundamental molecular mechanism by which two apposed membrane bilayers coalesce in rapid, transient steps that enable the successive merging of the outer and inner leaflets allowing lipid intermixing and subsequent mixing of the two previously separate compartments. The actual membrane merger mechanism – fusion, by definition – is conceptualized to be protein- or lipid-centric. According to the widely vetted stalk-pore hypothesis, membrane fusion proceeds via high curvature lipid intermediates. By cleaving membrane phospholipids at the sn-2 position, Phospholipase A_2 generates metabolites that exert spontaneous curvature stress (both negative and positive) on the membrane, thus influencing local membrane bending by altering the packing and conformation of lipids and proteins, respectively. Such changes could potentially modulate priming and attachment/docking steps that precede fusion, as well as the membrane merger steps *per se*.

1. Native membrane organization

The basic framework of native membranes is best described by the Fluid Mosaic Model: lipidic constituents of the membrane form bilayers in which polar head groups point outward and the acyl tails face each other to minimize contact with the aqueous medium (Singer and Nicolson, 1972). Membrane proteins associate with the hydrophilic polar head groups (peripheral proteins) and/or with the hydrophobic acyl-glycerol regions (integral proteins). The proteins and lipids in the membrane are in constant rotational and lateral motion, and lipids also move between the monolayers (i.e. *trans*-bilayer) via flip-, flop- and scramblases, contributing to the lipid asymmetry in the membrane leaflets (Contreras et al., 2010). Updates to the model include the presence of transient non-lamellar lipid phases, lipid rafts and inconsistent membrane thickness, and extreme protein overcrowding (Engelman, 2005). Nonetheless, cholesterol, sphingomyelin, phosphatidylcholine (PC), phosphatidylinositol (PI), phosphatidylethanolamine (PE), phosphatidylserine (PS), plasmalogen and phosphatidic acid (PA) are the core structural components of the membrane. PE, PS, and PI dominate in the cytoplasmic leaflet, whereas PC and cholesterol are relatively equally distributed between leaflets.

Lipids have intrinsic curvatures or conformations depending on the relative size of their polar head group to the acyl-glycerol region. The packing of similar lipids in the membrane thus exerts spontaneous local curvature stress (negative or positive) that influences local membrane bending; for example, lyso-phosphatidylcholine (LPC) with a large polar head group and proportionally 'slimmer' acyl-glycerol region, is defined as having positive spontaneous curvature (Fuller and Rand, 2001). Therefore, when introduced into one monolayer, LPC tends to curve the monolayer in the direction of the polar head groups. Conversely, sterols such as cholesterol, and free fatty acid (FFA) species such as arachidonic acid (ARA), have a small head group and proportionally larger hydrocarbon region; this is defined as negative spontaneous curvature, as the presence of such species curves the monolayer in the direction of the hydrocarbon chains. Membrane bending is further complicated by acyl chain length and degree of unsaturation. For instance, induction of the high curvature inverted hexagonal (HII) phase by diacylglycerol depends on the degree of unsaturation of the surrounding PC (Szule et al., 2002) or upon the presence of cholesterol (Coorssen and Rand, 1990). In order to understand potential effects on native membranes, it is thus critical to note that lipid assemblies can adopt a number of phases in excess aqueous medium in vitro (Fig. 1). These include (i) Lamellar (L) in which lipids (e.g. phospho- and glycolipids) adopt a bilayer con-

Abbreviation: ARA, arachidonic acid; DAG, diacylglycerol; FFA, free fatty acid; HD, hemifusion diaphragm; HII, inverted hexagonal; IM, inverted micellar; L, Lamellar; LPC, LPS, LPE, lysophosphatidyl-choline, -serine, - ethanolamine; PC, PS, PE, phosphatidyl - choline, - serine, - ethanolamine; PA, phosphatidic acid; PUFA, polyunsaturated free fatty acid; $[Ca^{2+}]i$, intracellular calcium concentration.

* Corresponding author.
E-mail address: jcoorssen@brocku.ca (J.R. Coorssen).

http://dx.doi.org/10.1016/j.biocel.2017.01.011
1357-2725/

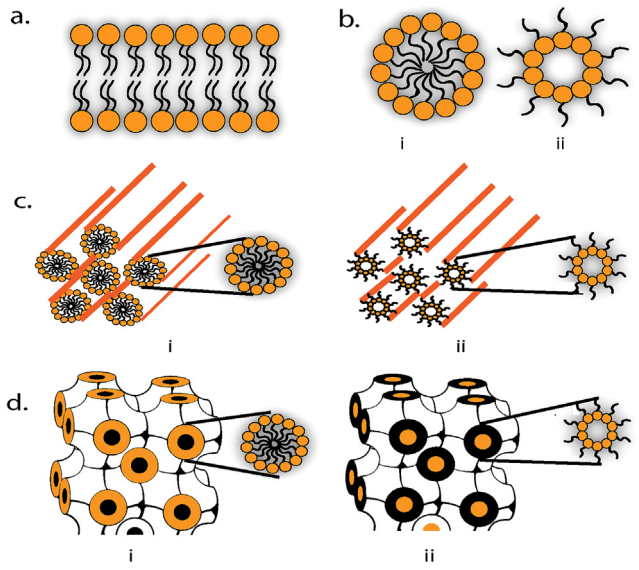

Fig. 1. Lipid polymorphism: a. Lamellar (phospholipids and glycolipids); b. (i) Micellar and (ii) inverted micellar (LPL and gangliosides); c. (i) Hexagonal and (ii) inverted hexagonal (PE and CL); d. (i) Cubic and (ii) inverted cubic (MAG) phases. (Adapted from reference (Jouhet, 2013)).

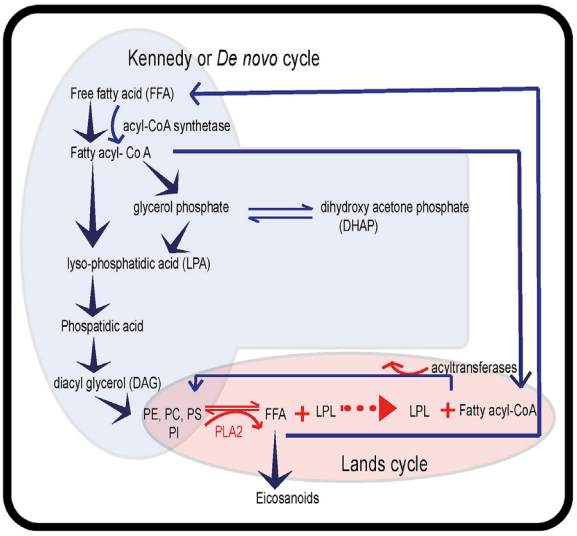

Fig. 2. Membrane remodeling via Kennedy and Lands cycles: In the Kennedy pathway, FFA is progressively converted to finally yield PE, PC, PS, and PI. In contrast, in Lands cycle, existing PE, PC, PS, and PI are metabolized by PLA_2, resulting in the formation of LPL and FFA. The released FFA is converted either to eicosanoids or into fatty acyl-CoA; the LPL is acylated by acyltransferases using fatty acyl-CoA. (Adapted from (Balsinde et al., 1995; Kennedy and Weiss, 1956; Lands et al., 1982)).

figuration; (ii) Micellar (M) in which lipids (e.g. lyso-phospholipids (LPL) and gangliosides) form spherical droplets with polar head groups facing outward and non-polar tails toward the interior; (iii) Inverted micellar (IM) in which lipids (e.g. PE) align to form inverted spherical droplets in which polar head groups face the interior and non-polar head groups face outward; (iv) Hexagonal or inverted hexagonal (HI or HII) in which lipids (e.g. PE and cardiolipin (CL)) forming M or IM phases arrange themselves in long tubular aggregates under certain temperature, pH, or ionic conditions; and (v) Cubic or reverse cubic (QI or QII), in which lipids adopt an even more complex arrangement (e.g. monoacylglycerol (MAG) can form a cubic phase which is an intermediate between HII and L phases). The significance of lipid phases in biological membrane is discussed elsewhere (reviewed in Jouhet, 2013); in context of the fusion mechanism, a transient non-lamellar (i.e. high curvature) hemifusion intermediate is one of the lipidic rearrangements said to underlie membrane fusion (Chernomordik et al., 1995).

2. PLA_2 and its role in membrane lipid homeostasis

The dynamic equilibrium of membrane lipid constituents is strongly regulated by the ratio of 'lamellar' to 'non-lamellar' lipids. Such control is enabled by lipid modifying enzymes such as Phospholipase A_2 (PLA_2) that hydrolyses membrane phospholipids at the sn-2 position producing LPL (often LPC) which are preferentially retained in the membrane, and a polyunsaturated free fatty acid (PUFA) – often Arachidonic acid (ARA; 20:4n-6) – that is somewhat more soluble and mobile with flipping efficiency of $t(1/2) < 1$ s; Hamilton, 1998), that can incorporate back into the phospholipids via acyl chain remodelling or Lands cycle (Balsinde et al., 1995; Lands et al., 1982). PLA_2 constitute a diverse enzyme family which is divided into groups based on sequence homology, sub-cellular localization, and calcium requirements. Broadly, these include (i) Ca^{2+}-dependent secretory forms ($sPLA_2$); (ii) Ca^{2+}-dependent cytoplasmic variants ($cPLA_2$); and (iii) Ca^{2+}-independent cytoplasmic types ($iPLA_2$).

At steady state, constituent molecular species in the membrane are regulated by interactions between *de novo* biosynthesis – Kennedy pathway (Kennedy and Weiss, 1956) – and Lands cycle, which is mediated by phospholipases and acyltransferases (i.e. transacylases) (Fig. 2). In the Kennedy pathway, free fatty acid (FFA) is converted into fatty acyl-CoA and then to glycerol phosphate or dihydroxyacetone phosphate (DHAP), resulting in the formation of PA or lysoPA. The PA is in turn converted to PI or to diacylglycerol (DAG), the latter of which is ultimately converted to PC, PE or PS. In Lands cycle, such existing phospholipids are hydrolysed to lyso-PC, −PE and −PS by the action of $iPLA_2$, releasing FFA. The liberated FFA is rapidly converted to acyl-CoA and finally incorporate back to the membrane via the Lands or Kennedy cycles. The incorporation of ARA into different cellular lipids, including signalling molecules (e.g. eicosanoids) depends upon their concentration; at nanomolar levels of free ARA, incorporation occurs almost exclusively into membrane phospholipids, while at micromolar levels, abundant incorporation occurs via the *de novo* pathway, ultimately leading to accumulation of ARA in triacylglycerol (TAG) (Balsinde and Dennis, 1996). TAG lacks a polar head group and instead carries three acyl chains that contribute to its intrinsic negative curvature.

3. The membrane fusion mechanism: Hypotheses

The prevailing protein-centric model of membrane fusion is based on the SNARE complex – an assembly of syntaxin, SNAP 25 (synaptosomal-associated protein, 25 kDa), and synaptobrevin/VAMP (vesicle associated membrane protein). All SNARE proteins contain a defining heptad repeat motif of hydrophobic residues. VAMP and syntaxin contain one SNARE motif connected to the C-terminal single *trans*-membrane domain (TMD) by a short linker region whereas SNAP-25 contains two SNARE motifs and is anchored to the membrane via palmitoylation. The *cis* complex involves proteins on the same membrane whereas *trans* SNARE complexes form between membranes (i.e. syntaxin and SNAP25 in one bilayer and VAMP in the apposed bilayer), holding the two distinct membranes together. It is speculated that inter-membrane 'zippering' of SNARE motifs, from N- toward C-termini, provides the necessary energy to facilitate membrane contact and fusion; that is, the mechanical force generated is postulated to be sufficient to overcome the hydration barrier and initiate formation of the fusion pore (Jackson, 2010; Min et al., 2013). Further, it has also been proposed that the rim of the fusion pore is proteinaceous,

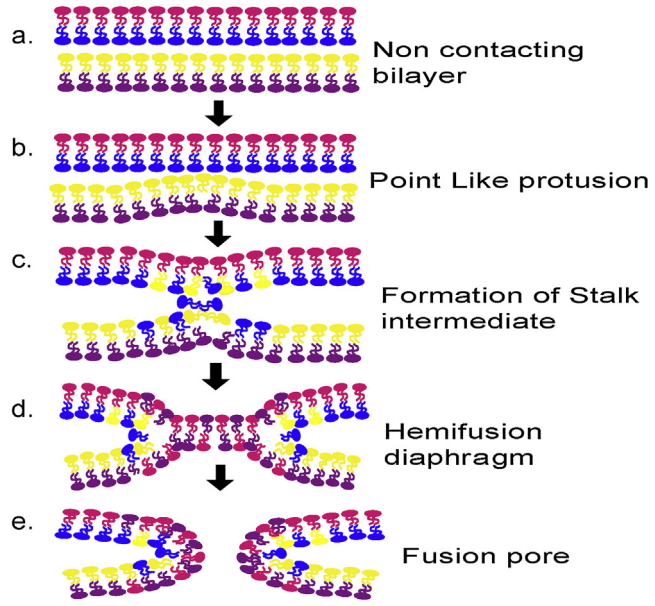

Fig. 3. Stalk-pore hypothesis: membrane fusion proceeds from point of contact through to opening of a fusion pore via high curvature intermediates. (Adapted from references (Churchward Matthew and Coorssen Jens, 2009)).

formed by the oligomerization of syntaxin TMDs (Han et al., 2004). However, there is evidence to indicate that neither the cytoplasmic domains of the SNAREs nor the TMD of syntaxin are directly involved in membrane fusion (Coorssen et al., 1998; Szule et al., 2003; Zhou et al., 2013; Zick et al., 2014). More recent work also suggests that a single *trans* SNARE complex may be sufficient to dock membranes and promote *subsequent* fusion, obviating the notion of a proteinaceous channel-like fusion pore composed of SNARE TMD (Shi et al., 2012). Furthermore, physiological levels of SNAREs do not support vacuolar fusion in the absence of negative curvature lipids (Zick et al., 2014). Together, these studies strongly argue against the SNARE-centric model of fusion, but not necessarily of the critical steps preceding membrane merger. Indeed, we have previously suggested that the *trans* SNARE complex could be a late if not the last step of docking and priming, ensuring fast efficient fusion (i.e. membrane merger) upon arrival of an appropriate trigger (e.g. calcium) (Coorssen et al., 2003; Coorssen et al., 1998; Szule et al., 2003).

The lipidic fusion pore model, or stalk-pore hypothesis, postulates that membrane fusion proceeds through merging of the proximal monolayers of adherent bilayer membranes followed by merger of the distal monolayers (i.e. outer leaflets of fusing bilayers); (Chernomordik et al., 1995). The entire fusion process proceeds from point of contact, formation of stalk and hemi-fusion diaphragm (HD), fusion pore opening and expansion, to content release or mixing (depending on the nature of the merging targets) (Fig. 3). The energy required to merge membranes is influenced by the spontaneous curvature of the constituent lipids (Fuller and Rand, 2001). Local lipids having intrinsic negative curvature thus promote merger of proximal leaflets of the contacting bilayers, leading to the formation of the HD or a localized stalk; introduction of positive curvature lipids (in particular LPC) at the contact site blocks membrane merger (Chernomordik et al., 1995; Vogel et al., 1993). Under fusogenic conditions, following merger of the proximal leaflets, distal leaflets merge resulting in formation, opening and expansion of the fusion pore. The merging of the distal leaflets is promoted by local lipids having net positive curvature. Therefore, membrane fusion proceeds rapidly through transient high curvature lipid intermediates. However, lipids may also have critical modulatory roles. Some (anionic) lipids are deprotonated, having a negative charge under physiological conditions, and can bind di- and trivalent cations, particularly free calcium ions. PS, for instance, may locally bind calcium or could modulate Synaptotagmin – a putative calcium sensor (Lai et al., 2011; Rogasevskaia et al., 2012). PA, on the other hand seems to have a role in vesicle docking and/or priming (Rogasevskaia and Coorssen, 2015; Starr et al., 2016) . In contrast, cholesterol has both an intrinsic negative curvature and defines membrane microdomains; it can directly facilitate membrane merger by lowering the energy barrier in the proximal monolayer mixing (Churchward and Coorssen, 2009; Churchward et al., 2008; Churchward et al., 2005), and could also promote the efficiency of the fusion mechanism by maintaining other key components in a localized, functional state – the physiological fusion machine (Churchward et al., 2005; Rogasevskaia et al., 2012).

4. How PLA_2 could modulate or facilitate membrane fusion

Studies have suggested a role for PLA_2 in regulated exocytosis, and perhaps in membrane merger in neuroendocrine cells, as treatment with PLA_2 inhibitors resulted in blockade of ARA production and a parallel inhibition of triggered exocytosis (Ray et al., 1993). Furthermore, increased synaptic vesicle fusion occurs in presynaptic membranes that are pre-treated with PLA_2 (Nishio et al., 1996). Conversely, there are also data suggesting separation of all major phospholipase activities from a direct effect on native membrane fusion (Coorssen, 1996).

Exogenous ARA increases catecholamine release from neurosecretory cells and has been shown to influence membrane fusion by enhancing vesicle docking (García-Martínez et al., 2013) perhaps by enhancing inter-membrane SNARE complex formation (Darios and Davletov, 2006; Johns et al., 2001; Latham et al., 2007). Munc18, a regulatory protein in the exocytotic pathway, is known to 'lock' syntaxin in the closed conformation (Yang et al., 2000); ARA interacts with the syntaxin/Munc18 complex, relieving syntaxin to engage in *trans*-SNARE complex formation (Connell et al., 2007; Rickman and Davletov, 2005). ARA has been suggested to directly interact with SNARE microdomains, limiting lateral motion of vesicles that are closer to the PM (Johns et al., 2001). In such lipid supplementation studies, prolonged cell incubations with exogenous ARA enhanced SNARE complex formation. Under these conditions, ARA (or indeed any exogenous lipid) could be rapidly metabolized, leading to accumulation of other Lands or Kennedy cycle intermediates depending on the rate limiting step(s) of the pathways; it is thus unclear whether ARA was the active lipid species in these studies. It would therefore be of interest to investigate the effect of PLA_2 derived endogenous ARA on SNARE complex formation and subsequent membrane fusion. Furthermore, since Phospholipase D (PLD) derived PA has a role in docking and priming (Rogasevskaia and Coorssen, 2015) and interactions between PLA_2 and PLD are also indicated (Wang et al., 1999) both phospholipases may have interacting roles in maintaining the docked, primed, fusion-ready state. It is also important to establish local concentrations of LPL and FFA species under conditions of both PLA_2 inhibition and stimulation, and to test for an increase or decrease, respectively, in exocytotic release.

The membrane concentration of LPC species required for ~50% inhibition of exocytotic fusion is ~1-2 mol% (Chernomordik et al., 1997). The resting concentration of arachidonic acid per cell is in the pico-to-nanomolar range; the release of even 1% of the total esterified pool of arachidonate could yield up to 50 μM local concentrations of FFA (Brash, 2001). Using the activity of native plasma membrane PLA_2 (human polymorphonuclear leukocytes; Victor et al., 1981) and the levels of PC and PE in both plasma and cortical secretory vesicle membranes (Kinsey et al., 1980; Churchward et al.,

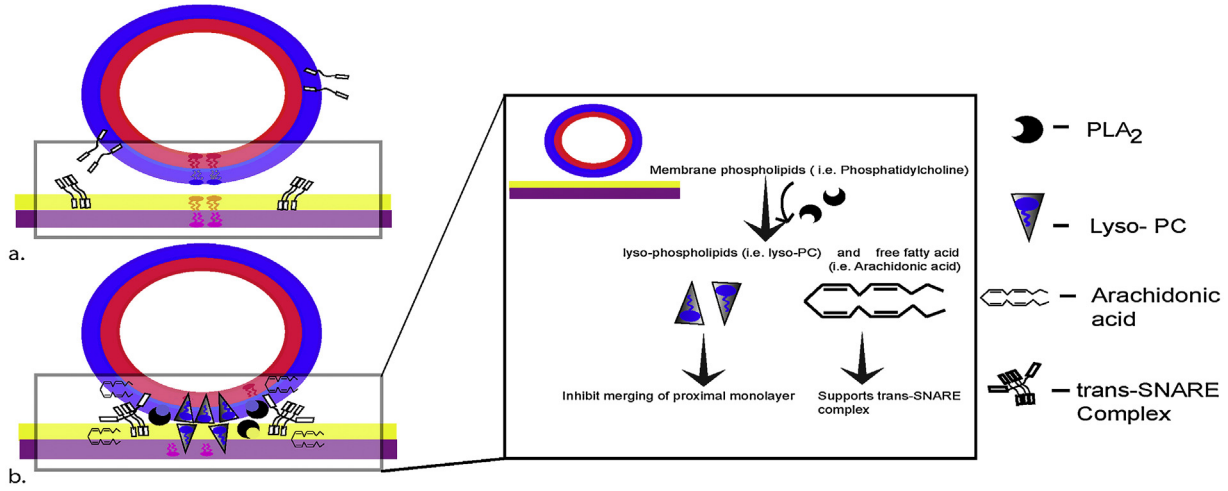

Fig. 4. a. Non-contacting membranes; b. membranes in close proximity. Working hypothesis: a fusion ready state is maintained by localized PLA_2 that produces LPL and ARA; LPL acts as a local 'fusion block' inhibiting the premature (i.e. pre-stimulus) merger of the proximal membranes while ARA supports the *trans* SNARE complex(es) in maintaining the fully primed, fusion-ready state.

2008a), one can estimate that the levels of LPC and LPE produced in the PM would be ≤0.162 and ≤0.61 nmoles/h/100 μg protein, respectively, and ≤0.14 and ≤0.04 mol%/h, respectively, in the vesicle membrane. It is also noteworthy that further metabolism of these LPL is unlikely to be uniform and this will also have a substantial impact on their lifetimes, as will the extent to which the PLA_2 activities may be localized at the docking/fusion sites. Furthermore, the characteristic flip-flop rate of LPCs is estimated in hours (Chernomordik et al., 1997), thus further emphasizing the significance of PLA_2 localization activity at the inner monolayer of the PM and the outer monolayer of the vesicle membrane yields 'proximal' LPC that would block fusion.

Therefore, with reference to the Stalk-pore hypothesis as well as evidence suggesting a stimulatory effect of ARA on SNARE complex formation, we propose that localized PLA_2 produce LPL that act as a basal local fusion 'block' or 'brake' inhibiting the premature merging of the proximal membranes, and ARA (or an active downstream metabolite) supports the SNAREs in maintaining a docked, primed state (Fig. 4). This implicates PLA_2 species as critical components of the physiological fusion machine, and one or more of their metabolites as potentially critical to the physiological fusion mechanism.

5. Conclusion and perspective

The actual role of SNAREs in membrane fusion has been debated, although even in the most extreme interpretation of their functions, fusion must still involve lipid mixing to effect membrane merger. It is nonetheless evident that lipids and proteins play integral and integrated roles in docking, priming, and membrane fusion. Lipids facilitate membrane bending by virtue of their intrinsic spontaneous curvature, form microdomains enriched in priming and/or docking factors, and also constitute critical interaction/binding sites for important protein components. There may well also be other important, yet undiscovered lipid-protein interactions that play modulatory or direct roles in membrane fusion. Thus, as outlined in Sections 3 and 4, PLA_2 derived endogenous ARA together with the SNAREs could play an integral role in docking and priming, while the LPC produced in parallel would serve as a local fusion block until such time as an appropriate trigger initiates rapid membrane merger. Studies of PLA_2 in local lipid homeostasis and the potential functions of its metabolites in maintaining the fusion-ready state and modulating membrane merger are thus warranted, particularly with regard to understanding modified membrane interactions in disease states.

Acknowledgements

DD thanks the School of Medicine, Western Sydney University, for scholarship funding. JRC acknowledges support of the National Health and Medical Research Council (NHMRC) of Australia (APP1065328), the Molecular Medicine Research Group, WSU, School of Medicine, and previous support from the CIHR, NSERC, and AHFMR (Canada).

References

Balsinde, J., Dennis, E.A., 1996. Bromoenol lactone inhibits magnesium-dependent phosphatidate phosphohydrolase and blocks triacylglycerol biosynthesis in mouse P388D1 macrophages. J. Biol. Chem. 271 (50), 31937–31941.
Balsinde, J., Bianco, I.D., Ackermann, E.J., Conde-Frieboes, K., Dennis, E.A., 1995. Inhibition of calcium-independent phospholipase A2 prevents arachidonic acid incorporation and phospholipid remodeling in P388D1 macrophages. Proc. Natl. Acad. Sci. U. S. A. 92 (18), 8527–8531.
Brash, A.R., 2001. Arachidonic acid as a bioactive molecule. J. Clin. Invest. 107 (11), 1339–1345.
Chernomordik, L., Chanturiya, A., Green, J., Zimmerberg, J., 1995. The hemifusion intermediate and its conversion to complete fusion: regulation by membrane composition. Biophys. J. 69 (3), 922–929.
Chernomordik, L.V., Leikina, E., Frolov, V., Bronk, P., Zimmerberg, J., 1997. An early stage of membrane fusion mediated by the low pH conformation of influenza hemagglutinin depends upon membrane lipids. J. Cell Biol. 136 (1), 81–93.
Churchward Matthew, A., Coorssen Jens, R., 2009. Cholesterol, regulated exocytosis and the physiological fusion machine. Biochem. J 423 (1), 1–14.
Churchward, M.A., Rogasevskaia, T., Höfgen, J., Bau, J., Coorssen, J.R., 2005. Cholesterol facilitates the native mechanism of Ca^{2+} triggered membrane fusion. J. Cell Sci. 118 (20), 4833–4848.
Churchward, M.A., Rogasevskaia, T., Brandman, D.M., Khosravani, H., Nava, P., Atkinson, J.K., Coorssen, J.R., 2008. Specific lipids supply critical negative spontaneous Curvature—an essential component of native Ca2+-triggered membrane fusion. Biophys. J. 94 (10), 3976–3986.
Connell, E., Darios, F., Broersen, K., Gatsby, N., Peak-Chew, S.Y., Rickman, C., Davletov, B., 2007. Mechanism of arachidonic acid action on syntaxin-Munc18. EMBO Rep. 8 (4), 414–419.
Contreras, F.X., Sánchez-Magraner, L., Alonso, A., Goñi, F.M., 2010. Transbilayer (flip-flop) lipid motion and lipid scrambling in membranes. FEBS Lett. 584 (9), 1779–1786.
Coorssen, J.R., Rand, R.P., 1990. Effects of cholesterol on the structural transitions induced by diacylglycerol in phosphatidylcholine and phosphatidylethanolamine bilayer systems. Biochem. Cell Biol. 68 (1), 65–69.
Coorssen, J.R., Blank, P.S., Tahara, M., Zimmerberg, J., 1998. Biochemical and functional studies of cortical vesicle fusion: the SNARE complex and Ca2+ sensitivity. J. Cell Biol. 143 (7), 1845–1857.

Coorssen, J.R., Blank, P.S., Albertorio, F., Bezrukov, L., Kolosova, I., Chen, X., Backlund, P.S., Zimmerberg, J., 2003. Regulated secretion: SNARE density, vesicle fusion and calcium dependence. J. Cell Sci. 116 (10), 2087–2097.
Coorssen, J.R., 1996. Phospholipase activation and secretion: evidence that PLA2, PLC, and PLD are not essential to exocytosis. Am. J. Physiol. – Cell Physiol. 270 (4), C1153–C1163.
Darios, F., Davletov, B., 2006. Omega-3 and omega-6 fatty acids stimulate cell membrane expansion by acting on syntaxin 3. Nature 440 (7085), 813–817.
Engelman, D.M., 2005. Membranes are more mosaic than fluid. Nature 438 (7068), 578–580.
Fuller, N., Rand, R.P., 2001. The influence of lysolipids on the spontaneous curvature and bending elasticity of phospholipid membranes. Biophys. J. 81 (1), 243–254.
García-Martínez, V., Villanueva, J., Torregrosa-Hetland, C.J., Bittman, R., Higdon, A., Darley-Usmar, V.M., Davletov, B., Gutiérrez, L.M., 2013. Lipid metabolites enhance secretion acting on SNARE microdomains and altering the extent and kinetics of single release events in bovine adrenal chromaffin cells. PLoS One 8 (9), e75845.
Hamilton, J.A., 1998. Fatty acid transport: difficult or easy? J. Lipid Res. 39 (3), 467–481.
Han, X., Wang, C.T., Bai, J., Chapman, E.R., Jackson, M.B., 2004. Transmembrane segments of syntaxin line the fusion pore of Ca2+-triggered exocytosis. Science 304 (5668), 289–292.
Jackson, M.B., 2010. SNARE complex zipping as a driving force in the dilation of proteinaceous fusion pores. J. Membr. Biol. 235 (2), 89–100.
Johns, L.M., Levitan, E.S., Shelden, E.A., Holz, R.W., Axelrod, D., 2001. Restriction of secretory granule motion near the plasma membrane of chromaffin cells. J. Cell Biol. 153 (1), 177–190.
Jouhet, J., 2013. Importance of the hexagonal lipid phase in biological membrane organization. Front. Plant Sci. 4, 494.
Kennedy, E.P., Weiss, S.B., 1956. The function of cytidine coenzymes in the biosynthesis of phospholipids. J. Biol. Chem. 222 (1), 193–214.
Kinsey, W.H., Decker, G.L., Lennarz, W.J., 1980. Isolation and partial characterization of the plasma membrane of the sea urchin egg. J. Cell Biol. 87 (1), 248–254.
Lai, A.L., Tamm, L.K., Ellena, J.F., Cafiso, D.S., 2011. Synaptotagmin 1 modulates lipid acyl chain order in lipid bilayers by demixing phosphatidylserine. J. Biol. Chem. 286 (28), 25291–25300.
Lands, W.E., Inoue, M., Sugiura, Y., Okuyama, H., 1982. Selective incorporation of polyunsaturated fatty acids into phosphatidylcholine by rat liver microsomes. J. Biol. Chem. 257 (24), 14968–14972.
Latham, C.F., Osborne, S.L., Cryle, M.J., Meunier, F.A., 2007. Arachidonic acid potentiates exocytosis and allows neuronal SNARE complex to interact with Munc18a. J. Neurochem. 100 (6), 1543–1554.
Min, D., Kim, K., Hyeon, C., Cho, Y.H., Shin, Y.K., Yoon, T.Y., 2013. Mechanical unzipping and rezipping of a single SNARE complex reveals hysteresis as a force-generating mechanism. Nat. Commun. 4, 1705.
Nishio, H., Takeuchi, T., Hata, F., Yagasaki, O., 1996. Ca(2+)-independent fusion of synaptic vesicles with phospholipase A2-treated presynaptic membranes in vitro. Biochem. J 318 (Pt 3), 981–987.
Ray, P., Berman, J.D., Middleton, W., Brendle, J., 1993. Botulinum toxin inhibits arachidonic acid release associated with acetylcholine release from PC12 cells. J. Biol. Chem. 268 (15), 11057–11064.
Rickman, C., Davletov, B., 2005. Arachidonic acid allows SNARE complex formation in the presence of Munc18. Chem. Biol. 12 (5), 545–553.
Rogasevskaia, T.P., Coorssen, J.R., 2015. The role of phospholipase D in regulated exocytosis. J. Biol. Chem. 290, 28683–28696.
Rogasevskaia, T.P., Churchward, M.A., Coorssen, J.R., 2012. Anionic lipids in Ca(2+)-triggered fusion. Cell Calcium 52 (3–4), 259–269.
Shi, L., Shen, Q.-T., Kiel, A., Wang, J., Wang, H.-W., Melia, T.J., Rothman, J.E., Pincet, F., 2012. SNARE proteins: one to fuse and three to keep the nascent fusion pore open. Science 335 (6074), 1355–1359.
Singer, S.J., Nicolson, G.L., 1972. The fluid mosaic model of the structure of cell membranes. Science 175 (4023), 720–731.
Starr, M.L., Hurst, L.R., Fratti, R.A., 2016. Phosphatidic acid sequesters sec18p from cis-SNARE complexes to inhibit priming. Traffic 17 (10), 1091–1109.
Szule, J.A., Fuller, N.L., Rand, R.P., 2002. The effects of acyl chain length and saturation of diacylglycerols and phosphatidylcholines on membrane monolayer curvature. Biophys. J. 83 (2), 977–984.
Szule, J.A., Jarvis, S.E., Hibbert, J.E., Spafford, J.D., Braun, J.E.A., Zamponi, G.W., Wessel, G.M., Coorssen, J.R., 2003. Calcium-triggered membrane fusion proceeds independently of specific presynaptic proteins. J. Biol. Chem. 278 (27), 24251–24254.
Victor, M., Weiss, J., Klempner, M.S., Elsbach, P., 1981. Phospholipase A2 activity in the plasma membrane of human polymorphonuclear leukocytes. FEBS Lett. 136 (2), 298–300.
Vogel, S.S., Leikina, E.A., Chernomordik, L.V., 1993. Lysophosphatidylcholine reversibly arrests exocytosis and viral fusion at a stage between triggering and membrane merger. J. Biol. Chem. 268 (34), 25764–25768.
Wang, Z., Clarke, C.R., Clinkenbeard, K.D., 1999. Role of phospholipase D in Pasteurella haemolytica leukotoxin-induced increase in phospholipase A2 activity in bovine neutrophils. Infect. Immun. 67 (8), 3768–3772.
Yang, B., Steegmaier, M., Gonzalez, L.C., Scheller, R.H., 2000. Nsec1 binds a closed conformation of syntaxin1a. J. Cell Biol. 148 (2), 247–252.
Zhou, P., Bacaj, T., Yang, X., Pang, Z.P., Sudhof, T.C., 2013. Lipid-anchored SNAREs lacking transmembrane regions fully support membrane fusion during neurotransmitter release. Neuron 80 (2), 470–483.
Zick, M., Stroupe, C., Orr, A., Douville, D., Wickner, W.T., 2014. Membranes linked by trans-SNARE complexes require lipids prone to non-bilayer structure for progression to fusion. eLife 3, e01879.

CHAPTER – 2

Combined Targeted Omic and Functional Assays Identify Phospholipases A_2 that Regulate Docking/Priming in Calcium-Triggered Exocytosis

(published in cells, 2019)

https://doi.org/10.3390/cells8040303

cells

MDPI

Article

Combined Targeted Omic and Functional Assays Identify Phospholipases A_2 that Regulate Docking/Priming in Calcium-Triggered Exocytosis

Deepti Dabral [1] and Jens R Coorssen [2,*]

[1] Molecular Physiology and Molecular Medicine Research Group, School of Medicine, Western Sydney University, Campbelltown Campus, NSW 2560, Australia; d.dabral@uws.edu.au
[2] Department of Health Sciences, Faculty of Applied Health Sciences and Department of Biological Sciences, Faculty of Mathematics & Science, Brock University, St. Catharines, ON L2S 3A1, Canada
* Correspondence: jcoorssen@brocku.ca

Received: 24 February 2019; Accepted: 28 March 2019; Published: 2 April 2019

Abstract: The fundamental molecular mechanism underlying the membrane merger steps of regulated exocytosis is highly conserved across cell types. Although involvement of Phospholipase A_2 (PLA_2) in regulated exocytosis has long been suggested, its function or that of its metabolites—a lyso-phospholipid and a free fatty acid—remain somewhat speculative. Here, using a combined bioinformatics and top-down discovery proteomics approach, coupled with lipidomic analyses, PLA_2 were found to be associated with release-ready cortical secretory vesicles (CV) that possess the minimal molecular machinery for docking, Ca^{2+} sensing and membrane fusion. Tightly coupling the molecular analyses with well-established quantitative fusion assays, we show for the first time that inhibition of a CV surface calcium independent intracellular PLA_2 and a luminal secretory PLA_2 significantly reduce docking/priming in the late steps of regulated exocytosis, indicating key regulatory roles in the critical step(s) preceding membrane merger.

Keywords: membrane merger; secretory vesicles; lysolipids; free fatty acids; regulated secretion; fusion

1. Introduction

Fusion is a ubiquitous fundamental cellular process enabling merger of biological membranes; this includes the defining release step of exocytosis following merger of secretory vesicles with the plasma membrane (PM). Studies over the last three-four decades have suggested a role of Phospholipase A_2 (PLA_2) in regulated exocytosis, generally arising from correlations of arachidonic acid (ARA) levels and vesicle content release [1–8]. In a cell free system, fusion of secretory vesicles with target membranes increased in the presence of PLA_2 suggesting that the enzyme or its metabolites affected membrane merger or the steps immediately preceding it [5,6,9]. Furthermore, addition of exogenous PLA_2 metabolites inhibits hemi-fusion formation or transition from hemi-fusion to pore opening depending upon their site of incorporation [10–12]. That PLA_2 species have been identified in secretory vesicles isolated from neutrophils [13], chromaffin cells [14], insulin secreting cells [15,16] and mast cells [17,18] highlights that these are conserved protein components of secretory vesicles. Early studies also identified endogenous PLA_2 activity in purified synaptic vesicles (SV) [5,6,19,20]. While some proteomic analyses have failed to identify SV associated PLA_2 [21,22], suggesting very low abundance and/or activity, at least one study identified iPLA2γ in synaptosomes [23]. Indeed, when synaptosomes were fractionated into free and docked SV pools prior to proteomic analysis, a patatin-like phospholipase domain containing 8 (Gene ID 157819923; also known as $iPLA_2\gamma$) was found to be more abundant in the docked SV pool [24].

Based on subcellular localization and Ca^{2+} requirement, PLA_2 isozymes are broadly classified as (i) Ca^{2+}-dependent secretory or $sPLA_2$, (ii) Ca^{2+}-independent cytoplasmic or membrane bound $iPLA_2$ and (iii) Ca^{2+}-dependent cytoplasmic or $cPLA_2$. Nevertheless, all PLA_2 cleave membrane phospholipids at the sn-2 position, producing a lyso-phospholipid (often lyso-phosphatidylcholine; LPC) which is preferentially retained in the membrane and a diffusible free fatty acid (FFA; often arachidonic acid (ARA; 20:4n-6)) that can incorporate back into the membrane via Lands cycle intermediates or is further metabolized to yield eicosanoids. $sPLA_2$ are generally 12–19 kDa proteins containing 5–7 conserved disulphide bonds and are characterized by an active site histidine in a DXCCXXHD consensus sequence and a conserved Ca^{2+}-binding loop with a XCGXGG consensus sequence [25,26]. Once secreted, their Ca^{2+} requirement for catalysis is in the low millimolar (mM) range with no strict fatty acid selectivity, although mostly target phosphatidyl-ethanolamine, -glycerol, -inositol and -serine (PE, PG, PI and PS) [26,27]. Although these enzymes are generally thought to be active only when released into the extracellular space, the possibility of basal $sPLA_2$ activity in the vesicle lumen has been suggested [17,28,29]. In transfected CHO-K1 and HEK293 cells that lack regulated secretory vesicles, expressed $sPLA_2$ was localized to the golgi and related intracellular vesicles and released ARA, indicating basal activity [28]. Of note is that adequate concentrations of free calcium ($[Ca^{2+}]_{free}$) may be (transiently) present within regulated secretory vesicles to support luminal $sPLA_2$ activity under basal conditions [30–33]. In contrast, $iPLA_2$ are intracellular enzymes that do not require Ca^{2+} beyond basal cytosolic levels for activity, contain serine in the GXSXG active site and possess a nucleotide-binding (GXGXXG) consensus sequence. The mammalian forms include $iPLA_2\beta$, $iPLA_2\gamma$, $iPLA_2\delta$, $iPLA_2\varepsilon$, $iPLA_2\zeta$ and $iPLA_2\eta$ with molecular weights ranging from 27 to 146 kDa. A well-established function of $iPLA_2\beta$ is membrane phospholipid remodelling via Lands cycle to maintain membrane integrity [29,34,35]. $cPLA_2$ are cytosolic proteins of molecular weights ranging from 61-114 kDa and require micromolar $[Ca^{2+}]_{free}$ for association with membrane phospholipids via their N-terminal C2 domain [25,26]. These enzymes also carry serine at GXSXG, GXSGS or GXSXV lipase consensus sequences [36]. There are six mammalian $cPLA_2$ isoforms, $cPLA_2$-α, β, γ, δ, ε, ζ of which all except $cPLA_2\gamma$ have a N-terminal C2 domain [36,37].

At the genomic level, sea urchin and human remain closely related (both are deuterostomes) relative to invertebrates [38–40]. SNARE (soluble N-ethylmaleimide-sensitive factor attachment protein receptor) proteins are highly conserved across species, having been identified on exocytotic vesicles from yeast to man, including the release-ready cortical vesicles (CV) isolated from unfertilized sea urchin eggs [40–46]. Furthermore, as CV retain the minimal molecular machinery for docking, Ca^{2+} sensing and membrane fusion, they are a well-established model to study the late steps of Ca^{2+}-triggered exocytosis [42,43,45,47–54]. CV are easily isolated with high purity and yield, either endogenously docked on the PM (i.e., cell surface complexes; CSC) or free-floating [42,49,51,55]. On triggering with Ca^{2+}, isolated CV fuse with each other in a manner indistinguishable from CV-PM fusion [42,45,49,55]. Using these fusion-ready native vesicles, we first identified catalytically active endogenous PLA_2 isozymes using a combined bioinformatics and top-down discovery proteomics approach coupled with lipidomic analyses. We then asked whether these isozymes have a role in the late steps of Ca^{2+}-triggered exocytosis. The enzymatic activities were localized to the CV lumen and vesicle surface and tightly coupled functional and molecular analyses were carried out to assess these PLA_2 activities and their associated effects on fusion parameters. A modulatory role in priming and/or docking is indicated.

2. Materials and Methods

2.1. Materials

2.1.1. Assessment of PLA_2 Activities and Fusion Assays

Native sea urchins (Heliocedaris tuberculata) were maintained at 7–8 °C in the local aquatic facility. CSC and CV were isolated as previously described [38,41,42,45,51,52,55]. Bromoenol lactone (BEL)

and 3-(3-acetamide-1-benzyl-2-ethylindolyl-5-oxy) propane sulfonic acid (LY311727) were purchased from Sigma Aldrich (St. Louis, MO USA); 1,1,1,2,2-Pentafluoro-7-phenyl-3-heptanone (FKGK-11) was from Cayman Chemicals (Ann Arbor, MI, USA).

CSC membrane labelling was carried out using 1-oleoyl-2-{12-[(7-nitro-2-1,3-benzoxadiazol-4-yl) amino] dodecanoyl} -sn-glycero-3-phospho-choline/-ethanolamine (NBD-PC/PE). Quantification of the generated NBD-FFA and NBD-PA was done using 1-oleoyl-2-{12-[(7-nitro-2-1,3-benzoxadiazol-4-yl) amino Arachidonic acid 20:4 (NBD-ARA) and 1-oleoyl-2-{12-[(7-nitro-2-1,3-benzoxadiazol-4-yl) amino] dodecanoyl}-sn-glycero-3-phosphate (NBD-PA) as reference standards. ARA (20:4) was purchased from Matreya LLC (State college, PA, USA) while all other lipids were purchased from Avanti Polar Lipids (Alabaster, AL, USA). Quantitative lipid analyses were carried out using High Performance Thin Layer Chromatography (HPTLC) [49–51,56]. Silica G-60 plates were purchased from Merck Millipore Ltd. (Darmstadt, Germany). All HPTLC solvents were minimally of analytical grade. High grade Trypsin was from Promega Corp. (Madison, WI, USA). The selective PLA_2 substrate, PED6 (*N*-((6-(2,4-Dinitrophenyl) amino) hexanoyl)-2-(4,4-Difluoro-5,7-Dimethyl-4-Bora-3a,4a-Diaza-s-Indacene-3-Pentanoyl)-1-Hexadecanoyl-sn-Glycero-3-Phosphoethanolamine, Triethylammonium Salt) was from Invitrogen (Carlsbad, CA, USA).

2.1.2. Protein Fractionation, Gel Electrophoresis and Western Blotting

Amicon Ultra-4 centrifugal filters (3kDa cut-off) came from Merck Millipore. Constituents of the Protease inhibitor cocktail [41,57] were purchased from Sigma-Aldrich (St. Louis) and AMRESCO Inc. (Dallas, TX, USA). All electrophoresis grade chemicals used in two-dimensional gel electrophoresis (2DE) were purchased from AMRESCO Inc. 3-10NL IPG strips, tributyl phosphine and Polyvinylidene difluoride (PVDF) membrane (0.2 μM pore size) were from Bio-Rad (Hercules, CA, USA). Anti-human rabbit polyclonal $iPLA_2$ antibody (PA5-27945) and anti-human mouse monoclonal $sPLA_2$ antibody (ab-24498) were from Invitrogen and Abcam (Cambridge, UK), respectively. Blocking agents—non-fat dry milk powder and BSA—were from Devondale (Saputo Dairy, Australia) and Sigma Aldrich, respectively. HRP linked anti-mouse IgG (NA93IV) and anti-rabbit IgG (NA934VS) antibodies came from GE Healthcare (Buckinghamshire, UK). Lumunata Cresendo Western HRP substrate was purchased from Merck Millipore. The blots and gels were imaged using the Image Quant™ LAS 4000 Biomolecular Imager (GE Healthcare, Chicago, Il, USA).

2.2. Methods

2.2.1. Molecular Analysis to Detect CSC Associated PLA_2 Activities

PLA_2 activities in intact unlabelled CSC suspensions (0.5 mL, OD 0.56 ± 0.02, n = 3–14) were assessed by measuring changes in FFA following treatments with the indicated concentrations of BEL, LY311727 and FKGK-11; exploratory experiments (n = 1–2) with 40 μM BEL, 10 μM FKGK-11, 100 nM LY311727 and higher concentrations were first carried out. Only those concentrations that significantly reduced endogenous FFA relative to control were selected for further study. CSC were isolated according to established protocols [49–52] and suspended in baseline intracellular medium (BIM; 210 mM potassium glutamate, 500 mM glycine, 10 mM NaCl, 10 mM PIPES, 50 μM $CaCl_2$, 1 mM $MgCl_2$, 1 mM EGTA pH 6.7) supplemented with 2.5 mM ATP, 2 mM DTT and 1X protease inhibitors [41–43,45,51,52]. Stock solutions of inhibitors were prepared in dimethyl sulfoxide and were delivered to CSC suspensions at a final solvent concentration of <1% [48,51,52]. At the end of the incubation, CV suspensions were immediately placed on ice, diluted with 5–8 mL of ice-cold BIM and aliquoted for rapid isolation of total lipids and for immediate assay of CV-PM fusion [49–51].

In separate experiments, CSC were allowed to incorporate NBD-PC or -PE for 15 min prior to the 20 min inhibitor treatments. Briefly, CSC suspensions (7 mL, OD 0.56 ± 0.005, n = 3) were labelled with 5600 picomoles NBD-PC or -PE for 15 min followed by treatment with the indicated doses of inhibitors. At the end of the treatments, all aliquots were washed three times in ice-cold BIM (pH 6.7) to remove

unlabelled NBD substrate and inhibitors and immediately placed on ice prior to rapid isolation of total CSC lipids and membrane proteins (see Section 2.2.4).

2.2.2. Quantitative Lipid Analyses

Total CSC or CV lipids were extracted according to Bligh and Dyer with established modifications [50–52,56,58]; total CV membrane proteins were also isolated from parallel aliquots by lysing CV with ice-cold PIPES (see Section 2.2.4). The resulting organic phases (and also aqueous phases in scaled-up experiments) were recovered, dried under nitrogen and suspended in $CHCl_3$:CH_3OH (2:1; *v*/*v*) for loading onto pre-conditioned silica gel 60 HPTLC plates. Sample loading was with the CAMAG automatic TLC sampler. Pre-conditioning of the plates was as previously described [50–52,56]. Using the CAMAG AMD 2 multi-development unit, neutral- and phospho-lipids were resolved using optimized protocols [48,49,51,52,56]. Resolved lipids were visualized on-plate by charring homogenously wetted plates with 10% cupric sulphate in 8% aqueous phosphoric acid at 145 °C for 10 min [56]; imaging was at 460 nm/605 nm (Ex/Em) using the LAS 4000 Biomolecular Imager and was analysed using MultiGauge v3.0 (Fuji Photo Film Co., Ltd. Tokyo, Japan). Quantification of endogenous CV or CSC lipids, NBD-FFA and -PA, was via calibration curves of the appropriate standards, resolved by HPTLC, in parallel with the experimental samples. To resolve neutral and phospholipids, well-established protocols were used [56]; NBD-FFA and -PA generated from NBD-PC labelled CSC were resolved together after confirming that the standard neutral lipid protocol was satisfactory for resolving both these species. To measure fluorescent signal from NBD-labelled lipids, uncharred plates were imaged at 460 nm/575 nm (Ex/Em) using the same imager and analysis software.

2.2.3. Sequence Alignments

To identify regions of homology, a sequence alignment of the putative urchin $sPLA_2$ (W4XE93) and $iPLA_2$ (XP_011669048.1) relative to characterized human and mouse isoforms was carried out using MEGA version 7.0.21 (free software downloaded from https://www.megasoftware.net/home) [59,60] and the ClustalW algorithm with default settings. All protein sequences, except that of the predicted urchin $iPLA_2$, were downloaded from Uniprot (February 2019). Of 22 putative urchin sequences, one with $sPLA_2$ characteristics (i.e., ~14kDa, likely to form intra-molecular disulphide bonds and prediction of Ca^{2+} as a cofactor [17,25]) was selected using the information available in Uniprot. Similarly, a putative urchin 80–85kDa $iPLA_2$ was selected from the 44 entries on the basis of characteristic molecular weight and presence of ankyrin repeats—a feature common to $iPLA_2$ forms across species [25,35]. As the predicted urchin 80–85kDa $iPLA_2$ is not present in the Uniprot database, the sequence was downloaded from PubMed. Human PLA_2 sequences used for the analyses were $sPLA_2$–P14555 and $iPLA_2$–O60733 and murine PLA_2 sequences were $sPLA_2$–Q9WVF6 and $iPLA_2$–P97819. Only those human and murine PLA_2 sequences identified at the protein level were selected. As the predicted urchin sequences present in Uniprot or PubMed (66 sequences in total) do not contain the C2 domain characteristic of $cPLA_2$, sequence alignment of $cPLA_2$ isozymes was not carried out and there was no further testing for this isozyme. Building from the in-silico analysis, validation at the protein level was then carried out using a well-established top-down proteomic approach coupling 2DE with high-sensitivity western blotting using anti-human $sPLA_2$ and $iPLA_2$ antibodies to conserved regions [45,57,61].

2.2.4. Sample Fractionation for 2DE Western Blotting

After de-jellying and thorough washing, unfertilized urchin eggs were homogenized in intracellular media (IM; 220 mM K-glutamate, 500 mM glycine, 10 mM NaCl, 5 mM $MgCl_2$, 5 mM EGTA, pH 6.7) supplemented with 2.5 mM ATP, 1 mM benzamidine HCl, 2 mg/mL aprotinin, 2 mg/mL pepstatin, 2 mg/mL leupeptin and 2 mM DTT) prior to standard isolation of high purity CSC or CV suspended in BIM [38,42,45,47–49,51,52]. For fractionation, CV were lysed using three volumes of ice-cold PIPES buffer (20 mM PIPES, pH 7.0 supplemented with protease, phosphatase and kinase inhibitors) for 90 s and isotonicity restored by adding an equal volume of 2 X IM (supplemented with protease,

phosphatase and kinase inhibitors). Samples were centrifuged at 125,000× g, 4 °C, for 3 h to recover membrane pellets and CV luminal proteins in the supernatant [50]. Membranes were solubilized in 2DE buffer (4% CHAPS, 8 M Urea and 2 M Thiourea supplemented with protease, phosphatase and kinase inhibitors [50,57]) while supernatant containing CV luminal proteins was buffer exchanged with 3M urea solution using Amicon filters. Solubilized membrane proteins and concentrated CV luminal proteins were resolved using a well-established 2DE protocol involving isoelectric focusing (IEF) followed by SDS-PAGE in 1 mm thick 10% resolving gels [57]. Subsequent high sensitivity western blotting was essentially as previously described [41,42,45,61]. Briefly, resolved proteins were transferred to 0.2 µM pore size PVDF membrane (Bio-Rad) using buffer containing 25 mm Tris, 192 mm glycine, 20% methanol and 0.025% SDS at 90 Volts for 1 h. Blots were blocked for 1 h at room temperature (RT) in a solution containing 20 mM Tris, 150 mM NaCl, 0.1% Tween (TBST) and 5% non-fat dry milk or 20 mg/mL BSA. Blots were incubated overnight (at least 16 h) with constant rocking at 4 °C with anti-human $sPLA_2$ (1:800) or $iPLA_2$ (1:2000) primary antibodies. After washing, blots were incubated with secondary antibodies conjugated to horseradish peroxidase (HRP) for 2 h at RT and then detected using Luminata Crescendo western HRP substrate and the LAS 4000 Biomolecular Imager. Secondary antibody controls were always carried out in parallel western blots and parallel 2DE gels were stained with colloidal Coomassie Brilliant Blue (cCBB) [62,63].

2.2.5. Molecular Analyses to Detect CV Associated PLA_2 Activities

Membrane and luminal fractions from purified CV suspensions were isolated using the same overall strategy as above except for the use of ice-cold BIM (pH 6.7) in the last step to maintain endogenous PLA_2 activity. This also ensured tight coupling of functional (i.e., fusion) and molecular analyses. PLA_2 activity in CV membrane and lumen fractions was measured by incubating 30 µg CV membrane or luminal protein with 200 picomoles NBD-PE or 170 picomoles NBD-PC for 30 s–10 min. PLA_2 activity was then stopped by adding 0.2 µL HCl and all aliquots were immediately placed on ice for rapid isolation of total lipids; scaled-up experiments were carried out using more CV luminal protein (120 µg) and NBD-PE (664 picomoles) to best detect NBD-FFA species. An equal volume of BIM without CV luminal or membrane protein was used as a control to which the indicated amount of NBD-PC or -PE was added and incubated for 10 min.

To further establish whether catalytically active PLA_2 was on the outer CV monolayer, well-established trypsin treatments were carried out to remove CV surface proteins and PLA_2 activity was measured using the selective PLA_2 substrate, PED6. Briefly, CV suspensions (2–4 mL; OD 0.95 + 0.04; n = 3) were treated with 700 U/mL trypsin for 1 h with gentle mixing every 15 min [42,45]. After treatment, CV suspensions were aliquoted into microplates and incubated with PED6 for 0–30 min; PLA_2 activity was measured at 485 nm/520 nm (Ex/Em) using a POLARstar Omega microplate reader. Fusion assays were also carried out to confirm the fusion competence of the treated CV. To confirm removal of $iPLA_2$ from the CV surface, western blotting was carried out on CV membrane proteins using the $iPLA_2$ antibody. Protein isolation and SDS-PAGE were as above with the exception that SDS sample buffer was used for solubilizing CV membrane proteins and detection was with cCBB [41,42,45,62,63]. In parallel replicates, absorbance at A405 was measured regularly during the incubations to assess for possible CV lysis; any drastic decrease in absorbance indicated marked loss of CV due to bursting (as seen with the addition of ddH_2O at the end of the experiment to confirm the intact state of CV).

2.2.6. Effects of PLA_2 Activities on Fusion Assays

Standard fusion and docking/priming assays were carried out as previously described [42,43,45,47–52,54,56]. All experiments were carried out in BIM pH 6.7 supplemented with 2.5 mM ATP, 2 mM DTT and 1X protease inhibitors [41–43,45,51,52]. Briefly, CSC (0.5 mL, OD 0.56 ± 0.02, n = 3–14) and CV (OD 0.94 ± 0.03, n = 22) suspensions were treated with the indicated inhibitor concentrations. Immediately following treatments, suspensions were diluted with 3–5 volumes of ice-cold BIM, pH 6.7 and aliquoted into microplates. Each condition was challenged with increasing concentrations of

$[Ca^{2+}]_{free}$ in quadruplicate, consistent with established protocol and this was repeated in separate experiments as indicated (n) [42,43,45,47–52]. The decrease in OD representing CV fusion was measured using a POLARstar Omega microplate reader [53,54]. Final $[Ca^{2+}]_{free}$ were measured with a Ca^{2+} sensitive electrode (Calcium Combination ISE, EDT directION Limited) as previously described [53,54]. All treatments were carried out at 25 °C. Parallel solvent controls were carried out in every experiment. A separate aliquot in each experiment was also snap-frozen in liquid N_2 and stored at −80 °C for subsequent molecular analyses.

3. Data Analyses

All data are reported as mean ± S.E.M. Two-sample two-tailed t-tests and 2-way ANOVA with Tukey's multiple comparisons were performed using GraphPad PRISM 7 version 7.04 to assess the difference between experimental conditions ($p \leq 0.05$ are considered significant).

4. Results

4.1. Identification of Endogenous PLA_2 Activities on CSC and Their Effects on CSC Fusion

As CSC consist of CV endogenously docked on the PM and undergo Ca^{2+}-triggered exocytosis in vitro, the potential presence and influence(s) of PLA_2 activities was first assessed using CSC and selective PLA_2 inhibitors. Treating CSC with LY311727 and BEL caused significant concentration-dependent decreases in endogenous FFA levels relative to a basal FFA level of 267.8 ± 29.8 femtomoles per μg CSC membrane protein (fmoles/μg MP) (Figure 1A; n = 3); 200 μM LY311727 reduced FFA levels to 122.7 ± 20.13 fmoles/μg MP while 100 μM and 500 μM BEL treatments reduced FFA levels below background values. No significant change in FFA levels was observed in any of the FKGK-11 treatments. As the lipid detection approach used is somewhat selective for unsaturated lipid species [56], in order to ensure a full assessment of potential PLA_2 activities, CSC were labelled with NBD-PC (fluorophore at the sn-2 fatty acid); as previously documented, such exogenous substrates are readily incorporated into CSC and CV membranes [49]. The generation of 3.8 ± 1.2 picomoles NBD-FFA/μg MP from hydrolysis of the incorporated NBD-PC further confirmed endogenous PLA_2 activity (Figure 1B; n = 3). The NBD-FFA was also generated from NBD-PE labelled CSC and CV (n = 1 confirmatory experiment, not shown). However, in contrast to Figure 1A, treating NBD-PC labelled CSC with increasing doses of BEL resulted in a concentration-dependent increase in NBD-FFA to 7.2 ± 3.0 and 9.8 ± 2.9 picomoles/μg MP. Similarly, a concentration-dependent increase in NBD-FFA to 8.9 ± 6.4 and 11.5 ± 8.2 picomoles/μg MP was observed in NBD-PC labelled CSC treated with 50 μM and 200 μM FKGK-11, respectively. No significant change in NBD-FFA levels were observed in any of the LY311727 treatments. As PLD also acts on PC, generation of 2.8 ± 0.5 picomoles NBD-PA/μg MP confirmed endogenous PLD activity (Figure 1B) consistent with previous findings [49]. However, none of the inhibitors caused significant change in NBD-PA with respect to the control. Importantly, the decrease in endogenous FFA levels (Figure 1A) and an increase in endogenous TAG, the *de novo* metabolite ([50,56]; Supplementary Figure 1A and also see [34,64,65]) in the BEL treated unlabelled CSC indicated the presence of a BEL sensitive PLA_2 on CSC. However, the significant increase in NBD-FFA levels in BEL and FKGK-11 treated NBD-PC labelled CSC also indicated the presence of a BEL insensitive PLA_2 species (Figure 1B). As BEL and FKGK-11 inhibit $iPLA_2$ and LY311727 is a selective inhibitor of $sPLA_2$ [26,35,64,66–68], the data suggested the presence of different catalytically active endogenous PLA_2 in CSC preparations.

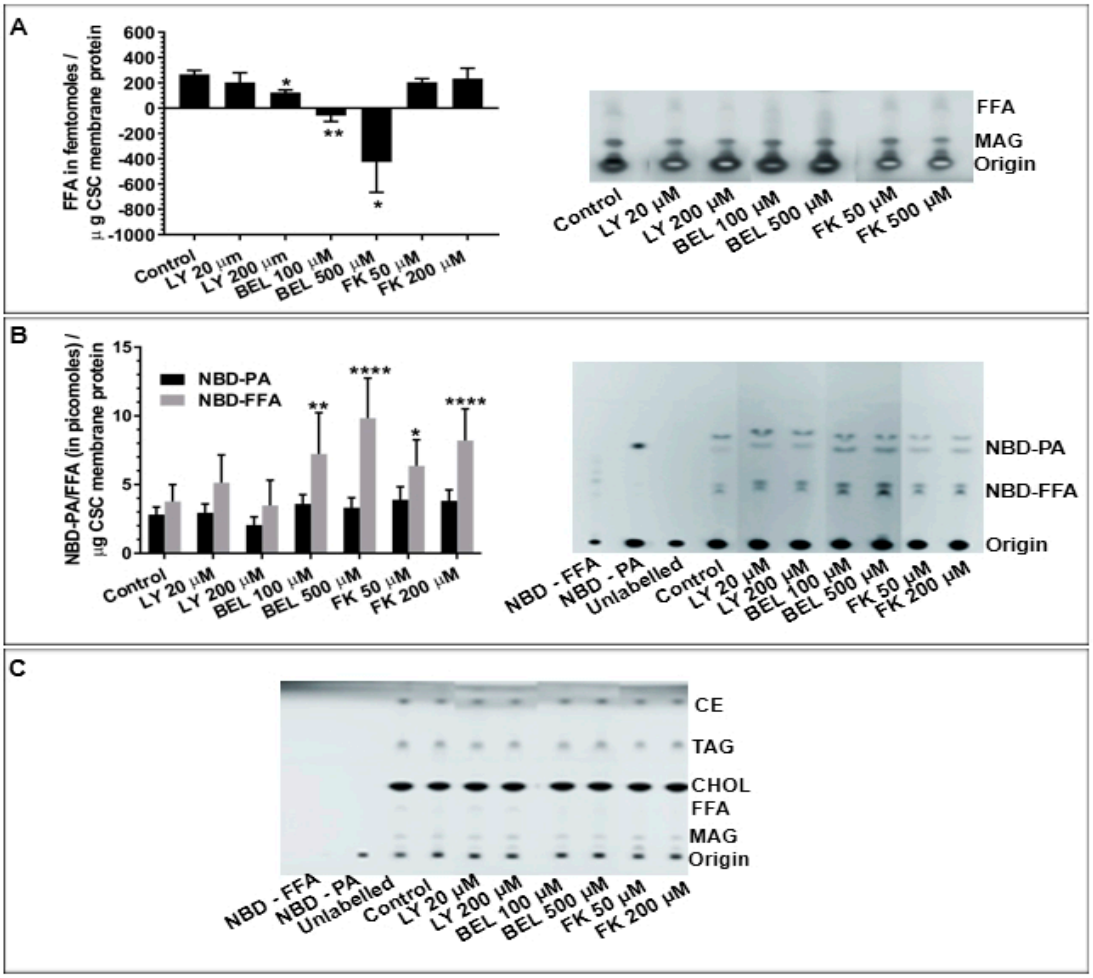

Figure 1. Detection and quantification of (**A**) endogenous CSC FFA, n = 3 separate experiments; (**B**) NBD-FFA and -PA in intact CSC after 15 min labelling with NBD-PC followed by 20 min inhibitor treatments, n = 3 separate experiments; (**C**) total CSC neutral lipids visualized on the same TLC plate as shown in B, after charring with $CuSO_4$. This also confirmed consistent lipid loading in each lane. Representative chromatograms showing indicated changes in lipids. (p-value, * < 0.05, ** < 0.005, **** < 0.0001 indicates relative difference to the control). Note: A section of chromatogram is shown in A and lanes in all chromatograms are grouped together from the same HPTLC plate following removal of lanes not associated with this study. A standard neutral lipid protocol was used to resolve the lipids [56].

With the evidence of active endogenous PLA_2, the effects of selective PLA_2 inhibitors were then tested on CV-PM fusion. The native, docked CV-PM preparations exposed to increasing $[Ca^{2+}]_{free}$ undergo exocytosis in vitro yielding a classic sigmoidal Ca^{2+} activity curve with an EC50 of 38.9 ± 6.4 µM $[Ca^{2+}]_{free}$ (Figure 2; n = 14) [42,45,48,49,52,69,70]. Treating CSC with 20 µM and 200 µM LY311727 [66,68] significantly decreased fusion extent to 44.1 ± 5.3% and 33.6 ± 20.8%, respectively (Figure 2; n = 3–4). On treating CSC with 100 µM and 500 µM BEL [35,64,71,72] a significant decrease in the fusion extent to 53.7 ± 24.6% and 54.2 ± 7.9%, respectively, was observed; 500 µM BEL also caused a progressive rightward shift in Ca^{2+} sensitivity to an EC50 of 230.6 ± 101.5 µM $[Ca^{2+}]_{free}$ (Figure 2; n = 3). CSC treated with 50 µM and 200 µM FKGK-11, another $iPLA_2$ inhibitor [67], also significantly reduced fusion extent to 71.4 ± 28.5% and 31.3 ± 23.6%, respectively (Figure 2; n = 3). Although, LY311727, BEL and FKGK-11 inhibited endogenous FFA production and blocked triggered fusion; PLA_2 species inhibited by LY311727 seem separate from the species which was inhibited by BEL and FKGK-11, in particular with reference to NBD-FFA generated from exogenous NBD-PC.

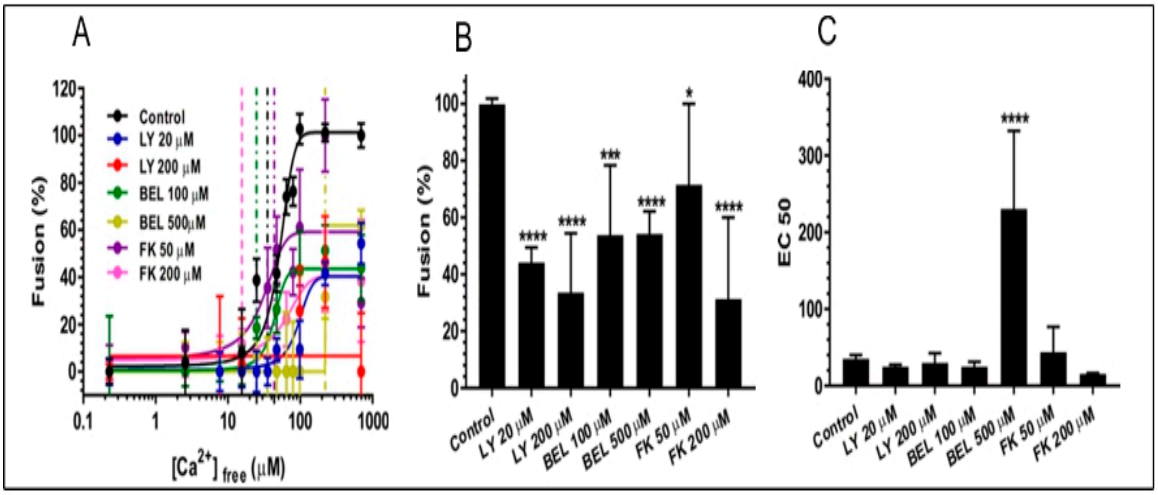

Figure 2. Effects of LY311727 (selective for $sPLA_2$) and BEL and FKGK-11 (both selective for $iPLA_2$) on (**A**) CSC Ca^{2+} activity curves (i.e., exocytosis *in vitro*); (**B**) fusion extent and; (**C**) Ca^{2+} sensitivity (EC50); n = 3–14. (p-value, * < 0.05, *** < 0.0005, **** < 0.0001 indicates difference relative to the control).

4.2. In-Silico Analysis

With initial evidence indicating the likely presence of more than one PLA_2 isozyme on CSC and their potential role in regulating late steps of regulated exocytosis, we sought to identify these isozymes, beginning with sequence alignment to identify regions of homology in putative urchin PLA_2 and characterized human and murine forms. The sequence alignment of $sPLA_2$ and $iPLA_2$ in the selected species clearly indicated conserved amino acid residues throughout the primary amino acid sequences, consistent with a high overall conservation from urchin to human (Figure 3) [40,73,74]. The urchin $sPLA_2$ and $iPLA_2$ forms showed high identity and similarity with both the human and murine species, particularly around the catalytic site histidine with >75% identity and similarity, as well as around the catalytic site serine with 100% identity and similarity (Figure 3A,B and Table 1). The $sPLA_2$ also have a histidine in the Ca^{2+} binding loop with a XCGXGG consensus sequence to which LY311727 binds to inhibit the enzyme [66,68]. The putative urchin $iPLA_2$ also contains a nucleotide binding site with a characteristic GGGVKG consensus sequence [35,75] and a caspase catalytic site with the DVTD consensus sequence [35,76,77]. Cysteine residues at C-67, C-185, C-240, C-344, C-465, C-550 and C-821 in the putative urchin $iPLA_2$ are also conserved and are thus likely susceptible to alkylation during BEL treatments [78].

Table 1. Identity and similarity of urchin PLA_2 isozymes to the human and murine forms.

	Target Species	Percent Identities	Percent Similarities	Percent Identities	Percent Similarities
Urchin Isozymes		**(Full Length)**		**(at Histidine Catalytic Site)**	
$sPLA_2$	Human	39	50	68	67
	Murine	36	46	74	74
		(Full Length)		**(at Serine Catalytic Site)**	
$iPLA_2$	Human	36	52	100	100
	Murine	36	53	100	100

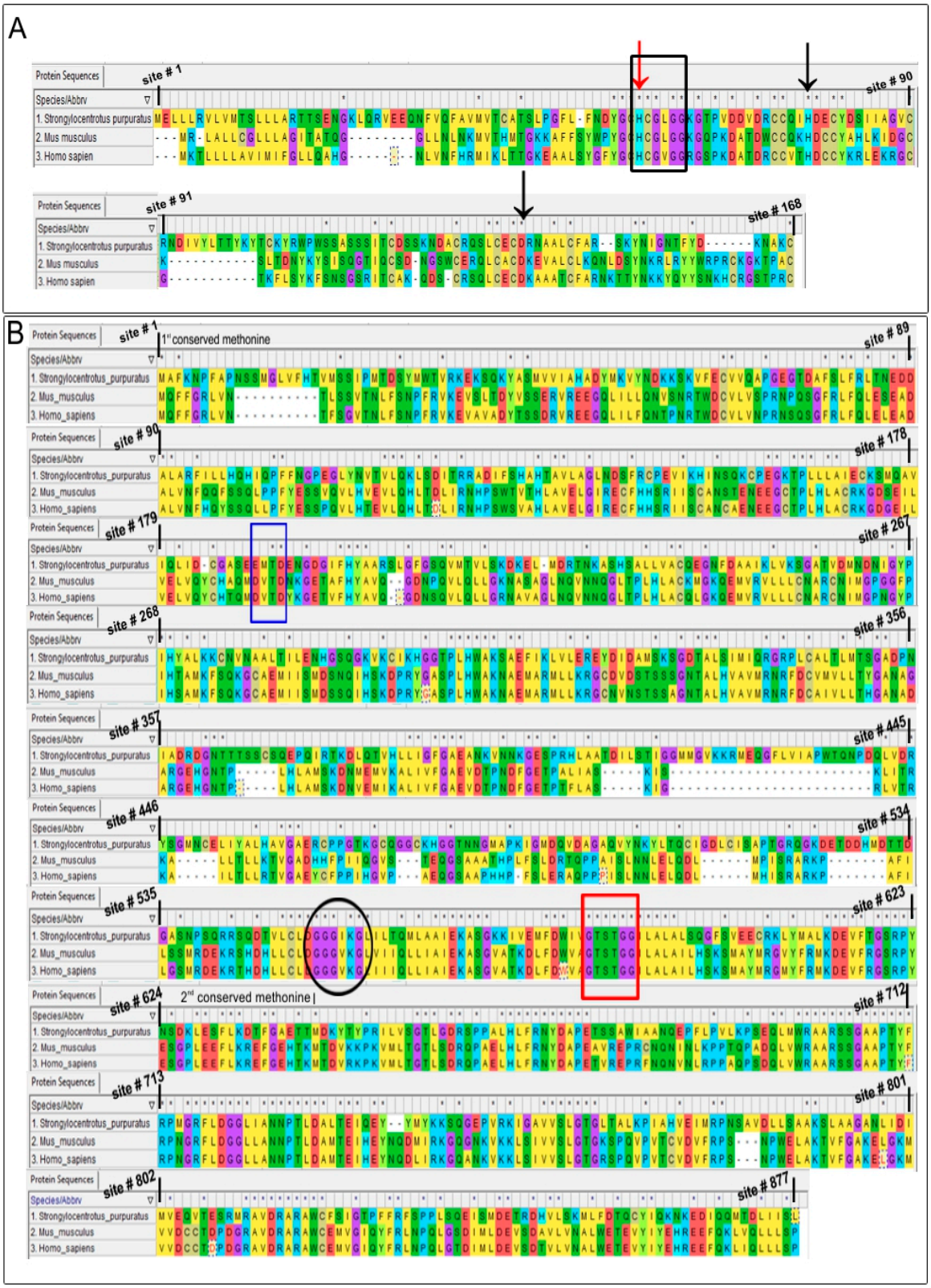

Figure 3. Sequence alignment of predicted urchin (**A**) sPLA$_2$ and (**B**) 80–85 kDa iPLA$_2$. The first row in each panel is the amino acid sequence of urchin PLA$_2$ isozymes and the subsequent two rows are of murine and human PLA$_2$ isozymes, respectively. Conserved amino acids are indicated with an asterisk

and site # represents the amino acid residue number in the primary urchin PLA_2 sequence (also considering gaps). The red arrow indicates conserved Histidine in the Ca^{2+} binding loop (Black box), the site at which LY311727 binds. Black arrows show conserved Histidine and Aspartic acid which form the catalytic site His-Asp dyad. Blue and red boxes indicate the caspase cleavage site and the active site serine in the GXSXG consensus sequence, respectively. The circle indicates the nucleotide binding site. Dissimilar residues with the same background colour indicate conservative substitution.

4.3. Western Blotting and Assays to Confirm Identity and Localization of PLA_2 Isozymes

After identifying conserved catalytic and regulatory domains in the putative urchin isozymes (Figure 3 and Table 1), enzyme localization in CSC and CV was probed using selective antibodies. The anti-human $sPLA_2$ antibody was raised against the entire length of human $sPLA_2$ and would thus identify putative urchin $sPLA_2$ considering the high identify and similarity, particularly within the catalytic region (Figure 3A and Table 1). Similarly, the anti-human $iPLA_2$ recognizes a region between amino acid 399–704, which is also highly conserved in the putative urchin $iPLA_2$ isozyme (54% identify, 67% similarity); this region also carries highly conserved GXSXG and GGGVKG catalytic and nucleotide binding consensus sequences (Figure 3B and Table 1). Western blotting of 2D gels identified two immune positive spots of ~14 kDa and pI of ~4.0 and ~4.9 in the CV lumen fraction using the $sPLA_2$ antibody (Figure 4A). An immune positive spot of ~63 kDa and pI ~6.2 and two immune positive spots of ~63 kDa and pI ~5.2 and 5.4 were detected in the CSC and CV membrane fractions, respectively, using the $iPLA_2$ antibody (Figure 4B,C, respectively). Of note is the relative high abundance of $iPLA_2$ on the CSC membrane in comparison to the CV membrane.

To further and more specifically localize the PLA_2 isozymes and explore possible substrate preferences, NBD-PE and -PC were used to assess the CV associated enzyme activities. First, an isolate of CV lumen proteins was incubated with NBD-PE or -PC for different interval (Figure 5A; n = 3). The NBD-PE in controls after 10 min incubation was 12.3 ± 0.9 picomoles which was significantly reduced to 9.0 ± 1.2, 7.4 ± 1.2, 6.8 ± 1.0 and 3.8 ± 2.3 picomoles following 30 s, 2 min, 5 min and 10 min incubations, respectively (Figure 5A). The generation of NBD-FFA having a retention factor (Rf) similar to NBD-ARA indicated PLA_2 activity; an ~70–90% increase in NBD-FFA over time was observed (Figure 5A; n = 2–3). Notably, a very large increase in NBD-FFA in CV aliquots that were pre-incubated with 104.0 μM $[Ca^{2+}]_{free}$ confirmed Ca^{2+} promoted CV luminal PLA_2 activity (Figure 5B, n = 3). In contrast, 18.4 ± 2.0 picomoles NBD-PC was detected in buffer controls and no significant change was detected even after 10 min incubation with the CV luminal protein (Figure 5A). This correlated with no detection of NBD-FFA species in NBD-PC labelled CSC (n = 2 confirmatory experiments, not shown). Thus, a decrease in NBD-PE and parallel increase in NBD-FFA over time and a large increase in the generation of NBD-FFA in the presence of higher $[Ca^{2+}]_{free}$ confirmed the presence of a Ca^{2+} dependent catalytically active $sPLA_2$ in the isolated CV luminal fraction, which is selective for PE over PC.

The substrate preference of the ~63kDa CV membrane $iPLA_2$ was also investigated by incubating isolated CV membrane fragments with NBD-PE or -PC (Figure 6A; n = 2–3). Buffer without CV membrane was used as the control to which the indicated amount of NBD-PC or -PE was added and incubated for 10 min. In all incubations, no significant change in the NBD-labelled lipids nor generation of NBD-FFA was observed. Therefore, to confirm whether the apparent membrane associated $iPLA_2$ was lost or became inactive during CV membrane isolation, intact CV were assayed for PLA_2 activity following trypsin treatment and loss of $iPLA_2$ was confirmed by western blotting. Loss of the ~63 kDa $iPLA_2$ protein band following trypsin treatment confirmed the presence of $iPLA_2$ on the CV surface (Figure 6B, n = 3; see also Figure S2). Both control and trypsin treated CV were then incubated with the PLA_2 selective substrate PED6—a glycerophosphoethanolamine with a BODIPY dye-labelled sn-2 acyl chain and a dinitrophenyl quencher-modified head group [79,80]. The cleavage of the BODIPY dye from the sn-2 position by the action of PLA_2 resulted in decreased quenching by the head group which specifically indicated PLA_2 activity. Relative to the 0 min control, there was no detectable PLA_2

activity in the trypsin treated CV, until 2 min. No significant change in the fluorescence intensity between 2–30 min in trypsin treated CV, relative to 0 min, indicated a complete loss of $iPLA_2$ activity that correlated with loss of the $iPLA_2$ band on the western blots (Figure 6C; n = 3). Absorbance measurements of parallel samples confirmed that there was no major loss of CV over the course of these incubations (not shown).

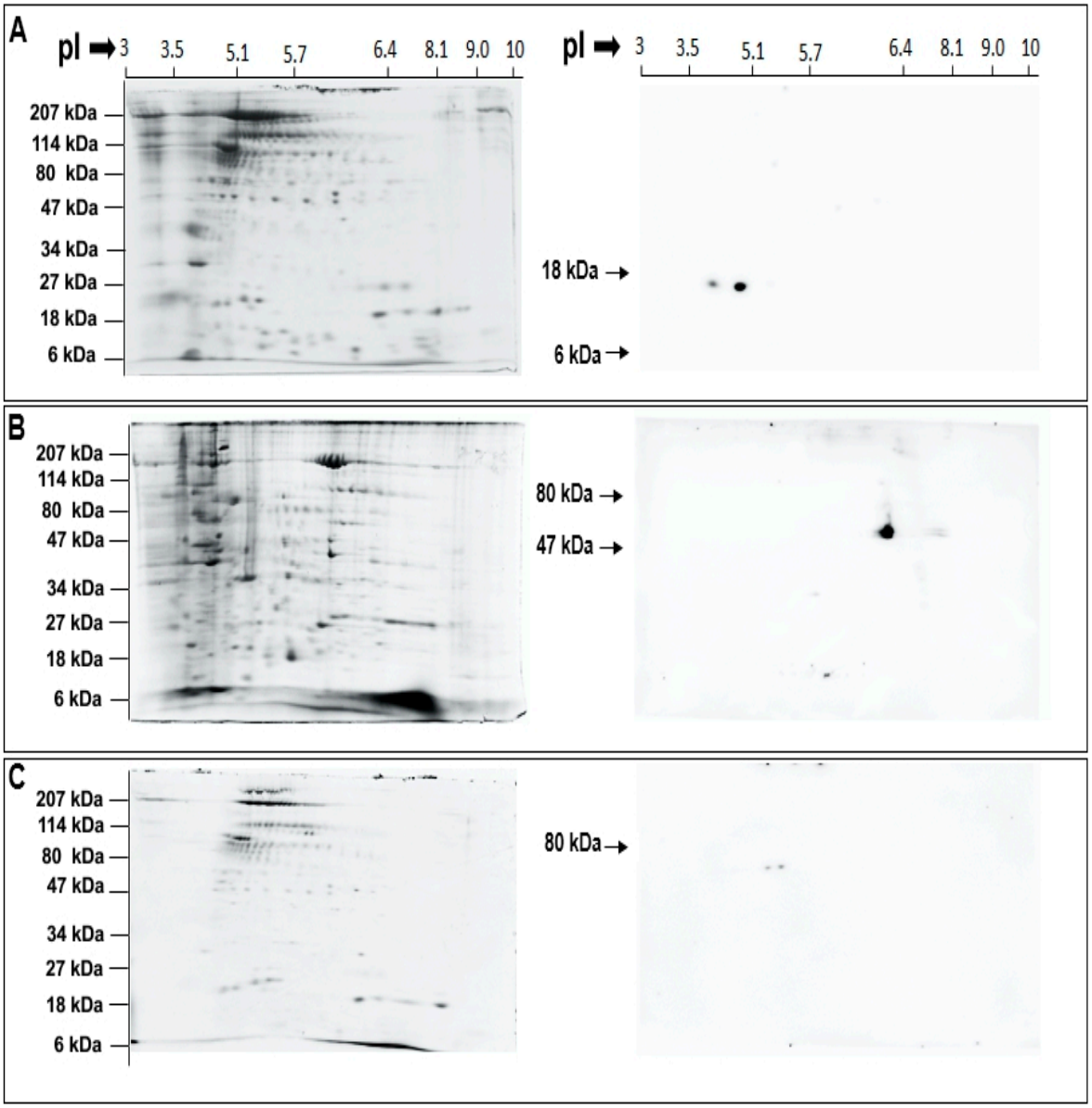

Figure 4. Immuno-reactive spots detected by (**A**) $sPLA_2$ antibody in the CV luminal fraction; (**B**) $iPLA_2$ antibody in the CSC membrane fraction; and (**C**) $iPLA_2$ antibody in the CV membrane fraction. cCBB stained 2D SDS-PAGE gels (left) and parallel western blots (right).

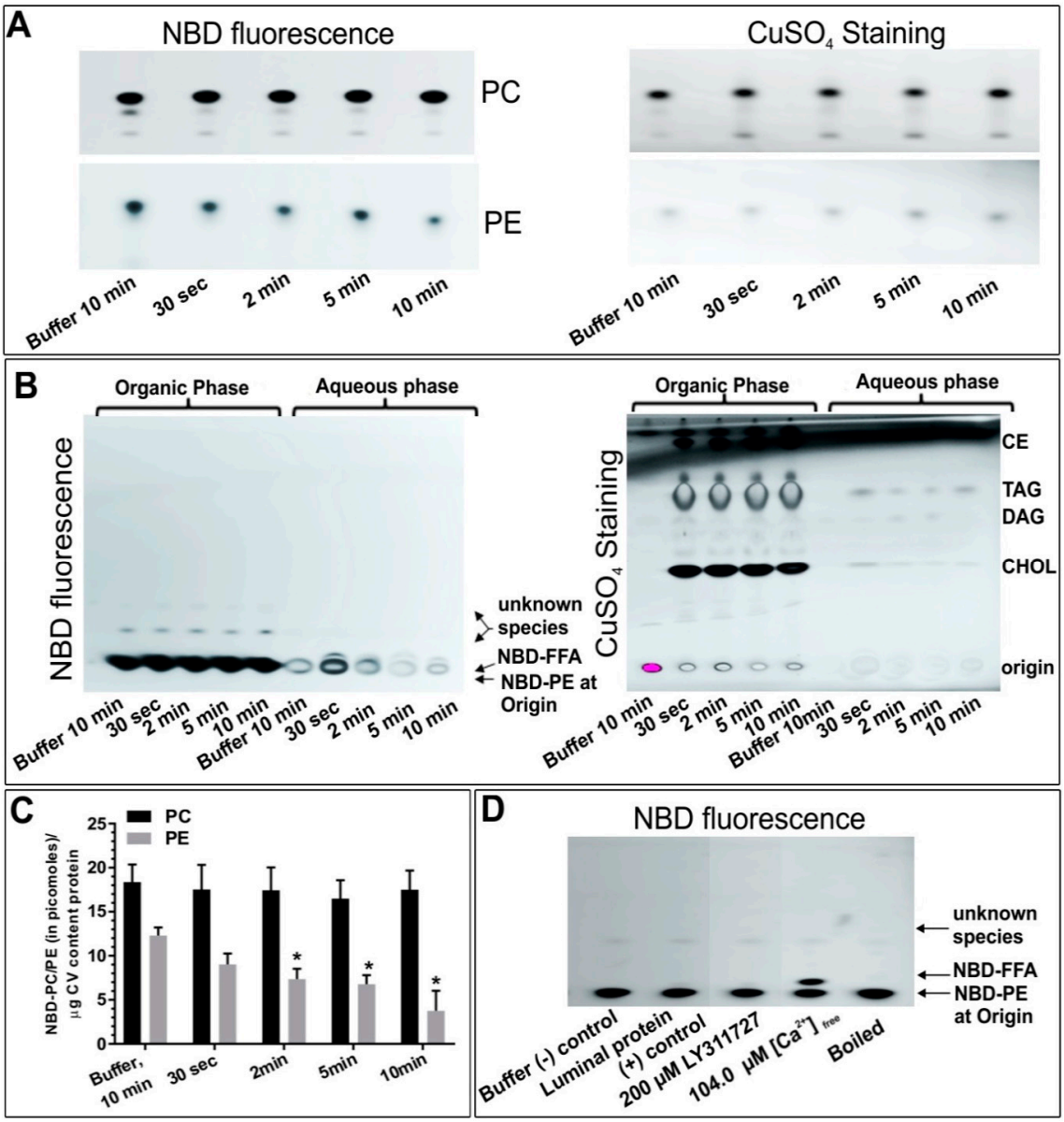

Figure 5. (**A**) Time-dependent decrease in NBD-PE and no change in NBD-PC, when incubated with isolated CV luminal proteins, $n = 3$; (**B**) Detection of NBD-FFA generated from NBD-PE, when incubated with CV luminal proteins; n = 2–3. After incubations, activity was stopped by adding 0.2 µL HCl, total lipids isolated, resulting organic and aqueous phases retained, dried and resolved. (**C**) Bar graph summarizing the changes in NBD-PC and -PE, indicating the presence of CV luminal PLA_2 with high catalytic activity for PE. (**D**) Effect of LY311727, increased $[Ca^{2+}]_{free}$ and boiling on luminal PLA_2 activity assessed by incubating isolated CV luminal proteins with NBD-PE; $n = 3$. (p-value, * < 0.05 indicates difference relative to the control). The chromatograms in A were resolved using a standard phospholipid protocol and in (**B**,**D**) using an established protocol for neutral lipids [56]. Note: Left panels in (**A**,**B**) show NBD fluorescence and the right panels show same section of the chromatogram after charring with $CuSO_4$ [56]. The lanes shown in (**D**) are grouped together from the same chromatogram following removal of lanes not associated with this study.

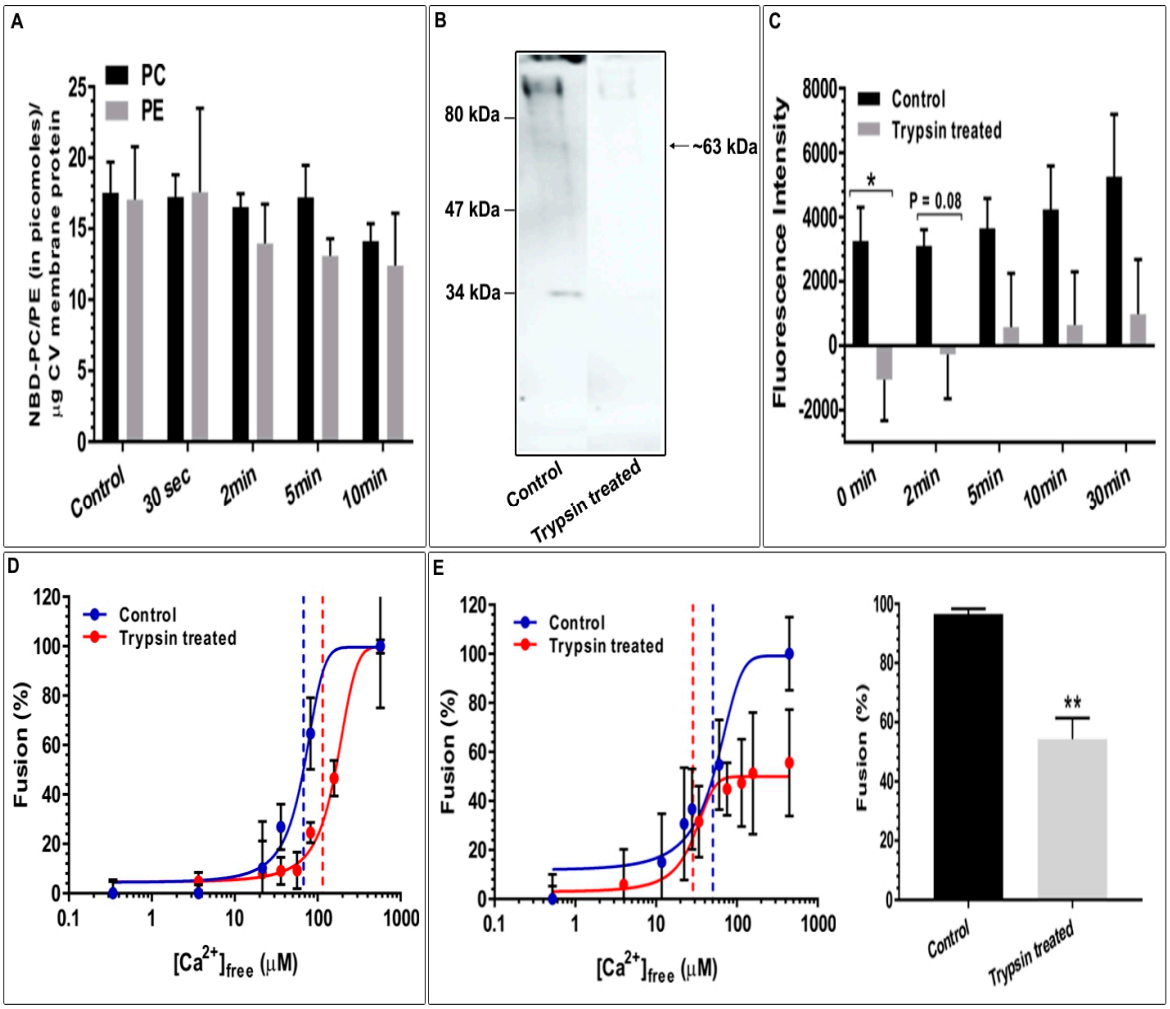

Figure 6. (**A**) Time-dependent changes in NBD-PC and -PE, when incubated with CV membrane fragments (n = 2–3); (**B**) Western blot showing an apparent complete loss of iPLA$_2$ in trypsin treated CV (n = 3). A total of 5µg CV membrane protein per lane was resolved; (**C**) Time-dependent changes in the CV surface PLA$_2$ activity in the intact CV assessed using PLA$_2$-selective substrate PED6 [79,80] (n = 3). The loss of the fluorescence signal is consistent with the loss of PLA$_2$ from the CV surface following ablation with trypsin. Functional assays showing the effects of trypsin treatment on CV-CV Ca^{2+} activity curves [45]; (**D**) Standard fusion assay (n = 2); (**E**) CV settle fusion assay (n = 3). (p-value, * < 0.05, ** < 0.005 indicates difference relative to the control). Note: The lanes in (**B**) are grouped together from the same western blot following removal of intervening lanes.

Considering the apparent complete loss of the ~63 kDa iPLA$_2$ from the external membrane of intact CV following trypsin treatment and the corresponding loss of activity assessed using the selective PED6 substrate (Figure 6B,C), we also tested these same batches of control and trypsin treated CV for functional activity. Parallel standard and settle fusion assays were thus carried out (Figure 6D,E, n = 2–3). In the standard assay, there was no significant change in the fusion extent although Ca^{2+} sensitivity appeared right-shifted following trypsin treatment; however, the shift was not significant relative to the untreated controls. Notably, in the settle assay used to assess docking and priming [42,47,49–52,54], fusion extent was significantly decreased to 54.3 ± 7.2% following trypsin treatment (Figure 6E; n = 3, (p < 0.004)).

4.4. The Effect of PLA_2 Activities on CV-CV Fusion

As in previous work, to enable a tight focus on the late steps of Ca^{2+} -triggered exocytosis, including the fusion mechanism itself, without having to contend with the 'background' of the PM, high purity CV preparations were used to further assess the potential influences of the endogenous CV-associated PLA_2 activities. Both the $sPLA_2$ and $iPLA_2$ were thus again targeted with selective inhibitors to better assess their potential influence(s) on the late steps of regulated exocytosis (Figure 7A,B; n = 3–19). The standard endpoint CV-CV fusion assays yielded a characteristic sigmoidal Ca^{2+} activity curve with an EC50 of 44.8 ± 3.8 μM $[Ca^{2+}]_{free}$ (Figure 7A; n = 19), which was translationally invariant with CV-PM fusion (Figure 1; n = 14) [42,45,49,51]. A significant decrease in fusion extent to 95.3 ± 2.9% and 80.0 ± 10.7%, was observed in CV treated with 20 μM and 200 μM LY311727, respectively (Figure 7A). Fusion of CV treated with 100 μM and 500 μM BEL were also reduced to 96.0 ± 3.2% and 90.0 ± 6.4%, respectively (Figure 7A); following treatment with 50 μM and 200 μM FKGK-11 fusion extent was reduced to 87.4 ± 8.5% and 75.4 ± 7.3%, respectively (Figure 7A). A significant right-shift in Ca^{2+} sensitivity, to yield EC50 of 78.9 ± 9.4 μM $[Ca^{2+}]_{free}$ and 79.8 ± 7.5 μM $[Ca^{2+}]_{free}$ was also observed following treatment with 50 μM and 200 μM FKGK-11.

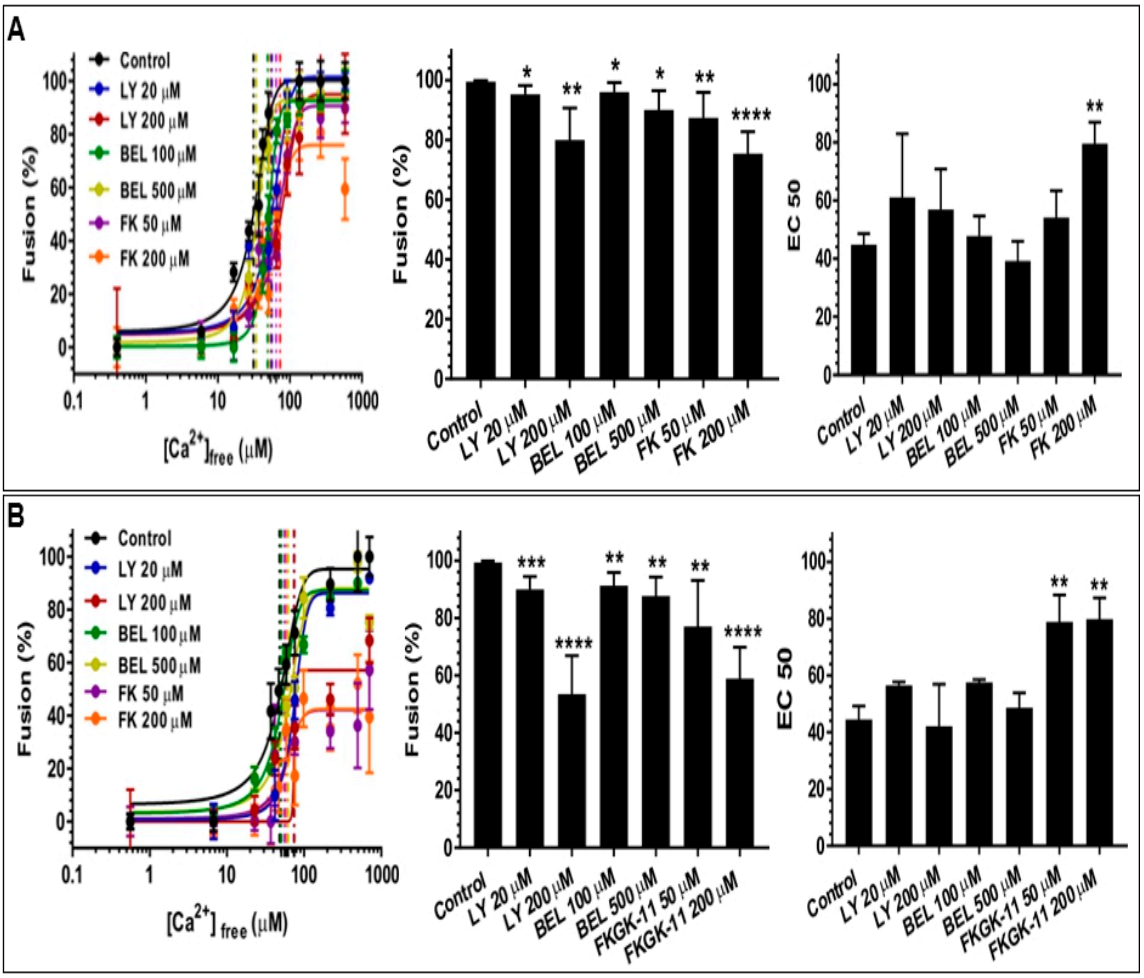

Figure 7. Effects of LY311727 (selective for $sPLA_2$) and BEL and FKGK-11 (both selective for $iPLA_2$) on CV-CV Ca^{2+} activity curves, fusion extent and Ca^{2+} sensitivity (EC50); (**A**) standard fusion assay, n = 3–19; (**B**) settle fusion assay, n = 3–19. (p-value, * < 0.05, ** < 0.005, *** < 0.0005, **** < 0.0001 indicates difference relative to the control.

When tested in the settle assay, CV treated with all doses of the inhibitors showed further decreases in fusion extent. These concentration-dependent decreases in fusion were to 89.9 ± 4.6% and 53.5 ± 13.4% in 20 μM and 200 μM LY311727 treated CV, respectively; 91.3 ± 4.6% and 87.6 ± 6.6% in 100 μM and 500 μM BEL treated CV, respectively; and 77.0 ± 16.0% and 58.9 ± 10.9% in 50 μM and 200 μM FKGK-11 treated CV, respectively, confirming the role(s) of PLA_2 isozymes in promoting and maintaining CV priming and/or docking (Figure 7B). To confirm that changes in the CV-CV fusion parameters were associated with perturbed PLA_2 activities, total lipid changes were assessed from the same preparations following inhibitor treatments. Treating CV with LY311727, BEL and FKGK-11 caused significant concentration-dependent decreases in endogenous FFA levels, relative to a basal FFA level of 15.7 ± 0.51 fmoles/μg MP (Figure 8; n = 3–4). FFA levels decreased to 12.9 ± 1.3 and 8.9 ± 3.5 fmoles/μg MP in CV treated with 20 μM and 200 μM LY311727, respectively. Additionally, a significant increase in the endogenous PE levels in the CV treated with 200 μM LY311727 (Table 2), confirmed the inhibitory action of LY311727 on PE-selective PLA_2. Treating CV with 500 μM BEL also significantly reduced FFA levels to 1.3 ± 6.7 fmoles/μg MP (Figure 8A,B; n = 4–12) and increased TAG levels to 376.7 ± 22.5 picomoles/μg MP, relative to the basal level of 217.2 ± 40.9 picomoles in the control (Figure S1B, n = 3–8; also seen in the BEL treated CSC, Figure S1A, n = 3–5).

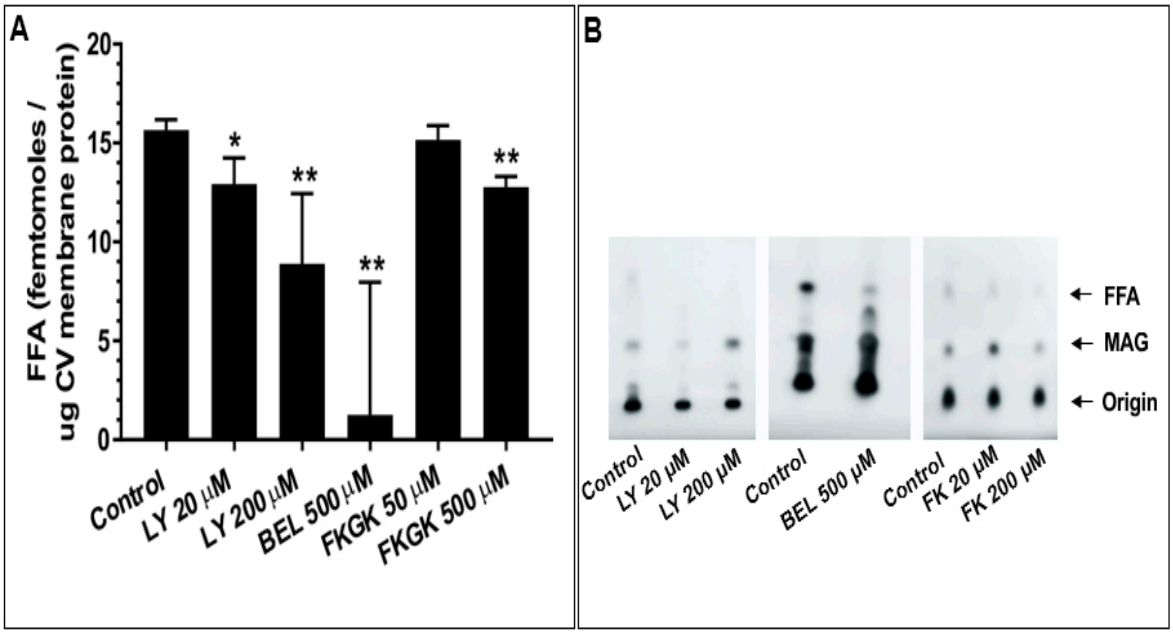

Figure 8. (**A**) Changes in the endogenous FFA in CV treated with indicated doses of LY311727, BEL and FKGK-11; n = 4–12; (**B**) Section of the chromatograms showing the changes in endogenous FFA. (p-value, * < 0.05, ** < 0.005 indicates difference relative to the control). A standard neutral lipid protocol was used to resolve the lipids [56].

Table 2. Endogenous PE and PC levels in (**A**) CSC and (**B**) CV, treated with the indicated doses of the inhibitors. ND-not done; NA-not applicable.

A

PE (Picomoles/μg CSC Membrane Protein)		Mean	SEM	Student *t*-Test	Sample Size (*n*)	PC (Picomoles/μg CSC Membrane Protein)		Mean	SEM	Student *t*-Test	Sample Size (*n*)
Control		29.5	7.5		5	**Control**		47.7	11.0		6
LY311727	**20 μM**	ND	NA	NA	NA	**LY311727**	**20 μM**	66.6	3.0	0.38	2
LY311727	**200 μM**	ND	NA	NA	NA	**LY311727**	**200 μM**	38.9	2.2	0.68	2
BEL	**100 μM**	ND	NA	NA	NA	**BEL**	**100 μM**	ND	ND	NA	NA
BEL	**500 μM**	28.0	7.5	0.90	3	**BEL**	**500 μM**	77.2	5.0	0.31	3
FKGK-11	**50 μM**	51.0	7.6	0.11	3	**FKGK-11**	**50 μM**	63.2	19.1	0.47	3
FKGK-11	**200 μM**	31.8	9.3	0.85	3	**FKGK-11**	**200 μM**	50.7	8.9	0.86	3

B

PE (Picomoles/μg CV Membrane Protein)		Mean	SEM	Student *t*-Test	Sample Size (*n*)	PC (Picomoles/μg CV Membrane Protein)		Mean	SEM	Student *t*-Test	Sample Size (*n*)
Control		46.0	5.5		11	**Control**		75.1	11.8		13
LY311727	**20 μM**	ND	NA	NA	NA	**LY311727**	**20 μM**	96.4	26.3	0.5	3
LY311727	**200 μM**	70.5	5.1	0.05	3	**LY311727**	**200 μM**	114.2	19.9	0.1	6
BEL	**100 μM**	ND	NA	NA	1	**BEL**	**100 μM**	ND	NA	NA	NA
BEL	**500 μM**	46.6	12.7	0.96	5	**BEL**	**500 μM**	57.3	7.2	0.4	5
FKGK-11	**50 μM**	40.4	12.9	0.66	3	**FKGK-11**	**50 μM**	53.5	26.0	0.4	3
FKGK-11	**200 μM**	22.5	6.7	0.06	3	**FKGK-11**	**200 μM**	42.4	16.5	0.2	3

5. Discussion

Using bioinformatics and a top-down proteomic approach combined with lipid analyses of isolated native CSC and CV, here we have identified endogenous, vesicle associated PLA_2—a $sPLA_2$ in the CV lumen and an $iPLA_2$ on the CV surface—and also demonstrated that their activities play a role in promoting and maintaining the docked and/or primed state of secretory vesicles. The results are consistent with previous findings in platelets that PLA_2 activity is not essential for fusion *per se* but has clear modulatory roles late in the exocytotic pathway [81].

5.1. PLA_2 Activity and Their Effects on CSC Fusion

Initial assessments of CSC confirmed the existence of endogenous PLA_2 activities and that these were associated with the late steps of the regulated exocytotic pathway (Figures 1 and 2). Blockade of these PLA_2 activities using the well-characterized $iPLA_2$ inhibitors, BEL [35,64,66,78] and FKGK-11 [35,67] and the $sPLA_2$ inhibitor LY311727 [68], caused significant decreases in endogenous FFA levels (Figure 1A) and an increase in PE levels (Table 2). Importantly, a significant decrease in endogenous FFA but increase in NBD-FFA in BEL treated CSC also indicated the presence of BEL sensitive as well as insensitive PLA_2 isozymes, the latter seemingly an $sPLA_2$ (Figure 1A,B). Furthermore, to assess for potential nonspecific inhibitory effects of BEL on other enzymes [78], unlabelled and NBD-PC labelled CSC were treated with another $iPLA_2$ inhibitor, FKGK-11. The significant concentration-dependent increase in NBD-FFA (similar to that seen with BEL; Figure 1B) supported the interpretation that BEL and FKGK-11 targeted at least one common molecular entity. This might also indicate that alternate $iPLA_2$ isoforms or proteoforms compensated for the loss, in the presence of BEL or FKGK-11. In contrast, using LY311727 to block $sPLA_2$ resulted in a concentration-dependent decrease in endogenous FFA with no change in NBD-FFA, generated from NBD-PC labelled CSC (or NBD-PE labelled CSC; $n = 1$, not shown). These data indicated an active $sPLA_2$ that could not access the exogenous NBD-PE or -PC (Figure 1A,B), despite the fact that NBD-PE was also seen to be a preferred substrate of CV luminal PLA_2 (Figure 5A). Also, no significant change in the fluorescence intensity in the 30 min control, relative to the 0 min control (Figure 6C), indicated that 30 min was insufficient for any putative CV flippase to translocate PED6 (a modified PE) toward the CV lumen; had there been such translocation of PED6, a significant increase in fluorescence intensity should have occurred within 30 min due to luminal $sPLA_2$ activity.

Notably, a significant increase in TAG in the BEL treated unlabelled CSC provided an early indication that $iPLA_2$ could be the isozyme on CSC (Figure S1A and [34,64]). The proposed 'housekeeping' function of $iPLA_2$ is to generate lyso-phospholipid acceptors for the incorporation of FFA into membrane phospholipids [34,35,64,82]. Upon $iPLA_2$ inhibition, lyso-phospholipid acceptor levels decrease, consequently leading to an increase in FFA concentration [29,64]. Under such a condition, the bulk of FFA is incorporated in the de novo metabolites TAG, DAG and MAG (Figure S1A,B) [64]. BEL also inhibits magnesium-dependent phosphatidate phosphohydrolase (PAP), an enzyme catalysing the conversion of PA to DAG; however, there were no changes in PA in BEL treated CSC (Figure 1B).

Overall, the data suggested the presence of more than one catalytically active form of PLA_2 on CSC, some of which may be strategically localized to maintain the docked and release-ready state of CV on the PM [29]. Blocking PLA_2 activities using well characterized $iPLA_2$ inhibitors (BEL [78] and FKGK-11 [35,67]) and an $sPLA_2$ inhibitor (LY311727 [68]) caused significant inhibition of CSC fusion suggesting that even fully docked and fusion-ready CV are sensitive to changes in local PLA_2 activity (Figures 1B and 2).

5.2. Bioinformatics

With functional confirmation of the presence of active PLA_2 species and association of their metabolites with the late steps of Ca^{2+}-triggered exocytosis, we used a combined bioinformatics and top-down proteomics approach to identify and localize the active isoforms. Orthologs and paralogs are

hypothesized to share high structural and functional similarity [83]; proteins essential to fundamental molecular mechanisms have a similar structure and function from urchin to mammals [37,73,74,83]. Accordingly, there was substantial homology in amino acid sequence between urchin and mammalian $sPLA_2$ and $iPLA_2$, particularly at the catalytic sites (Figure 3 and Table 1) [37]. The putative urchin $sPLA_2$ shares conserved catalytic and regulatory regions of >75% identity and similarity with the mammalian orthologs (Table 1), including the highly conserved histidine and aspartic acid in the catalytic site consensus sequence (HDCCY) and the histidine in the Ca^{2+} binding loop (HCGVGG) (Figure 3A), at which LY311727 binds via its amide group [66]. Similarly, the $iPLA_2$ share conserved catalytic and regulatory domains, including the conserved active site serine in the GXSXG consensus sequence that interacts with FKGK-11 [37,69] and the conserved cysteine residues are alkylated by the active BEL metabolites [78]. The urchin $iPLA_2$ thus shares conserved catalytic and regulatory domains with the human and murine orthologs (Figure 3B and Table 1). Additionally, it also contains an ATP binding consensus motif (GGGVKG) and a N-terminal caspase-3 cleavage site (DVTD), that are all characteristic of $iPLA_2\beta$ (Figure 3) [35,84]. Notably, $iPLA_2\beta$ and $sPLA_2$ genes are conserved in lower eukaryotes, further indicating an essential role of these enzymes [37].

5.3. Top-Down Proteomics Identify CV Associated PLA_2 Isozymes

Based on the bioinformatics we then carried out targeted top-down proteomic analyses using 2DE and immunoblotting. These analyses identified a highly conserved catalytically active ~14 kDa CV luminal $sPLA_2$ isozyme (Figure 4A) [25,26,36,85,86] having substrate preference for PE over PC (Figure 5A,B) [26]. Indeed, there are other reports of 14 kDa $sPLA_2$ species having a substrate selectivity for PE over PC [17,87]. An increase in the activity of this CV luminal $sPLA_2$ species in the presence of $[Ca^{2+}]_{free}$ was also confirmatory of its identification (Figure 5B) [25,27]. Similarly, using an antibody to the human form, we detected an ~63 kDa $iPLA_2$ on both CSC and CV membranes (Figure 4B,C), although having different isoelectric points (pI). One of the most common post-translation modifications (PTM) causing a shift in pI is phosphorylation, resulting in an increase in the net negative charge on the protein. Hence, CV membrane $iPLA_2$ isozymes with pI of ~5.2 and 5.4 may be phosphorylated (or otherwise modified) species relative to the bulk of the enzyme found on CSC (pI of ~6.2) (Figure 4B,C); the broad potential influence of protein phosphorylation on the late steps of exocytosis has been well documented [52]. The ~63kDa $iPLA_2$ is proposed to arise from the proteolytic cleavage of a nascent full length 80–85 kDa $iPLA_2$ [35,76,77]. Therefore, together with in-silico analysis (Figure 3B), identification of an ~63 kDa $iPLA_2$ on the CV membrane (Figure 4C) and the significant decrease in endogenous FFA in BEL and FKGK-11 treated CV (Figure 8A,B) with a parallel increase in TAG (Figure S1B), confirmed a catalytically active membrane bound CV $iPLA_2$ [35,64,76,77,82]. Notably, on comparing CSC and CV data (Figure 4B,C), it would seem that much more of the $iPLA_2$ may be localized to the PM, some (small) fraction presumably near or at sites of CV docking and fusion. The putative urchin $iPLA_2$ contains 57 potential trypsin cleavage sites, predicted by PeptideMass [88] and thus cleavage at even a few of these sites would destroy the enzyme. Hence, loss of the 63 kDa CV $iPLA_2$ following trypsin treatment (Figure 6B) and associated decrease in signal from the PLA_2 selective PED6 substrate (Figure 6C), further confirmed the presence of an active $iPLA_2$ on the external CV membrane. Thus, proteolytic removal of CV surface proteins, including $iPLA_2$, caused a significant decrease in fusion extent to 54.3 ± 7.2% in the settle fusion assay that evaluates the priming and docking capacity of CV (Figure 6E), indicating that vesicle surface proteins including $iPLA_2$ and SNAREs [29,41–45,89]—and possibly other as yet unidentified proteins—are critical for priming and/or docking. This is consistent with a suggested link between the CV surface PLA_2 activity and influences on the late steps of the exocytotic pathway [29].

5.4. CV Associated PLA_2 Isozymes Regulate Docking and/or Priming

Finally, we sought to test whether the identified PLA_2 isozymes are components of the minimal molecular machinery present on CV which enables docking, Ca^{2+} sensing and membrane

merger [38,42,43,45,47–52,55,90–92]. Thus, CV were treated with selective PLA_2 inhibitors and changes in the fusion parameters were assessed using the well-established standard and settle fusion assays [38,42,43,45,47–54,90–92]. Consistent with the significant concentration-dependent decrease in fusion extent in CSC fusion assays, comparable effects were seen in the standard CV fusion assay following treatments with LY311727, BEL and FKGK-11 (Figure 7A). However, a far more pronounced decrease in the fusion extent in the settle assays (Figure 7B) confirmed that CV associated PLA_2 isozymes or their metabolites play a critical role in docking and/or priming. The significant concentration-dependent decrease in endogenous CV FFA following the inhibitor treatments (Figure 8A,B), significant increase in PE (Table 2; in CV treated with 200 μM LY311727) and parallel increase in TAG (Figure S1B; in CV treated with 500 μM BEL) confirmed that these inhibitors targeted CV associated PLA_2 isozymes.

Furthermore, $iPLA_2$ hydrolyse BEL to generate diffusible Bromomethyl Keto Acid (BMKA), which alkylates cysteine thiols in $iPLA_2$ causing its inhibition, in addition to non-specific alkylation of cysteine thiols present in other proteins [78]. Therefore, the significant reduction in the Ca^{2+} sensitivity of CSC treated with 500 μM BEL (Figure 2), relative to a lack of effect on CV treated identically (Figure 7A,B), suggested that BMKA acted (to some extent) like N-ethylmaleimide (NEM) in CSC [90,92]. This indicates additional thiol sites on the PM that regulate efficiency of the fusion mechanism (i.e., Ca^{2+} sensing). In terms of targeted inhibition, it should be noted that the compounds, LY311727, BMKA and FKGK-11 are highly hydrophobic with log P values of 1.92 ± 0.62, 3.90 ± 0.37 and 5.40 ± 0.89, respectively, where the partition coefficient (P) = [organic]/[aqueous] (calculated using ADC/ChemSketch [93]). Hence, these compounds have a high likelihood to intercalate into or cross the CV membrane. Indeed, the significant concentration-dependent decrease in fusion extent upon 200 μM LY311727 treatments, to 33.6 ± 20.8%, 80.0 ± 10.7% and 53.5 ± 13.4% in the CSC, CV-CV standard and settle fusion assays, respectively, (Figure 2A,B and Figure 7A,B) and; the parallel decrease in endogenous FFA (Figures 1A and 8A,B) indicated that inhibition of the CV luminal $sPLA_2$ reduced CV priming and/or docking. Although BMKA and FKGK-11 may also have crossed the CV membrane, it seems unlikely that these would inhibit the $sPLA_2$—its sulfhydryl groups would already be engaged in intra-molecular disulphide bonding and thus would not be susceptible to BMKA induced alkylation [78] and the absence of a catalytic site serine would obviate FKGK-11 binding [67]. Therefore, overall, the inhibitors chosen are expected to be highly selective for the PLA_2 species in question and thus reflect selective influences on the functional assays.

5.5. Concluding Remarks

According to the Stalk-pore hypothesis, the fusion of two distinct membrane bilayers proceeds through sequential steps resulting in the localized mixing of proximal monolayers followed by fusion of the distal monolayers [94–97]. This enables vesicle content mixing (homotypic fusion) or release (heterotypic fusion) and subsequent content dispersal. PLA_2 activity produces both negative and positive curvature lipids—LPC and FFA, respectively—which are known to inhibit or promote fusion depending on their site of incorporation [10,11,29,94,95,98]. In this regard, localization of the endogenous catalytically active PLA_2 isozymes that supply LPC and FFA near the docking and/or fusion site is of critical importance. The internal CV microenvironment has a pH of ~5.5 and contains ~100 mM calcium, mostly in a bound state, as has also been found in other (mammalian) secretory vesicles [30,86,99–101]; however, the estimated global luminal $[Ca^{2+}]_{free}$ is ~1–10 μM, occurring as transients, linked in part to the opening of p-type Ca^{2+} channels [30]. As these are global measures, the local $[Ca^{2+}]_{free}$ at the CV membrane would be much higher. This is also consistent with the estimates of luminal $[Ca^{2+}]_{free}$ in chromaffin granules under basal conditions [100]. Hence, in response to CV luminal Ca^{2+} transients in vivo, the activity of localized luminal $sPLA_2$ would increase, preferentially hydrolysing PE on the inner CV monolayer (Figures 4A and 5A,B), at or immediately adjacent to the docking/fusion site. Thus, under basal conditions, the external CV membrane associated $iPLA_2$ generates LPC and FFA by cleaving PC on the outer CV monolayer, while luminal $sPLA_2$ produces LPE

and FFA on the inner CV monolayer. Such localization of $iPLA_2$ on the outer vesicle (and inner plasma) membrane, near docking/fusion sites, would block spontaneous merger of the vesicle and PM due to high local levels of LPC at membrane contact sites, in particular considering the substantially higher positive intrinsic curvature of LPC relative to LPE [98]. As such, this might act as a native fusion 'brake' that must be overcome by the Ca^{2+}-triggered fusion mechanism [29], in which basal LPC production is somewhat balanced by intermittent LPE production via transient $sPLA_2$ activity (Figure 9). In this regard and that of FFA (see below) it would also be important to assess the distribution of fatty acid species at sn-1 and sn-2 of the endogenous CV membrane PC and PE. The net accumulation of FFA on *cis* or *trans* monolayers and any associated effects would be dependent on the rate of passive diffusion, flipping efficiency, rate of metabolism, site of incorporation, chain length and degree of unsaturation [10,95,102–107]. Notably, perhaps complimentary to the actions of LPC and LPE, PLA_2 derived FFA has been proposed to support the formation of *trans* SNARE complexes to maintain the primed and/or docked state of vesicles [4,29,108,109]. Importantly, basal CV luminal $sPLA_2$ activity supported CV-PM and CV-CV fusion (Figure 2, Figure 6D,E and Figure 7A,B); whether the activity is also sensitive to transient changes in luminal $[Ca^{2+}]_{free}$ and how these may be linked to the final membrane merger steps are unknown. However, the likely coordinated action (i.e., cross-talk) of the CV luminal $sPLA_2$ and outer membrane bound $iPLA_2$ in maintaining the docked, fusion-ready state of vesicles on the PM is evident as both interventions used here—pharmacological inhibition of CV luminal $sPLA_2$ and membrane associated $iPLA_2$ and proteolytic removal of $iPLA_2$—significantly impaired priming and/or docking.

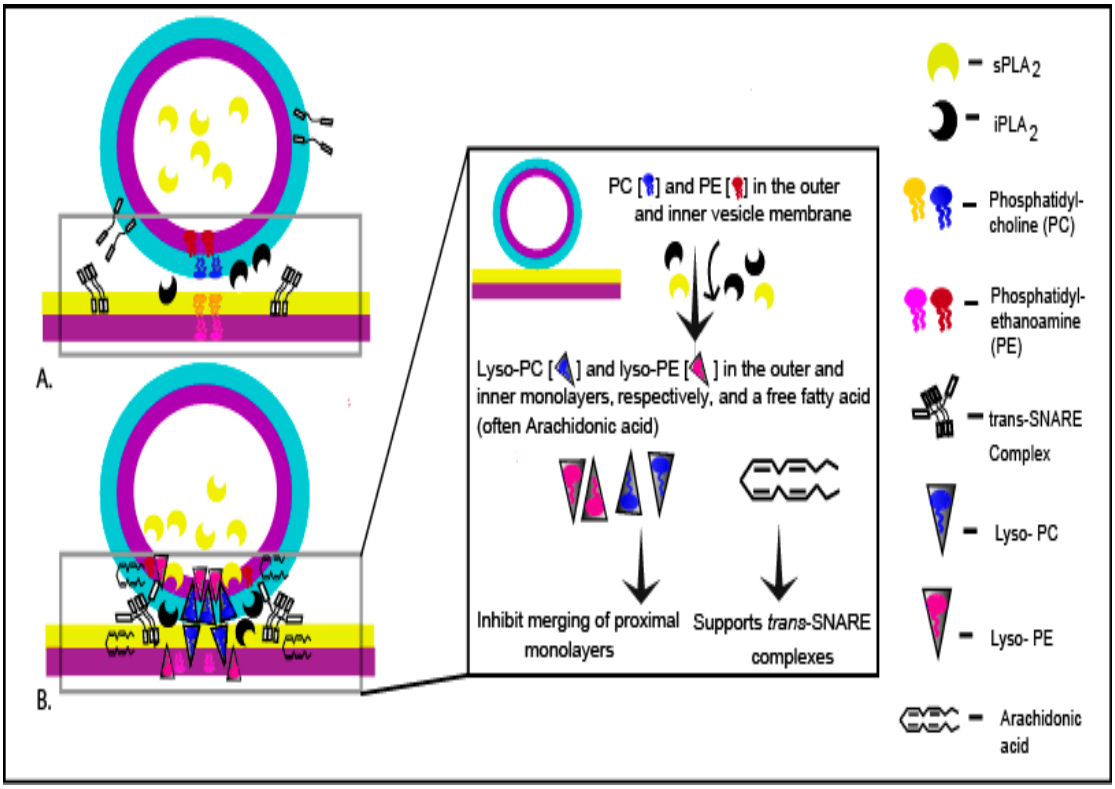

Figure 9. Working hypothesis: (**A**) Non-contacting membranes (**B**) Vesicle docked with the plasma membrane (PM). At basal rate, the vesicle luminal $sPLA_2$ and membrane bound $iPLA_2$ cleave PE and PC in the inner and outer monolayer, respectively; PM bound $iPLA_2$ also cleaves PC in the inner monolayer of the PM. This causes a local increase in LPC at the membrane contact site that is balanced by intermittent LPE production at the adjacent inner membrane via transient $sPLA_2$ activity. This mechanism may thus act as a native fusion 'brake' and the released FFA (often Arachidonic acid) may support *trans* SNARE complex formation to ensure and maintain efficient priming/docking. (adapted from [29] with permission).

6. Conclusions

The data confirm (i) the presence of endogenous, catalytically active CV associated PLA_2 isozymes—a CV luminal $sPLA_2$ and an $iPLA_2$ associated with the outer CV membrane; and (ii) that proteolytic removal of CV surface proteins including $iPLA_2$ or the pharmacological inhibition of both the isozymes significantly reduces priming and/or docking. Based on this as well as previously measured vesicular Ca^{2+} transients, basal Ca^{2+} dependent CV luminal $sPLA_2$ activity and CV membrane attached $iPLA_2$ would appear to act together to support efficient vesicle priming and/or docking. While intriguing, this warrants further study, particularly relating to the apparent effects of FFA on the formation of SNARE complexes and/or in modulating membrane biophysical properties, as FFA is also known to induce the transition from the bilayer to the hexagonal phase upon its incorporation in the membrane [10,107,110].

Supplementary Materials: The following are available online at http://www.mdpi.com/2073-4409/8/4/303/s1. Figure S1: Endogenous TAG levels in (**A**) CSC; n = 3–5 and (**B**) CV; n = 3–8 treated with the indicated doses of LY311727, BEL and FKGK-11, including representative chromatograms showing changes in neutral lipids. Figure S2: (**A**) SDS-PAGE of total CV membrane protein isolated from trypsin treated CV and the parallel untreated control; (**B**) secondary antibody control western blot to identify non-specific protein binding. A total of 5 µg CV membrane protein per lane was resolved.

Author Contributions: J.R.C. conceptualized the study and provided all resources and funding. J.R.C. and D.D. designed the methodology. D.D. carried out the investigation, data curation and analysis. D.D. and J.R.C. interpreted the data. D.D. wrote the original draft. D.D. and J.R.C. wrote the final manuscript.

Funding: This study is supported by funding from the National Health and Medical Research Council (NHMRC–APP1065328) of Australia and an anonymous family foundation.

Acknowledgments: J.R.C. is grateful to an anonymous family foundation for providing initial financial support for this work and acknowledges targeted funding from the National Health and Medical Research Council (NHMRC–APP1065328). DD thanks Western Sydney University (WSU), School of Medicine (SOM) for a Post Graduate Research Award. DD and JRC thank Ashleigh Deschamps WSU, SOM for urchin collections and maintenance of the aquatic facility. We also thank David Messiah, Lana Kajlich and the Underwater Research Group of NSW for additional urchin collections.

Conflicts of Interest: The authors declare no conflict of interest.

Abbreviations

ARA	arachidonic acid
$[Ca^{2+}]$free	free calcium ion concentration
cCBB	colloidal Coomassie brilliant blue G-250 dye
CHAPS	3-[(3-Cholamidopropyl) dimethylammonio]-1-propanesulfonate hydrate
CHOL	cholesterol
CE	cholesterol ester
CSC	cell surface complexes
CV	cortical vesicles
FFA	free fatty acid
DAG	diacylglycerol
LPC	lyso-phosphatidylcholine
PC, PE, PI, PG, PS	phosphatidyl-choline, -ethanolamine, -inositol, -glycerol, -serine
MAG	monoacylglycerol
pI	isoelectric point
PED6	(*N*-((6-(2,4-dinitrophenyl) amino) hexanoyl)-2-(4,4-difluoro-5,7-dimethyl-4-Bora-3a,4a-diaza-s-Indacene-3-pentanoyl)-1-hexadecanoyl-sn-glycero-3-phosphoethanolamine, triethylammonium salt
SV	synaptic vesicles
TAG	triacylglycerol

References

1. Frye, R.A.; Holz, R.W. The relationship between arachidonic acid release and catecholamine secretion from cultured bovine adrenal chromaffin cells. *J. Neurochem.* **1984**, *43*, 146–150. [CrossRef]
2. Frye, R.A.; Holz, R.W. Arachidonic acid release and catecholamine secretion from digitonin-treated chromaffin cells: Effects of micromolar calcium, phorbol ester and protein alkylating agents. *J. Neurochem.* **1985**, *44*, 265–273. [CrossRef]
3. Juhl, K.; Hoy, M.; Olsen, H.L.; Bokvist, K.; Efanov, A.M.; Hoffmann, E.K.; Gromada, J. cPLA$_2$ alpha-evoked formation of arachidonic acid and lysophospholipids is required for exocytosis in mouse pancreatic beta-cells. *Am. J. Physiol. Endocrinol. Metab.* **2003**, *285*, E73–E81. [CrossRef]
4. Latham, C.F.; Osborne, S.L.; Cryle, M.J.; Meunier, F.A. Arachidonic acid potentiates exocytosis and allows neuronal SNARE complex to interact with Munc18a. *J. Neurochem.* **2007**, *100*, 1543–1554. [CrossRef]
5. Matsuzawa, A.; Murakami, M.; Atsumi, G.; Imai, K.; Prados, P.; Inoue, K.; Kudo, I. Release of secretory phospholipase A2 from rat neuronal cells and its possible function in the regulation of catecholamine secretion. *Biochem. J.* **1996**, *318*, 701–709. [CrossRef] [PubMed]
6. Moskowitz, N.; Schook, W.; Puszkin, S. Interaction of brain synaptic vesicles induced by endogenous Ca^{2+}-dependent phospholipase A2. *Science* **1982**, *216*, 305–307. [CrossRef] [PubMed]
7. Ray, P.; Berman, J.D.; Middleton, W.; Brendle, J. Botulinum toxin inhibits arachidonic acid release associated with acetylcholine release from PC12 cells. *J. Biol. Chem.* **1993**, *268*, 11057–11064. [PubMed]
8. Ray, P.; Ishida, H.; Millard, C.B.; Petrali, J.P.; Ray, R. Phospholipaise A2 and arachidonic acid-mediated mechanism of neuroexocytosis: A possible target of botidinum neurotoxin A other then SNAP-25. *J. Appl. Toxicol.* **1999**, *19*, S27–S28. [CrossRef]
9. Karli, U.O.; Schafer, T.; Burger, M.M. Fusion of neurotransmitter vesicles with target membrane is calcium independent in a cell-free system. *Proc. Natl. Acad. Sci. USA* **1990**, *87*, 5912–5915. [CrossRef] [PubMed]
10. Chernomordik, L.; Chanturiya, A.; Green, J.; Zimmerberg, J. The hemifusion intermediate and its conversion to complete fusion: Regulation by membrane composition. *Biophys. J.* **1995**, *69*, 922–929. [CrossRef]
11. Chernomordik, L.V.; Vogel, S.S.; Sokoloff, A.; Onaran, H.O.; Leikina, E.A.; Zimmerberg, J. Lysolipids reversibly inhibit Ca^{2+}-, GTP- and pH-dependent fusion of biological membranes. *FEBS Lett.* **1993**, *318*, 71–76. [CrossRef]
12. Reese, C.; Mayer, A. Transition from hemifusion to pore opening is rate limiting for vacuole membrane fusion. *J. Cell Biol.* **2005**, *171*, 981–990. [CrossRef] [PubMed]
13. Uriarte, S.M.; Powell, D.W.; Luerman, G.C.; Merchant, M.L.; Cummins, T.D.; Jog, N.R.; Ward, R.A.; McLeish, K.R. Comparison of Proteins Expressed on Secretory Vesicle Membranes and Plasma Membranes of Human Neutrophils. *J. Immunol.* **2008**, *180*, 5575–5581. [CrossRef] [PubMed]
14. Wegrzyn, J.L.; Bark, S.J.; Funkelstein, L.; Mosier, C.; Yap, A.; Kazemi-Esfarjani, P.; La Spada, A.R.; Sigurdson, C.; O'Connor, D.T.; Hook, V. Proteomics of Dense Core Secretory Vesicles Reveal Distinct Protein Categories for Secretion of Neuroeffectors for Cell−Cell Communication. *J. Proteome Res.* **2010**, *9*, 5002–5024. [CrossRef]
15. Brunner, Y.; Couté, Y.; Iezzi, M.; Foti, M.; Fukuda, M.; Hochstrasser, D.F.; Wollheim, C.B.; Sanchez, J.-C. Proteomics Analysis of Insulin Secretory Granules. *Mol. Cell. Proteom.* **2007**, *6*, 1007–1017. [CrossRef] [PubMed]
16. Schvartz, D.; Brunner, Y.; Coute, Y.; Foti, M.; Wollheim, C.B.; Sanchez, J.C. Improved characterization of the insulin secretory granule proteomes. *J. Proteom.* **2012**, *75*, 4620–4631. [CrossRef] [PubMed]
17. Chock, S.P.; Schmauder-Chock, E.A.; Cordella-Miele, E.; Miele, L.; Mukherjee, A.B. The localization of phospholipase A2 in the secretory granule. *Biochem. J.* **1994**, *300*, 619–622. [CrossRef]
18. Bingham, C.O.; Fijneman, R.J.A.; Friend, D.S.; Goddeau, R.P.; Rogers, R.A.; Austen, K.F.; Arm, J.P. Low Molecular Weight Group IIA and Group V Phospholipase A2 Enzymes Have Different Intracellular Locations in Mouse Bone Marrow-derived Mast Cells. *J. Biol. Chem.* **1999**, *274*, 31476–31484. [CrossRef]
19. Moskowitz, N.; Puszkin, S.; Schook, W. Characterization of brain synaptic vesicle phospholipase A2 activity and its modulation by calmodulin, prostaglandin E2, prostaglandin F2 alpha, cyclic AMP and ATP. *J. Neurochem.* **1983**, *41*, 1576–1586. [CrossRef]
20. Moskowitz, N.; Schook, W.; Puszkin, S. Regulation of endogenous calcium-dependent synaptic membrane phospholipase A2. *Brain Res.* **1984**, *290*, 273–280. [CrossRef]
21. Takamori, S.; Holt, M.; Stenius, K.; Lemke, E.A.; Grønborg, M.; Riedel, D.; Urlaub, H.; Schenck, S.; Brügger, B.; Ringler, P.; et al. Molecular Anatomy of a Trafficking Organelle. *Cell* **2006**, *127*, 831–846. [CrossRef] [PubMed]

22. Marco, M.; Jacqueline, B.; Carsten, C.; Michael, K.; Herbert, Z.; Walter, V. Immunoisolation of two synaptic vesicle pools from synaptosomes: A proteomics analysis. *J. Neurochem.* **2005**, *95*, 1732–1745. [CrossRef]
23. Heo, S.; Diering, G.H.; Na, C.H.; Nirujogi, R.S.; Bachman, J.L.; Pandey, A.; Huganir, R.L. Identification of long-lived synaptic proteins by proteomic analysis of synaptosome protein turnover. *Proc. Natl. Acad. Sci. USA* **2018**, *115*, E3827–E3836. [CrossRef]
24. Boyken, J.; Grønborg, M.; Riedel, D.; Urlaub, H.; Jahn, R.; Chua, J.J.E. Molecular Profiling of Synaptic Vesicle Docking Sites Reveals Novel Proteins but Few Differences between Glutamatergic and GABAergic Synapses. *Neuron* **2013**, *78*, 285–297. [CrossRef] [PubMed]
25. Dennis, E.A. The growing phospholipase A2 superfamily of signal transduction enzymes. *Trends Biochem. Sci.* **1997**, *22*, 1–2. [CrossRef]
26. Farooqui, A.A.; Yang, H.C.; Rosenberger, T.A.; Horrocks, L.A. Phospholipase A2 and its role in brain tissue. *J. Neurochem.* **1997**, *69*, 889–901. [CrossRef] [PubMed]
27. Kudo, I.; Murakami, M.; Hara, S.; Inoue, K. Mammalian non-pancreatic phospholipases A2. *Biochim. Biophys. Acta (Bba) Lipids Lipid Metab.* **1993**, *1170*, 217–231. [CrossRef]
28. Mounier, C.M.; Ghomashchi, F.; Lindsay, M.R.; James, S.; Singer, A.G.; Parton, R.G.; Gelb, M.H. Arachidonic Acid Release from Mammalian Cells Transfected with Human Groups IIA and X Secreted Phospholipase A2 Occurs Predominantly during the Secretory Process and with the Involvement of Cytosolic Phospholipase A2-α. *J. Biol. Chem.* **2004**, *279*, 25024–25038. [CrossRef]
29. Dabral, D.; Coorssen, J.R. Phospholipase A2: Potential roles in native membrane fusion. *Int. J. Biochem. Cell Biol.* **2017**, *85*, 1–5. [CrossRef]
30. Raveh, A.; Valitsky, M.; Shani, L.; Coorssen, J.R.; Blank, P.S.; Zimmerberg, J.; Rahamimoff, R. Observations of Calcium Dynamics in Cortical Secretory Vesicles. *Cell Calcium* **2012**, *52*, 217–225. [CrossRef]
31. Estévez-Herrera, J.; Domínguez, N.; Pardo, M.R.; González-Santana, A.; Westhead, E.W.; Borges, R.; Machado, J.D. ATP: The crucial component of secretory vesicles. *Proc. Natl. Acad. Sci. USA* **2016**, *113*, E4098–E4106. [CrossRef]
32. Winkler, H.; Westhead, E. Th molecular organization of adrenal chromaffin granules. *Neuroscience* **1980**, *5*, 1803–1823. [CrossRef]
33. Jaime, S.; Laura, V.; Marcial, C.; Esther, H.S.; Fonteriz, R.I.; Lobaton, C.D.; Mayte, M.; Alfredo, M.; Javier, A. Calcium dynamics in bovine adrenal medulla chromaffin cell secretory granules. *Eur. J. Neurosci.* **2008**, *28*, 1265–1274. [CrossRef]
34. Balsinde, J.; Balboa, M.A.; Dennis, E.A. Antisense inhibition of group VI Ca^{2+}-independent phospholipase A2 blocks phospholipid fatty acid remodeling in murine P388D1 macrophages. *J. Biol. Chem.* **1997**, *272*, 29317–29321. [CrossRef] [PubMed]
35. Ramanadham, S.; Ali, T.; Ashley, J.W.; Bone, R.N.; Hancock, W.D.; Lei, X. Calcium-independent phospholipases A2 and their roles in biological processes and diseases. *J. Lipid Res.* **2015**, *56*, 1643–1668. [CrossRef]
36. Six, D.A.; Dennis, E.A. The expanding superfamily of phospholipase A(2) enzymes: Classification and characterization. *Biochim. Biophys. Acta* **2000**, *1488*, 1–19. [CrossRef]
37. Murakami, M.; Taketomi, Y.; Miki, Y.; Sato, H.; Hirabayashi, T.; Yamamoto, K. Recent progress in phospholipase A2 research: From cells to animals to humans. *Prog. Lipid Res.* **2011**, *50*, 152–192. [CrossRef]
38. Abbineni, P.S.; Wright, E.P.; Rogasevskaia, T.P.; Killingsworth, M.C.; Malladi, C.S.; Coorssen, J.R. The Sea Urchin Egg and Cortical Vesicles as Model Systems to Dissect the Fast, Ca^{2+}-Triggered Steps of Regulated Exocytosis. In *Exocytosis Methods*; Thorn, P., Ed.; Humana Press: Totowa, NJ, USA, 2014; pp. 221–241.
39. Zimmerberg, J.; Coorssen, J.R.; Vogel, S.S.; Blank, P.S. Sea urchin egg preparations as systems for the study of calcium-triggered exocytosis. *J. Physiol.* **1999**, *520*, 15–21. [CrossRef]
40. Sodergren, E.; Weinstock, G.M.; Davidson, E.H.; Cameron, R.A.; Gibbs, R.A.; Angerer, R.C.; Angerer, L.M.; Arnone, M.I.; Burgess, D.R.; Burke, R.D.; et al. The genome of the sea urchin Strongylocentrotus purpuratus. *Science* **2006**, *314*, 941–952. [CrossRef]
41. Tahara, M.; Coorssen, J.R.; Timmers, K.; Blank, P.S.; Whalley, T.; Scheller, R.; Zimmerberg, J. Calcium Can Disrupt the SNARE Protein Complex on Sea Urchin Egg Secretory Vesicles without Irreversibly Blocking Fusion. *J. Biol. Chem.* **1998**, *273*, 33667–33673. [CrossRef]
42. Coorssen, J.R.; Blank, P.S.; Tahara, M.; Zimmerberg, J. Biochemical and Functional Studies of Cortical Vesicle Fusion: The SNARE Complex and Ca^{2+} Sensitivity. *J. Cell Biol.* **1998**, *143*, 1845–1857. [CrossRef]

43. Szule, J.A.; Jarvis, S.E.; Hibbert, J.E.; Spafford, J.D.; Braun, J.E.A.; Zamponi, G.W.; Wessel, G.M.; Coorssen, J.R. Calcium-triggered Membrane Fusion Proceeds Independently of Specific Presynaptic Proteins. *J. Biol. Chem.* **2003**, *278*, 24251–24254. [CrossRef] [PubMed]
44. Sean, C.; David, L.; Gary, W. Members of the SNARE hypothesis are associated with cortical granule exocytosis in the sea urchin egg. *Mol. Reprod. Dev.* **1997**, *48*, 106–118. [CrossRef]
45. Coorssen, J.R.; Blank, P.S.; Albertorio, F.; Bezrukov, L.; Kolosova, I.; Chen, X.; Backlund, P.S.; Zimmerberg, J. Regulated secretion: SNARE density, vesicle fusion and calcium dependence. *J. Cell Sci.* **2003**, *116*, 2087–2097. [CrossRef] [PubMed]
46. Avery, J.; Hodel, A.; Whitaker, M. In vitro exocytosis in sea urchin eggs requires a synaptobrevin-related protein. *J. Cell Sci.* **1997**, *110*, 1555–1561. [PubMed]
47. Rogasevskaia, T.; Coorssen, J.R. Sphingomyelin-enriched microdomains define the efficiency of native Ca^{2+}-triggered membrane fusion. *J. Cell Sci.* **2006**, *119*, 2688–2694. [CrossRef] [PubMed]
48. Rogasevskaia, T.P.; Churchward, M.A.; Coorssen, J.R. Anionic lipids in Ca(2+)-triggered fusion. *Cell Calcium* **2012**, *52*, 259–269. [CrossRef]
49. Rogasevskaia, T.P.; Coorssen, J.R. The role of phospholipase D in regulated exocytosis. *J. Biol. Chem.* **2015**, *290*, 28683–28696. [CrossRef]
50. Rogasevskaia, T.P.; Coorssen, J.R. A new approach to the molecular analysis of docking, priming and regulated membrane fusion. *J. Chem. Biol.* **2011**, *4*, 117–136. [CrossRef]
51. Churchward, M.A.; Rogasevskaia, T.; Höfgen, J.; Bau, J.; Coorssen, J.R. Cholesterol facilitates the native mechanism of Ca^{2+}-triggered membrane fusion. *J. Cell Sci.* **2005**, *118*, 4833–4848. [CrossRef]
52. Churchward, M.A.; Rogasevskaia, T.; Brandman, D.M.; Khosravani, H.; Nava, P.; Atkinson, J.K.; Coorssen, J.R. Specific Lipids Supply Critical Negative Spontaneous Curvature—An Essential Component of Native Ca^{2+}-Triggered Membrane Fusion. *Biophys. J.* **2008**, *94*, 3976–3986. [CrossRef]
53. Abbineni, P.; Coorssen, J. Application of High-Throughput Assays to Examine Phospho-Modulation of the Late Steps of Regulated Exocytosis. *High.-Throughput* **2017**, *6*, 17. [CrossRef] [PubMed]
54. Abbineni, P.S.; Coorssen, J.R. Sphingolipids modulate docking, Ca^{2+} sensitivity and membrane fusion of native cortical vesicles. *Int. J. Biochem. Cell Biol.* **2018**, *104*, 43–54. [CrossRef] [PubMed]
55. Zimmerberg, J.; Blank, P.S.; Kolosova, I.; Cho, M.-S.; Tahara, M.; Coorssen, J.R. A stage-specific preparation to study the Ca^{2+}-triggered fusion steps of exocytosis: Rationale and perspectives. *Biochimie* **2000**, *82*, 303–314. [CrossRef]
56. Churchward, M.A.; Brandman, D.M.; Rogasevskaia, T.; Coorssen, J.R. Copper (II) sulfate charring for high sensitivity on-plate fluorescent detection of lipids and sterols: Quantitative analyses of the composition of functional secretory vesicles. *J. Chem. Biol.* **2008**, *1*, 79–87. [CrossRef] [PubMed]
57. Butt, R.H.; Coorssen, J.R. Postfractionation for Enhanced Proteomic Analyses: Routine Electrophoretic Methods Increase the Resolution of Standard 2D-PAGE. *J. Proteome Res.* **2005**, *4*, 982–991. [CrossRef] [PubMed]
58. Bligh, E.G.; Dyer, W.J. A rapid method of total lipid extraction and purification. *Can. J. Biochem. Physiol.* **1959**, *37*, 911–917. [CrossRef] [PubMed]
59. Hall, B.G. Building Phylogenetic Trees from Molecular Data with MEGA. *Mol. Biol. Evol.* **2013**, *30*, 1229–1235. [CrossRef]
60. Kumar, S.; Stecher, G.; Tamura, K. MEGA7: Molecular Evolutionary Genetics Analysis Version 7.0 for Bigger Datasets. *Mol. Biol. Evol.* **2016**, *33*, 1870–1874. [CrossRef]
61. Coorssen, J.R.; Blank, P.S.; Albertorio, F.; Bezrukov, L.; Kolosova, I.; Backlund, P.S., Jr.; Zimmerberg, J. Quantitative femto- to attomole immunodetection of regulated secretory vesicle proteins critical to exocytosis. *Anal. Biochem.* **2002**, *307*, 54–62. [CrossRef]
62. Gauci, V.J.; Padula, M.P.; Coorssen, J.R. Coomassie blue staining for high sensitivity gel-based proteomics. *J. Proteom.* **2013**, *90*, 96–106. [CrossRef]
63. Noaman, N.; Abbineni, P.S.; Withers, M.; Coorssen, J.R. Coomassie staining provides routine (sub)femtomole in-gel detection of intact proteoforms: Expanding opportunities for genuine Top-down Proteomics. *Electrophoresis* **2017**, *38*, 3086–3099. [CrossRef]
64. Balsinde, J.; Bianco, I.D.; Ackermann, E.J.; Conde-Frieboes, K.; Dennis, E.A. Inhibition of calcium-independent phospholipase A2 prevents arachidonic acid incorporation and phospholipid remodeling in P388D1 macrophages. *Proc. Natl. Acad. Sci. USA* **1995**, *92*, 8527–8531. [CrossRef] [PubMed]

65. Jenkins, C.M.; Mancuso, D.J.; Yan, W.; Sims, H.F.; Gibson, B.; Gross, R.W. Identification, Cloning, Expression and Purification of Three Novel Human Calcium-independent Phospholipase A2 Family Members Possessing Triacylglycerol Lipase and Acylglycerol Transacylase Activities. *J. Biol. Chem.* **2004**, *279*, 48968–48975. [CrossRef] [PubMed]
66. Farooqui, A.A.; Litsky, M.L.; Farooqui, T.; Horrocks, L.A. Inhibitors of intracellular phospholipase A2 activity: Their neurochemical effects and therapeutical importance for neurological disorders. *Brain Res. Bull.* **1999**, *49*, 139–153. [CrossRef]
67. Hsu, Y.-H.; Bucher, D.; Cao, J.; Li, S.; Yang, S.-W.; Kokotos, G.; Woods, V.L.; McCammon, J.A.; Dennis, E.A. Fluoroketone Inhibition of Ca^{2+}-Independent Phospholipase A2 through Binding Pocket Association Defined by Hydrogen/Deuterium Exchange and Molecular Dynamics. *J. Am. Chem. Soc.* **2013**, *135*, 1330–1337. [CrossRef]
68. Tibes, U. Phospholipase A2 inhibitors in development. *Expert Opin. Investig. Drugs* **1997**, *6*, 279–298. [CrossRef]
69. Baker, P.F.; Whitaker, M.J. Influence of ATP and calcium on the cortical reaction in sea urchin eggs. *Nature* **1978**, *276*, 513. [CrossRef] [PubMed]
70. Vacquier, V.D. The isolation of intact cortical granules from sea urchin eggs: Calcium lons trigger granule discharge. *Dev. Biol.* **1975**, *43*, 62–74. [CrossRef]
71. Balsinde, J.; Dennis, E.A. Bromoenol lactone inhibits magnesium-dependent phosphatidate phosphohydrolase and blocks triacylglycerol biosynthesis in mouse P388D1 macrophages. *J. Biol. Chem.* **1996**, *271*, 31937–31941. [CrossRef]
72. Ramanadham, S.; Wolf, M.J.; Jett, P.A.; Gross, R.W.; Turk, J. Characterization of an ATP-stimulatable Ca(2+)-independent phospholipase A2 from clonal insulin-secreting HIT cells and rat pancreatic islets: A possible molecular component of the beta-cell fuel sensor. *Biochemistry* **1994**, *33*, 7442–7452. [CrossRef] [PubMed]
73. Cameron, R.A. Comparing the Human and Sea Urchin Genomes. In *eLS*; John Wiley & Sons, Inc.: Hoboken, NJ, USA, 2013. [CrossRef]
74. Bradham, C.A.; Foltz, K.R.; Beane, W.S.; Arnone, M.I.; Rizzo, F.; Coffman, J.A.; Mushegian, A.; Goel, M.; Morales, J.; Geneviere, A.-M.; et al. The sea urchin kinome: A first look. *Dev. Biol.* **2006**, *300*, 180–193. [CrossRef] [PubMed]
75. Ramanadham, S.; Hsu, F.F.; Zhang, S.; Jin, C.; Bohrer, A.; Song, H.; Bao, S.; Ma, Z.; Turk, J. Apoptosis of insulin-secreting cells induced by endoplasmic reticulum stress is amplified by overexpression of group VIA calcium-independent phospholipase A2 (iPLA2 beta) and suppressed by inhibition of iPLA2 beta. *Biochemistry* **2004**, *43*, 918–930. [CrossRef] [PubMed]
76. Song, H.; Bao, S.; Lei, X.; Jin, C.; Zhang, S.; Turk, J.; Ramanadham, S. Evidence for proteolytic processing and stimulated organelle redistribution of iPLA2β. *Biochim. Biophys. Acta (Bba) Mol. Cell Biol. Lipids* **2010**, *1801*, 547–558. [CrossRef]
77. Larsson, P.K.A.; Claesson, H.-E.; Kennedy, B.P. Multiple Splice Variants of the Human Calcium-independent Phospholipase A2 and Their Effect on Enzyme Activity. *J. Biol. Chem.* **1998**, *273*, 207–214. [CrossRef]
78. Song, H.; Ramanadham, S.; Bao, S.; Hsu, F.-F.; Turk, J. A Bromoenol Lactone Suicide Substrate Inactivates Group VIA Phospholipase A(2) by Generating a Diffiusible Bromomethyl Keto Acid That Alkylates Cysteine Thiols. *Biochemistry* **2006**, *45*, 1061–1073. [CrossRef] [PubMed]
79. Darrow, A.L.; Olson, M.W.; Xin, H.; Burke, S.L.; Smith, C.; Schalk-Hihi, C.; Williams, R.; Bayoumy, S.S.; Deckman, I.C.; Todd, M.J.; et al. A novel fluorogenic substrate for the measurement of endothelial lipase activity. *J. Lipid Res.* **2011**, *52*, 374–382. [CrossRef]
80. Kim, Y.J.; Kim, K.P.; Rhee, H.J.; Das, S.; Rafter, J.D.; Oh, Y.S.; Cho, W. Internalized group V secretory phospholipase A2 acts on the perinuclear membranes. *J. Biol. Chem.* **2002**, *277*, 9358–9365. [CrossRef] [PubMed]
81. Coorssen, J.R. Phospholipase activation and secretion: Evidence that PLA2, PLC and PLD are not essential to exocytosis. *Am. J. Physiol. Cell Physiol.* **1996**, *270*, C1153–C1163. [CrossRef] [PubMed]
82. Balsinde, J.; Winstead, M.V.; Dennis, E.A. Phospholipase A2 regulation of arachidonic acid mobilization. *FEBS Lett.* **2002**, *531*, 2–6. [CrossRef]
83. Peterson, M.E.; Chen, F.; Saven, J.G.; Roos, D.S.; Babbitt, P.C.; Sali, A. Evolutionary constraints on structural similarity in orthologs and paralogs. *Protein Sci. A Publ. Protein Soc.* **2009**, *18*, 1306–1315. [CrossRef]

84. Hazen, S.L.; Stuppy, R.J.; Gross, R.W. Purification and characterization of canine myocardial cytosolic phospholipase A2. A calcium-independent phospholipase with absolute f1-2 regiospecificity for diradyl glycerophospholipids. *J. Biol. Chem.* **1990**, *265*, 10622–10630. [PubMed]
85. Rosenthal, M.D.; Gordon, M.N.; Buescher, E.S.; Slusser, J.H.; Harris, L.K.; Franson, R.C. Human Neutrophils Store Type II 14-kDa Phospholipase A2 in Granules and Secrete Active Enzyme in Response to Soluble Stimuli. *Biochem. Biophys. Res. Commun.* **1995**, *208*, 650–656. [CrossRef] [PubMed]
86. Suzuki, N.; Ishizaki, J.; Yokota, Y.; Higashino, K.; Ono, T.; Ikeda, M.; Fujii, N.; Kawamoto, K.; Hanasaki, K. Structures, enzymatic properties and expression of novel human and mouse secretory phospholipase A(2)s. *J. Biol. Chem.* **2000**, *275*, 5785–5793. [CrossRef]
87. Zupan, L.A.; Steffens, D.L.; Berry, C.A.; Landt, M.; Gross, R.W. Cloning and expression of a human 14-3-3 protein mediating phospholipolysis. Identification of an arachidonoyl-enzyme intermediate during catalysis. *J. Biol. Chem.* **1992**, *267*, 8707–8710. [PubMed]
88. Wilkins, M.R.; Lindskog, I.; Gasteiger, E.; Bairoch, A.; Sanchez, J.C.; Hochstrasser, D.F.; Appel, R.D. Detailed peptide characterization using PEPTIDEMASS—A World-Wide-Web-accessible tool. *Electrophoresis* **1997**, *18*, 403–408. [CrossRef] [PubMed]
89. Szule, J.A.; Fuller, N.L.; Rand, R.P. The effects of acyl chain length and saturation of diacylglycerols and phosphatidylcholines on membrane monolayer curvature. *Biophys. J.* **2002**, *83*, 977–984. [CrossRef]
90. Furber, K.L.; Churchward, M.A.; Rogasevskaia, T.P.; Coorssen, J.R. Identifying Critical Components of Native Ca^{2+}-triggered Membrane Fusion. *Ann. N. Y. Acad. Sci.* **2009**, *1152*, 121–134. [CrossRef]
91. Furber, K.L.; Dean, K.T.; Coorssen, J.R. Dissecting the mechanism of Ca^{2+} triggered membrane fusion: Probing protein function using thiol reactivity. *Clin. Exp. Pharmacol. Physiol.* **2010**, *37*, 208–217. [CrossRef]
92. Furber, K.L.; Brandman, D.M.; Coorssen, J.R. Enhancement of the Ca(2+)-triggering steps of native membrane fusion via thiol-reactivity. *J. Chem. Biol.* **2009**, *2*, 27–37. [CrossRef]
93. Spessard, G.O. ACD Labs/LogP dB 3.5 and ChemSketch 3.5. *J. Chem. Inf. Comput. Sci.* **1998**, *38*, 1250–1253. [CrossRef]
94. Chernomordik, L.; Kozlov, M.M.; Zimmerberg, J. Lipids in biological membrane fusion. *J. Membarin Biol.* **1995**, *146*, 1–14. [CrossRef]
95. Chernomordik, L.V.; Kozlov, M.M. Mechanics of membrane fusion. *Nat. Struct. Mol. Biol.* **2008**, *15*, 675–683. [CrossRef]
96. Kozlov, M.M.; Leikin, S.L.; Chernomordik, L.V.; Markin, V.S.; Chizmadzhev, Y.A. Stalk mechanism of vesicle fusion. *Eur. Biophys. J.* **1989**, *17*, 121–129. [CrossRef]
97. Kozlovsky, Y.; Kozlov, M.M. Stalk Model of Membrane Fusion: Solution of Energy Crisis. *Biophys. J.* **2002**, *82*, 882–895. [CrossRef]
98. Fuller, N.; Rand, R.P. The influence of lysolipids on the spontaneous curvature and bending elasticity of phospholipid membranes. *Biophys. J.* **2001**, *81*, 243–254. [CrossRef]
99. Gillot, I.; Ciapa, B.; Payan, P.; Sardet, C. The calcium content of cortical granules and the loss of calcium from sea urchin eggs at fertilization. *Dev. Biol.* **1991**, *146*, 396–405. [CrossRef]
100. Mahapatra, N.R.; Mahata, M.; Hazra, P.P.; McDonough, P.M.; O'Connor, D.T.; Mahata, S.K. A Dynamic Pool of Calcium in Catecholamine Storage Vesicles: Exploration in living cells by a novel vesicle-targeted chromogranin a-aequorin chimeric photoprotein. *J. Biol. Chem.* **2004**, *279*, 51107–51121. [CrossRef] [PubMed]
101. Leitner, J.W.; Sussman, K.E.; Vatter, A.E.; Schneider, F.H. Adenine nucleotides in the secretory granule fraction of rat islets. *Endocrinology* **1975**, *96*, 662–677. [CrossRef] [PubMed]
102. Brash, A.R. Arachidonic acid as a bioactive molecule. *J. Clin. Investig.* **2001**, *107*, 1339–1345. [CrossRef] [PubMed]
103. Hamilton, J.A. Fatty acid transport: Difficult or easy? *J. Lipid Res.* **1998**, *39*, 467–481.
104. Alder-Baerens, N.; Lisman, Q.; Luong, L.; Pomorski, T.; Holthuis, J.C.M. Loss of P4 ATPases Drs2p and Dnf3p Disrupts Aminophospholipid Transport and Asymmetry in Yeast Post-Golgi Secretory Vesicles. *Mol. Biol. Cell* **2006**, *17*, 1632–1642. [CrossRef] [PubMed]
105. Galli, C.; Risé, P.; Marangoni, F. Fate of exogenous arachidonic acid in THP-1 cells: Incorporation in cell lipids and conversion to other N-6 fatty acids. *ProstaglandinsLeukot. Essent. Fat. Acids* **1995**, *52*, 103–106. [CrossRef]
106. Ibarguren, M.; López, D.J.; Escribá, P.V. The effect of natural and synthetic fatty acids on membrane structure, microdomain organization, cellular functions and human health. *Biochim. Biophys. Acta (Bba) Biomembr.* **2014**, *1838*, 1518–1528. [CrossRef] [PubMed]

107. Epand, R.M.; Epand, R.F.; Ahmed, N.; Chen, R. Promotion of hexagonal phase formation and lipid mixing by fatty acids with varying degrees of unsaturation. *Chem. Phys. Lipids* **1991**, *57*, 75–80. [CrossRef]
108. Darios, F.; Davletov, B. Omega-3 and omega-6 fatty acids stimulate cell membrane expansion by acting on syntaxin 3. *Nature* **2006**, *440*, 813–817. [CrossRef] [PubMed]
109. Dulubova, I.; Sugita, S.; Hill, S.; Hosaka, M.; Fernandez, I.; Sudhof, T.C.; Rizo, J. A conformational switch in syntaxin during exocytosis: Role of munc18. *EMBO J.* **1999**, *18*, 4372–4382. [CrossRef] [PubMed]
110. Chernomordik, L. Non-bilayer lipids and biological fusion intermediates. *Chem. Phys. Lipids* **1996**, *81*, 203–213. [CrossRef]

CHAPTER – 3

Arachidonic acid and lysophosphatidylcholine inhibit multiple late steps of regulated exocytosis.

(published in Biochemical and Biophysical Research Communications, 2019)

https://doi.org/10.1016/j.bbrc.2019.05.106

Biochemical and Biophysical Research Communications xxx (xxxx) xxx

Contents lists available at ScienceDirect

Biochemical and Biophysical Research Communications

journal homepage: www.elsevier.com/locate/ybbrc

Arachidonic acid and lysophosphatidylcholine inhibit multiple late steps of regulated exocytosis

Deepti Dabral [a], Jens R. Coorssen [b, *]

[a] Molecular Physiology, Molecular Medicine Research Group, School of Medicine, Western Sydney University, Campbelltown Campus, NSW, 2560, Australia
[b] Departments of Health Sciences and Biological Sciences, Faculties of Applied Health Sciences and Mathematics & Science, Brock University, St. Catharines, ON, L2S 3A1, Canada

ARTICLE INFO

Article history:
Received 27 April 2019
Accepted 15 May 2019
Available online xxx

Keywords:
Native membrane fusion
Arachidonic acid
Lysophosphatidylcholine
Phospholipase A_2
ETYA
ET-18-OCH3

ABSTRACT

The canonical Phospholipase A_2 (PLA_2) metabolites lysophosphatidylcholine (LPC) and arachidonic acid (ARA) affect regulated exocytosis in a wide variety of cells and are proposed to directly influence membrane merger owing to their respective spontaneous curvatures. According to the Stalk-pore hypothesis, negative curvature ARA inhibits and promotes bilayer merger upon introduction into the distal or proximal monolayers, respectively; in contrast, with positive curvature, LPC has the opposite effects. Using fully primed, release-ready native cortical secretory vesicles (CV), well-established fusion assays and standardized lipid analyses, we show that exogenous ARA and LPC, as well as their non-metabolizable analogous, ETYA and ET-18-OCH3, inhibit the docking/priming and membrane merger steps, respectively, of regulated exocytosis.

1. Introduction

Membrane merger and fusion pore opening are the final steps in regulated exocytosis enabling the release of vesicular content into the extracellular space. Prior to this merger, vesicles must attach to the plasma membrane (PM) and undergo a series of molecular reactions to become fully docked, primed and release-ready, including formation of *trans* SNARE (soluble NSF attachment protein receptor; NSF, *N*-ethylmaleimide-sensitive factor) complexes. The proposed functions of SNARE complexes include docking and priming [1–5], and membrane fusion [3,5] (but also see Ref. [5] for other proposed functions); the latter is suggested to be driven by NH_2 terminus-to-COOH terminus 'zippering' of the parallel coiled-coil SNARE domains, that are proposed to pull adjacent membranes together [3], purportedly with sufficient energy to overcome intermembrane repulsive forces [3,5,6]. Yet, at native densities, in native membranes, such SNARE interactions alone do not 'drive' fusion [1,6–9]; indeed, complete ablation of SNAREs did not block Ca^{2+}-triggered fusion, implicating critical role(s) of other proteins and lipids in membrane merger and other late steps of exocytosis [1,2,10–12]. The *trans* SNARE interactions are said to initiate once membranes are ~8 nm apart, and zippering continues until membranes are ~2–4 nm apart, bringing adjacent membrane bilayers into their closest *estimated* proximity [13,14]. Although in close apposition (~3–8 nm, predicted by course-grain models; [13]), membranes still do not merge spontaneously due, at least in part, to intermembrane repulsive forces [14,15]. This may yield apposing contact sites that are (almost) purely lipidic. Furthermore, decreasing lysophosphatidylethanolamine (LPE), in the distal monolayers of contacting vesicles reduces docking/priming [12], consistent with a reduced fusion of dense core vesicles (DCV) to SNARE containing bilayers that have higher phosphatidylethanolamine (PE) in the distal monolayer [16]. Also, it is well known that lysophosphatidylcholine (LPC) in the proximal monolayers inhibits membrane merger [17–19]. In this regard, optimum levels and a critical balance between LPE and LPC on the distal and proximal monolayers of the apposed bilayers, respectively, at or near fusion sites, together seem to serve as a molecular brake to block 'spontaneous' membrane merger in an unstimulated state [11,12]. Nevertheless, upon Ca^{2+} triggering, membranes at the fusion site quickly merge, resulting in content release [20–22]. These fusion sites in native membranes are rich in cholesterol and sphingomyelin, that together organize microdomains that ensure fusion

Abbreviations: ARA, Arachidonic acid; ET-18-OCH3, 1-O-octadecyl-2-Omethyl-rac-*glycero*-3-phosphocholine; ETYA, Eicosatetraynoic Acid; LPC, lysophosphatidylcholine.

* Corresponding author.
E-mail addresses: d.dabral@uws.edu.au (D. Dabral), jcoorssen@brocku.ca (J.R. Coorssen).

https://doi.org/10.1016/j.bbrc.2019.05.106
0006-291X/

efficiency (e.g., Ca^{2+} sensing, docking/priming) [4,22–24]. Additionally, cholesterol acts as a key local contributor of negative curvature for progression to the hemifusion stage [4,22,25], while optimal levels of sphingolipids contribute to both the efficiency and capacity for fusion [23,26]. Other Ca^{2+} binding sites and effectors that may be localized at the fusion site as 'efficiency' factors include PS, cholesterol sulfate, and synaptotagmin [4,23,26,27].

Apart from modifying membrane biophysical properties, exogenous lipids, including (arachidonic acid; ARA) and LPC, alter protein-protein interactions [28–31], membrane enzyme activities [32,33] and membrane lipid homeostasis [11,32,34,35]. ARA enhances SNARE complex formation *in vitro* by acting on the regulatory Munc18, thus releasing syntaxin from Munc18/syntaxin complexes [30]. However, considering the high flip-flop rate of ARA ($t_{1/2}$ of seconds) [3, 50, 51], lateral movement [51, 52], rate of passive diffusion [53], conversion to other membrane lipid species [46,47] and its downstream metabolism to generate eicosanoids, it remains uncertain that ARA would be the active species to enhance *trans* SNARE complex formation *in vivo*. Importantly, native membranes contain enzymes that maintain lipid homeostasis [11,12,26], therefore, to tightly couple functional and molecular analyses, a quantitative assessment of the fate of exogenous lipids is always necessary [12,22,26,36].

Here we assessed the effects of the canonical PLA_2 metabolites, ARA and LPC, on the late steps of Ca^{2+} triggered native membrane fusion; their metabolic fate and functional contributions were confirmed by the parallel use of non-metabolizable analogous (Fig. 1).

2. Materials and methods

Reference lipids and oleoyl-LPC were from Avanti Polar Lipids (Alabaster, AL, USA). Arachidonic acid (20:4) was from Matreya LLC (Pennsylvania, USA). 1-*O*-octadecyl-2-*O*methyl-*rac*-*glycero*-3-phosphocholine (ET-18-OCH3) and Eicosatetraynoic Acid (ETYA) were from Cayman Chemical (Ann Arbor, USA). Silica G-60 High-Performance Thin Layer Chromatography (HPTLC) plates were from Merck Millipore Ltd. (Darmstadt, Germany). All salts, buffer components, and organic solvents were of at least analytical grade. All glassware used during lipid isolation was silanized (SigmaCote; Darmstadt, Germany). The dried samples were stored in silanized glass vials from Thermo Fisher Scientific (Oregon, USA).

CV treatment and Fusion assays: Native brown sea urchins (*Heliocedaris tuberculata*) were maintained at ~7° - 8 °C in the in-house aquatic facility [12]. CV were isolated from unfertilized eggs using a standardized protocol and suspended in Baseline Intracellular Medium, (BIM, 210 mM potassium glutamate, 500 mM glycine, 10 mM NaCl, 10 mM PIPES, 50 μM $CaCl_2$, 1 mM $MgCl_2$, 1 mM EGTA, pH 6.7) supplemented with 2.5 mM ATP, 2 mM DTT and protease inhibitors [1,2,10,12,22,25,36]. CV suspensions (OD 0.9 ± 0.05; $n = 10$) were treated with indicated concentrations of ARA, ETYA, LPC and ET-18-OCH3 for 10 min at 25 °C and diluted with 3–5 vol of ice-cold BIM, pH 6.7 immediately after incubation. Stock solutions of LPC and ARA were prepared in ethanol and delivered to CV suspensions to a final solvent concentration <0.1% [25]. ET-18-OCH3 and ETYA were dissolved in BIM (pH 6.7) and dimethyl sulfoxide, respectively; ETYA was delivered to a final solvent concentration <1% [12,22,25]. LPC and ET-18-OCH3 concentrations were selected based on previous work [10,37]; ARA and ETYA concentrations were selected based on considerations provided in Refs. [11,38]. CV fusion indicated by decrease in optical density (OD) was measured using a POLARstar Omega microplate reader (BMG Labtech, Offenburg, Germany). The final free Ca^{2+} concentration ($[Ca^{2+}]_{free}$) in parallel mock samples was measured with a Ca^{2+} sensitive electrode (Calcium Combination ISE, EDT directION Limited) [12,26]. Standard and 'settle' fusion assays were carried out as previously described [1,2,10,12,22,23,25,26,36]. Aliquots of CV suspension were snap frozen in liquid N_2 and stored at −80 °C for later molecular analyses.

Lipid normalization and analyses: Membrane protein was isolated in parallel with the total lipids, from the same CV aliquot, as described previously [12]. Briefly, CV were lysed for 90 s and isotonicity of the suspension immediately restored [12]. Membranes were recovered by centrifuging at 125,000×*g*, 4 °C, for 3 h

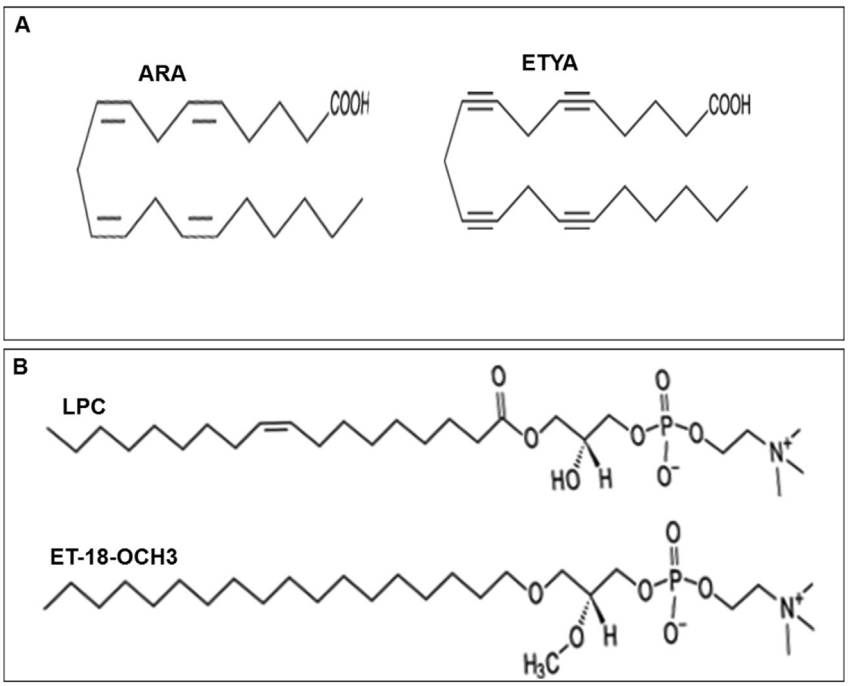

Fig. 1. Structures of (A) ARA and ETYA and; (B) LPC and ET-18-OCH3.

Please cite this article as: D. Dabral, J.R. Coorssen, Arachidonic acid and lysophosphatidylcholine inhibit multiple late steps of regulated exocytosis, Biochemical and Biophysical Research Communications, https://doi.org/10.1016/j.bbrc.2019.05.106

using a Beckman Coulter Optima™ L-100XP Ultracentrifuge. The resulting membrane pellet was solubilized in two-dimensional gel electrophoresis (2DE) buffer [39]. Protein quantification was via a solid-phase fluorescence-based assay using EZQ™ reagent from Invitrogen (Carlsbad, CA) [12]. Total CV lipids were extracted according to Bligh and Dyer, with established modifications [12,22,25,40,41]. Lipid corresponding to 1 μg and 2 μg of total membrane protein were assessed for neutral and phospholipids, respectively [12,40]. Activation of silica plates was by wetting with CH_3OH:ethyl acetate (6:4) using the AMD 2 multi-development unit (Muttenz, Switzerland) and subsequent heating at 110 °C for 30 min [12,22,25,40]. To resolve lipids, dried samples were dissolved in $CHCl_3$:CH_3OH (2:1 *v/v*) and loaded onto activated HPTLC plates using the CAMAG automated TLC Sampler (Muttenz, Switzerland). Neutral and phospholipids were resolved according to established methods [22,25,36,40] and visualized on-plate at 460 nm/605 nm (Ex/Em) using the ImageQuant™ LAS 4000 Biomolecular Imager (GE Healthcare, Buckinghamshire, UK) [12,40]. Images were analyzed using MultiGauge *v* 3.0 (Fuji Photo Film Co., Ltd. Tokyo, Japan). Lipids of interest were quantified via calibration curves of the appropriate standards, resolved in parallel with the sample lipids.

2.1. Data analysis

All conditions were tested in quadruplicate, and experiments replicated as indicated (n). Data were normalized by setting zero % fusion at <0.3 μM $[Ca^{2+}]_{free}$ and 100% fusion at >100 μM $[Ca^{2+}]_{free}$. Ca^{2+} activity curves were fit using a sigmoidal 4-parameter logistic model (PRISM 7.03; GraphPad, San Diego, US). Data are reported as mean ± SEM. Two-sample, two-tailed t-tests with $P < 0.05$ were considered significant.

3. Results and discussion

Using stage-specific, release-ready CV isolated from unfertilized sea urchin eggs, well-established fusion assays, and standardized lipid analyses [1,2,4,10,12,23,25,26,36,40], exogenous ARA and LPC are shown to inhibit vesicle docking/priming and membrane merger, respectively. This was further confirmed by their respective non-metabolizable analogues, ET-18-OCH3 and ETYA (Fig. 1).

ARA and LPC are ubiquitous, and small amounts of these metabolites are produced *in vivo* at any instant by endogenous PLA_2 [11,38]; limited enzyme activity also occurs in the CV membrane, maintaining FFA levels at ~15 fmol/μg MP in an unstimulated state [12]. Complexity arises due to various cellular PLA_2 isozymes [42], the high flipping rate of ARA [11,43,44], and the fact that both lysophospholipids and FFA promote as well as inhibit membrane merger based on their site of incorporation [11,18–20], thus posing challenges to dissect their specific roles in regulated exocytosis. Hence, high purity CV preparations lacking cytosolic components but retaining the minimal machinery necessary for Ca^{2+} sensing, docking/priming, and fusion [1,2,4,10,12,25,26,36], are exceptional models with which to dissect the role(s) of PLA_2 metabolites in the late stages of regulated exocytosis.

3.1. Effects of exogenous ARA and ETYA on fusion and their metabolic fate

Triggering CV with increasing $[Ca^{2+}]_{free}$ yielded a characteristic sigmoidal Ca^{2+} activity curve with an EC50 of 55.6 ± 3.8 μM $[Ca^{2+}]_{free}$ (Fig. 2A; $n = 5$) [1,10,12,22,36]. Treating CV with 85 nM ARA or 85 nM ETYA, significantly reduced fusion to 59.8 ± 13.1% and 19.7 ± 5.0%, respectively, but only in the settle fusion assay (Fig. 2; $n = 2–3$). The significant decrease in fusion extent in ARA treated CV correlated with a select increase in endogenous free fatty acid (FFA) (Fig. 2C; $n = 4$), confirming incorporation of the exogenous ARA into the CV membrane. There were no significant changes in other neutral (Fig. 2C, representative chromatogram) and phospholipid species (not shown). The basal endogenous FFA in untreated controls was 14.9 ± 2.0 fmol/μg CV membrane protein (fmol/μg MP) (Fig. 2C; $n = 4$), consistent with previous measures [12]. The ~22% increase in endogenous FFA to 18.4 ± 0.7 fmol/μg MP was significant in the ARA treated CV, relative to 14.3 ± 0.7 fmol/μg MP in the ETYA treated CV, confirming that ETYA was not metabolized (Fig. 2C; $n = 4$). No significant change in Ca^{2+} sensitivity was observed in either of these treatments (Fig. 2).

ARA maintained optimum fusion (i.e., 100 ± 1.3%) in the standard assay (Fig. 2A; $n = 3–5$), and thus did not interfere with the fundamental ability of CV to fuse. That ARA can rapidly diffuse across the membrane [38] and also be rapidly metabolized [34,35], suggested that (exogenous) ARA could directly alter membrane biophysical properties owing to its negative spontaneous curvature or exert an indirect effect by generating 'active' downstream metabolite(s). To dissociate these potential effects, a metabolically stable analogue, ETYA, having four alkyne bonds, in contrast to alkene bonds in ARA, was used (Fig. 1A). ETYA also had no effect on fusion extent in the standard assay, confirming that neither ARA nor its analogue had a direct effect on fusion. However, in the settle assay, fusion was reduced to ~40% and ~20% in ARA and ETYA treated CV, respectively, confirming that ARA and ETYA selectively impaired docking/priming (Fig. 2A and B). Furthermore, an ~20% increase in endogenous FFA in ARA treated CV, indicated conversion of exogenous ARA into endogenous FFA, while no such change was seen in ETYA treated CV (Fig. 2C). Hence, membrane incorporated ETYA most likely acted directly to reduce docking/priming by ~80%, suggesting that ARA also acted comparably, at least until metabolized. It is well-known that incorporation of ARA into the distal monolayers of contacting bilayers directly inhibits membrane merger owing to its negative spontaneous curvature [17,18,20]. Therefore, it seems likely that ARA (and potentially ETYA) equilibrated between the monolayers of the CV membrane, negating specific curvature effects but perhaps overwhelming the basal balance of FFA necessary to promote and maintain docking/priming under basal conditions [11].

3.2. Effects of exogenous LPC and ET-18-OCH3 on fusion and their metabolic fate

Treating CV with 100 μM LPC or 100 μM ET-18-OCH3, significantly reduced fusion to 33.0 ± 5.6% and 26.3 ± 13.2% respectively, in the standard fusion assay (Fig. 3A; $n = 3–6$). However, in the settle fusion assay, fusion was further reduced to 24.0 ± 5.4% and 3.0 ± 2.9%, respectively, in aliquots of the same treated CV (Fig. 3B; $n = 3–6$). Additionally, treating CV with 100 μM ET-18-OCH3 reduced Ca^{2+} sensitivity causing a significant rightward shift in EC50 to 171.0 ± 53.4 μM $[Ca^{2+}]_{free}$, relative to the control EC50 of 65.7 ± 8.5 μM $[Ca^{2+}]_{free}$ in the standard fusion assay (Fig. 3A); fusion was abolished in the settle assay following incorporation of ET-18-OCH3 (Fig. 3B). Notably, an ~30% increase in endogenous PC to 41.0 ± 1.9 pmol/μg MP was significant in the LPC treated CV, relative to 30.4 ± 2.9 pmol/μg MP in the control (Fig. 3C; $n = 5–8$); there was no significant change in PC levels in ET-18-OCH3 treated CV. No significant changes were detected for any other phospholipids (not shown).

Since 100 μM LPC reduced fusion by ~70% in both the standard and settle fusion assays (Fig. 3A and B), it is essential to differentiate whether this occurred due to blockade of membrane merger [10,18,37] or reflected reduced docking/priming. The significant decrease in fusion extent even after establishing membrane contact

Please cite this article as: D. Dabral, J.R. Coorssen, Arachidonic acid and lysophosphatidylcholine inhibit multiple late steps of regulated exocytosis, Biochemical and Biophysical Research Communications, https://doi.org/10.1016/j.bbrc.2019.05.106

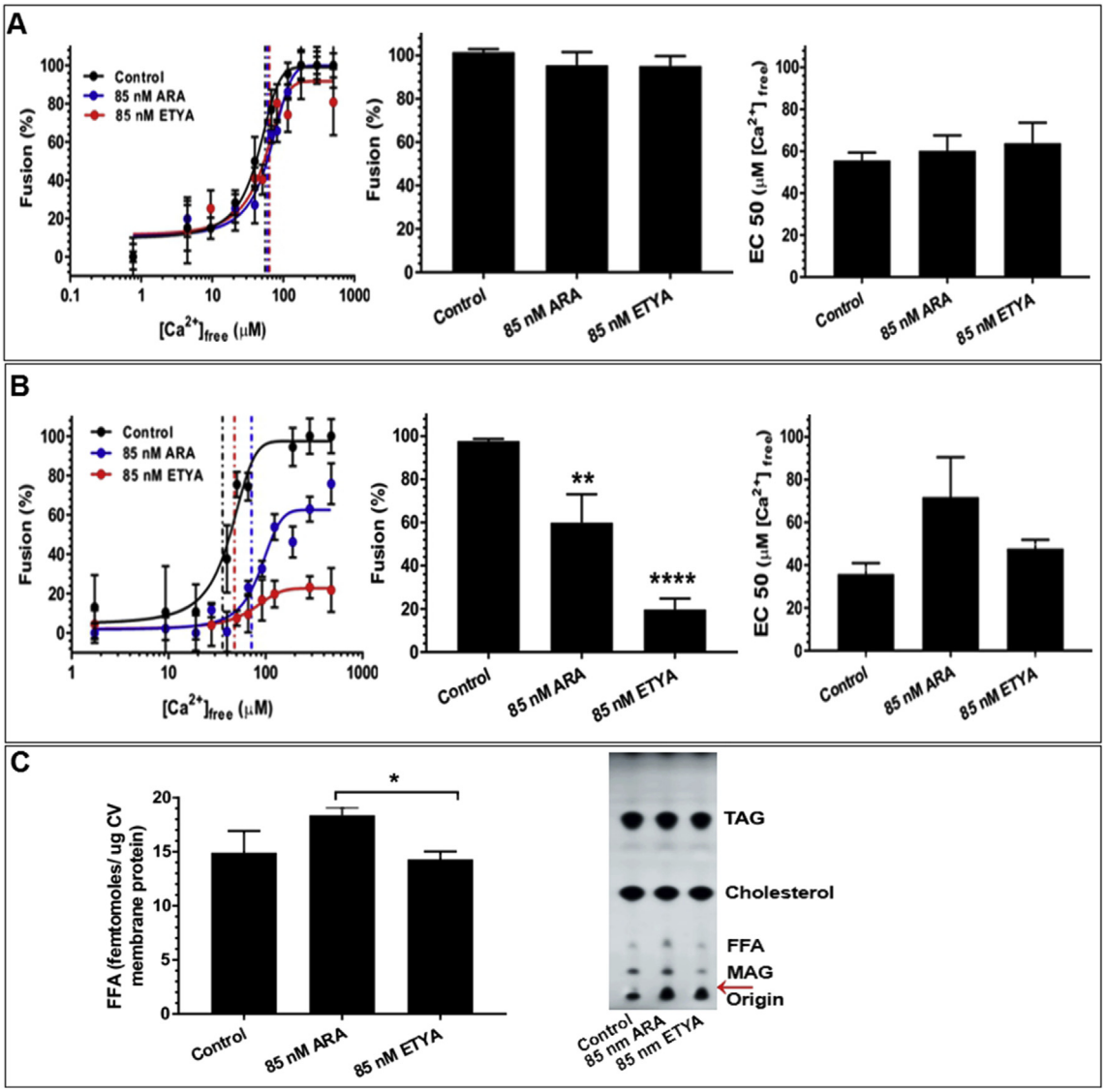

Fig. 2. Effects of 85 nM ARA and ETYA on CV-CV fusion. Changes in the Ca^{2+} activity curves, fusion extent and Ca^{2+} sensitivity (EC50); (A) standard fusion assay ($n = 3–5$); (B) CV settle fusion assay ($n = 2–3$) and; (C) the changes in endogenous FFA following treatment with indicated concentrations of ARA and ETYA, with a representative chromatogram; $n = 4$ separate experiments. (** = 0.009; **** < 0.0001 represent significant differences from control; *<0.05 represent significant difference as indicated). Red arrow indicates exogenous ARA and ETYA. The total lipid load in each lane corresponds to 1 μg CV membrane protein. (For interpretation of the references to colour in this figure legend, the reader is referred to the Web version of this article.)

(i.e., the standard fusion assay) indicated that LPC inhibited membrane merger, as has been well documented [18–20,37]. Also, an ~30% increase in endogenous PC indicated the conversion of exogenous LPC in the CV membrane (Fig. 3C). Importantly, PC essentially has zero intrinsic curvature, thus forming flat lamellar L_α phases [17,45], and the flip-flop rates of PC and LPC in native membranes are in the range of hours [44,46]. Therefore, exogenous LPC as well as the small amounts of PC produced from it likely accumulated in the outer CV monolayer. Nonetheless, with such bulk lipid supplementation, it is clear that complex nonspecific effects on native membranes are likely to occur, necessitating additional assessments to confirm functional contributions of these lipids. Thus, as above, treating CV with a non-metabolizable analogue, 100 μM ET-18-OCH3, reduced fusion to a comparable extent in the standard fusion assay, but completely blocked fusion in the settle assay, likely due to the consistent presence of the analogue (Fig. 3B). Nonetheless, decreased Ca^{2+} sensitivity in the standard fusion assay with ET-18-OCH3 treated CV also indicated an effect on fusion efficiency, which has been linked to disruption of critical local microdomains [23,24,26]. Thus, one must consider the structural differences between LPC and ET-18-OCH3 that include replacement of a hydroxyl group (OH) in LPC with a methoxy group (OCH3), and addition of a carbonyl group (C═O) on the fatty acid (Fig. 1B). The absence of OH in ET-18-OCH3 precludes the possibility of hydrogen bonding with the membrane phospholipids [47,48] and thus may contribute to the select decrease in Ca^{2+} sensitivity (Fig. 3A). In this regard, it is notable that ET-18-OCH3 is known to destabilize membrane domain structures by competing with sphingomyelin to interact with cholesterol [49] and forms fewer and smaller microdomains in monolayers of complex lipid extracts *in vivo* [50]. Therefore, it seems that ET-18-OCH3 additionally disrupted microdomains defining fusion sites to an extent sufficient to reduce the efficiency (i.e., Ca^{2+} sensitivity) of the mechanism [23,24,26,49]. As ET-18-OCH3 was a more potent inhibitor of fusion

Please cite this article as: D. Dabral, J.R. Coorssen, Arachidonic acid and lysophosphatidylcholine inhibit multiple late steps of regulated exocytosis, Biochemical and Biophysical Research Communications, https://doi.org/10.1016/j.bbrc.2019.05.106

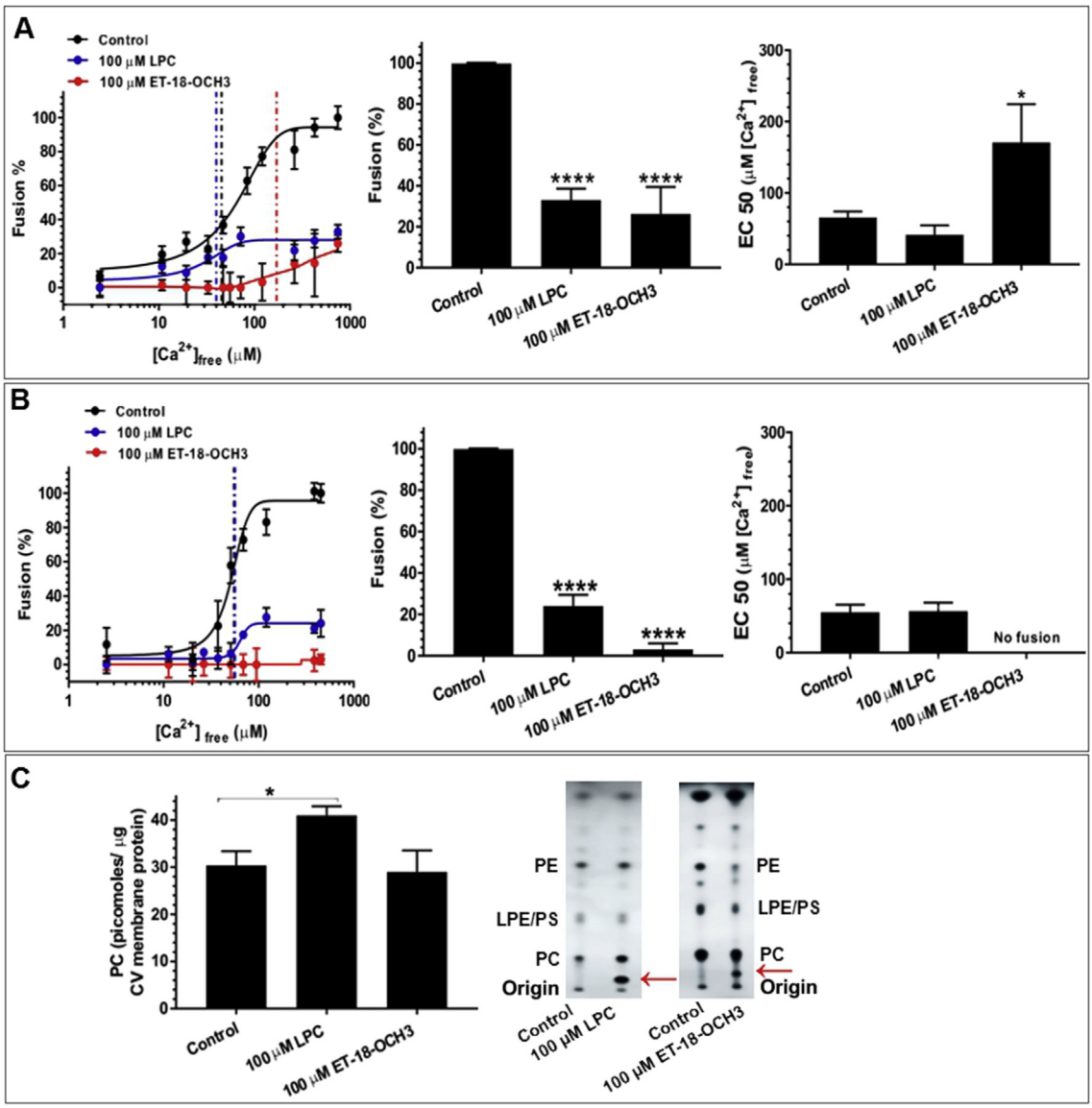

Fig. 3. Effects of 100 μM LPC and ET-18-OCH3 on CV-CV fusion. Changes in the Ca^{2+} activity curves, fusion extent and Ca^{2+} sensitivity (EC50); (A) Standard fusion assay ($n = 3–6$); (B) CV settle fusion assay ($n = 3–6$) and; (C) the changes in endogenous PC following treatment with indicated concentrations of LPC and ET-18-OCH3, $n = 3$ separate experiments. (* < 0.05; **** < 0.0001 represent significant differences from control). Red arrows indicate exogenous LPC and ET-18-OCH3. Note: The apparent difference in the intensity of lipid species between the two chromatograms is due to the necessity for different exposures during image capture. The total lipid load in each lane corresponds to 2 μg CV membrane protein. (For interpretation of the references to colour in this figure legend, the reader is referred to the Web version of this article.)

(Fig. 3), it seems the production of PC from LPC contributed little to the inhibitory process except perhaps to limit the effects by reducing the amount of exogenous LPC. Indeed, local production of PC may have contributed to the stabilization of critical microdomains, consistent with a lack of influence of the LPC treatment on Ca^{2+} sensitivity (Fig. 3A and B).

Thus, the data indicate that exogenous LPC and ET-18-OCH3 in the proximal monolayers of contacting CV block membrane merger due to their positive spontaneous curvature; the metabolic stability of ET-18-OCH3 and its likely disruption of microdomains thus resulted in a complete inhibition of fusion (Fig. 3). As the docked/primed state of release-ready CV is maintained by the basal activities of CV surface $iPLA_2$ that preferentially generate LPC in the outer CV monolayer, it acts as a molecular 'fusion brake' to ensure efficient maintenance of docking/priming prior to the triggering of fusion [11,12] (Fig. 4A and B); here, exogenous LPC in the proximal monolayer likely augmented the effects of the existing endogenous fusion brake owing to its added positive spontaneous curvature [11] (Figs. 3 and 4C). In contrast, exogenous ARA, likely equilibrated between the CV monolayers [38,43,44] upsetting the balance of native FFA and thereby caused a nonspecific inhibition of docking/priming (Figs. 2 and 4D). Furthermore, as *in vitro* experiments have suggested that ARA promotes SNARE complex formation yet the data here indicate blockade of docking/priming, it seems unlikely that ARA itself performs such a function in native membranes.

4. Conclusion

Exogenous ARA selectively inhibits docking/priming but does not have a direct role in membrane merger. In contrast, exogenous LPC, in the proximal monolayers, blocked membrane merger, consistent with previous studies. These outcomes were confirmed by using the non-metabolizable analogues, ETYA and ET-18-OCH3. The data also highlight the importance of transbilayer balance of

Please cite this article as: D. Dabral, J.R. Coorssen, Arachidonic acid and lysophosphatidylcholine inhibit multiple late steps of regulated exocytosis, Biochemical and Biophysical Research Communications, https://doi.org/10.1016/j.bbrc.2019.05.106

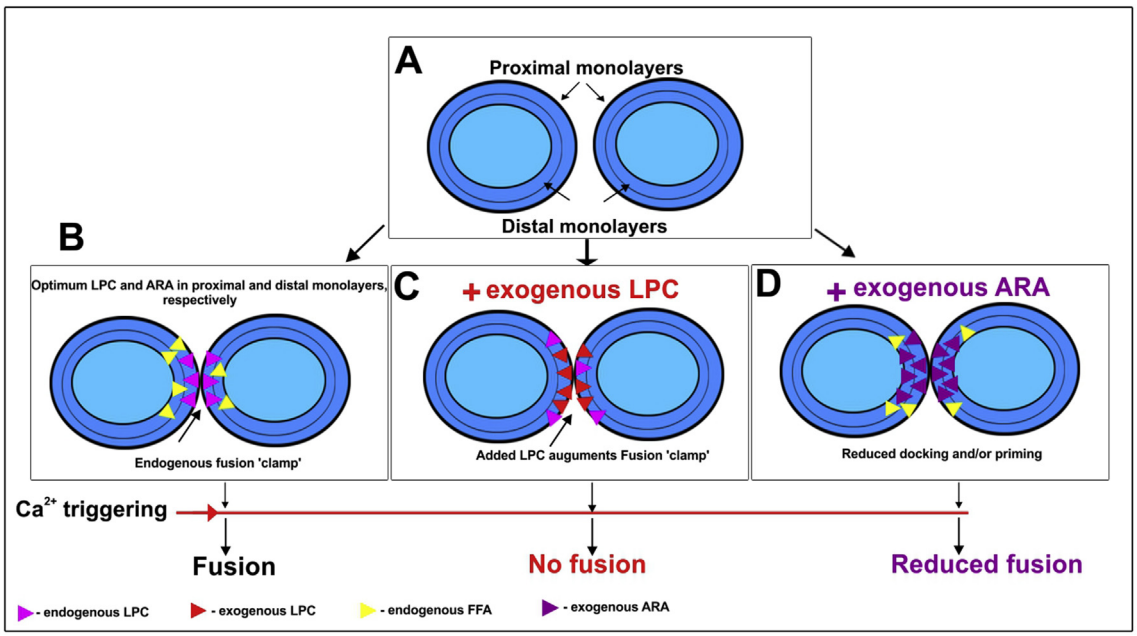

Fig. 4. Effects of exogenous LPC and ARA on late steps of native Ca^{2+} triggered fusion. (A) Non-contacting vesicles (B) Contacting vesicles with optimum levels of endogenous LPC and FFA undergo fusion upon Ca^{2+} triggering (C) Contacting vesicles with exogenous LPC incorporated in the proximal monolayers, increasing potency of the endogenous fusion 'clamp' and (D) Exogenous ARA equilibrates in the bilayers of the contacting vesicle, reducing docking and/or priming.

lipid species in native molecular mechanisms, as well as the need to carefully consider and control for bulk supplementation of exogenous lipids.

Conflicts of interest

None.

Author contributions

JRC conceived of the study and designed it with DD. JRC provided all resources and funding. DD performed the experiments, analyzed, interpreted the data and wrote the original draft. JRC interpreted the data and completed the final manuscript.

Acknowledgments

DD thanks Western Sydney University (WSU) for the Post Graduate Research Award. DD and JRC thank Ashleigh Deschamps WSU, SOM for urchin collections and aquatic facility maintenance. JRC notes research support from the NHMRC, Australia (Project Grant APP1065328).

Transparency document

Transparency document related to this article can be found online at https://doi.org/10.1016/j.bbrc.2019.05.106.

References

[1] J.R. Coorssen, P.S. Blank, F. Albertorio, L. Bezrukov, I. Kolosova, X. Chen, P.S. Backlund, J. Zimmerberg, Regulated secretion: SNARE density, vesicle fusion and calcium dependence, J. Cell Sci. 116 (2003) 2087–2097. https://doi.org/10.1242/jcs.00374.

[2] J.A. Szule, S.E. Jarvis, J.E. Hibbert, J.D. Spafford, J.E.A. Braun, G.W. Zamponi, G.M. Wessel, J.R. Coorssen, Calcium-triggered membrane fusion proceeds independently of specific presynaptic proteins, J. Biol. Chem. 278 (2003) 24251–24254. https://doi.org/10.1074/jbc.C300197200.

[3] D. Fasshauer, H. Otto, W.K. Eliason, R. Jahn, A.T. Brunger, Structural changes are associated with soluble N-ethylmaleimide-sensitive fusion protein attachment protein receptor complex formation, J. Biol. Chem. 272 (1997) 28036–28041. https://doi.org/10.1074/jbc.272.44.28036.

[4] Matthew A. Churchward, Jens R. Coorssen, Cholesterol, regulated exocytosis and the physiological fusion machine, Biochem. J. 423 (2009) 1–14. https://doi.org/10.1042/bj20090969.

[5] J.G. Duman, J.G. Forte, What is the role of SNARE proteins in membrane fusion? Am. J. Physiol. Cell Physiol. 285 (2003) C237–C249. https://doi.org/10.1152/ajpcell.00091.2003.

[6] T.J. Melia, T. Weber, J.A. McNew, L.E. Fisher, R.J. Johnston, F. Parlati, L.K. Mahal, T.H. Sollner, J.E. Rothman, Regulation of membrane fusion by the membrane-proximal coil of the t-SNARE during zippering of SNAREpins, J. Cell Biol. 158 (2002) 929–940. https://doi.org/10.1083/jcb.200112081.

[7] P.I. Kuzmin, J. Zimmerberg, Y.A. Chizmadzhev, F.S. Cohen, A quantitative model for membrane fusion based on low-energy intermediates, Proc. Natl. Acad. Sci. U.S.A. 98 (2001) 7235–7240. https://doi.org/10.1073/pnas.121191898.

[8] X. Chen, D. Araç, T.-M. Wang, C.J. Gilpin, J. Zimmerberg, J. Rizo, SNARE-mediated lipid mixing depends on the physical state of the vesicles, Biophys. J. 90 (2006) 2062–2074. https://doi.org/10.1529/biophysj.105.071415.

[9] M. Zick, W. Wickner, Improved reconstitution of yeast vacuole fusion with physiological SNARE concentrations reveals an asymmetric Rab(GTP) requirement, Mol. Biol. Cell 27 (2016) 2590–2597. https://doi.org/10.1091/mbc.e16-04-0230.

[10] J.R. Coorssen, P.S. Blank, M. Tahara, J. Zimmerberg, Biochemical and functional studies of cortical vesicle fusion: the SNARE complex and Ca2+ sensitivity, J. Cell Biol. 143 (1998) 1845–1857. https://doi.org/10.1083/jcb.143.7.1845.

[11] D. Dabral, J.R. Coorssen, Phospholipase A2: potential roles in native membrane fusion, Int. J. Biochem. Cell Biol. 85 (2017) 1–5. https://doi.org/10.1016/j.biocel.2017.01.011.

[12] D. Dabral, J.R. Coorssen, Combined targeted omic and functional assays identify phospholipases A2 that regulate docking/priming in calcium-triggered exocytosis, Cells 8 (2019) 303. https://doi.org/10.3390/cells8040303.

[13] C. Imig, S.-W. Min, S. Krinner, M. Arancillo, C. Rosenmund, Thomas C. Südhof, J. Rhee, N. Brose, Benjamin H. Cooper, The morphological and molecular nature of synaptic vesicle priming at presynaptic active zones, Neuron 84 (2014) 416–431. https://doi.org/10.1016/j.neuron.2014.10.009.

[14] T. Fukuma, M.J. Higgins, S.P. Jarvis, Direct imaging of individual intrinsic hydration layers on lipid bilayers at Ångstrom resolution, Biophys. J. 92 (2007) 3603–3609. https://doi.org/10.1529/biophysj.106.100651.

[15] R.P. Rand, V.A. Parsegian, Hydration forces between phospholipid bilayers, Biochim. Biophys. Acta Rev. Biomembr. 988 (1989) 351–376. https://doi.org/10.1016/0304-4157(89)90010-5.

[16] A.J.B. Kreutzberger, V. Kiessling, B. Liang, S.-T. Yang, J.D. Castle, L.K. Tamm, Asymmetric phosphatidylethanolamine distribution controls fusion pore lifetime and probability, Biophys. J. 113 (2017) 1912–1915. https://doi.org/10.1016/j.bpj.2017.09.014.

[17] L. Chernomordik, Non-bilayer lipids and biological fusion intermediates,

Chem. Phys. Lipids 81 (1996) 203–213. https://doi.org/10.1016/0009-3084(96)02583-2.
[18] L. Chernomordik, M.M. Kozlov, J. Zimmerberg, Lipids in biological membrane fusion, J. Membarin Biol. 146 (1995) 1–14. https://doi.org/10.1007/BF00232676.
[19] L.V. Chernomordik, S.S. Vogel, A. Sokoloff, H.O. Onaran, E.A. Leikina, J. Zimmerberg, Lysolipids reversibly inhibit Ca2+-, GTP- and pH-dependent fusion of biological membranes, FEBS (Fed. Eur. Biochem. Soc.) Lett. 318 (1993) 71–76. https://doi.org/10.1016/0014-5793(93)81330-3.
[20] L. Chernomordik, A. Chanturiya, J. Green, J. Zimmerberg, The hemifusion intermediate and its conversion to complete fusion: regulation by membrane composition, Biophys. J. 69 (1995) 922–929. https://doi.org/10.1016/s0006-3495(95)79966-0.
[21] Y. Kozlovsky, M.M. Kozlov, Stalk model of membrane fusion: solution of energy crisis, Biophys. J. 82 (2002) 882–895. https://doi.org/10.1016/S0006-3495(02)75450-7.
[22] M.A. Churchward, T. Rogasevskaia, J. Höfgen, J. Bau, J.R. Coorssen, Cholesterol facilitates the native mechanism of Ca2+-triggered membrane fusion, J. Cell Sci. 118 (2005) 4833–4848. https://doi.org/10.1242/jcs.02601.
[23] T. Rogasevskaia, J.R. Coorssen, Sphingomyelin-enriched microdomains define the efficiency of native Ca^{2+}-triggered membrane fusion, J. Cell Sci. 119 (2006) 2688–2694. https://doi.org/10.1242/jcs.03007.
[24] M. Mahadeo, K.L. Furber, S. Lam, J.R. Coorssen, E.J. Prenner, Secretory vesicle cholesterol: correlating lipid domain organization and Ca2+ triggered fusion, Biochim. Biophys. Acta Biomembr. 1848 (2015) 1165–1174. https://doi.org/10.1016/j.bbamem.2015.02.005.
[25] M.A. Churchward, T. Rogasevskaia, D.M. Brandman, H. Khosravani, P. Nava, J.K. Atkinson, J.R. Coorssen, Specific lipids supply critical negative spontaneous curvature—an essential component of native Ca2+-triggered membrane fusion, Biophys. J. 94 (2008) 3976–3986. https://doi.org/10.1529/biophysj.107.123984.
[26] P.S. Abbineni, J.R. Coorssen, Sphingolipids modulate docking, Ca2+ sensitivity and membrane fusion of native cortical vesicles, Int. J. Biochem. Cell Biol. 104 (2018) 43–54. https://doi.org/10.1016/j.biocel.2018.09.001.
[27] T.P. Rogasevskaia, M.A. Churchward, J.R. Coorssen, Anionic lipids in Ca(2+)-triggered fusion, Cell Calcium 52 (2012) 259–269. https://doi.org/10.1016/j.ceca.2012.03.006.
[28] F. Darios, B. Davletov, Omega-3 and omega-6 fatty acids stimulate cell membrane expansion by acting on syntaxin 3, Nature 440 (2006) 813–817. https://doi.org/10.1038/nature04598.
[29] C. Rickman, B. Davletov, Arachidonic acid allows SNARE complex formation in the presence of Munc18, Chem. Biol. 12 (2005) 545–553. http://doi.org/10.1016/j.chembiol.2005.03.004.
[30] I. Dulubova, S. Sugita, S. Hill, M. Hosaka, I. Fernandez, T.C. Sudhof, J. Rizo, A conformational switch in syntaxin during exocytosis: role of munc18, EMBO J. 18 (1999) 4372–4382. https://doi.org/10.1093/emboj/18.16.4372.
[31] C.F. Latham, S.L. Osborne, M.J. Cryle, F.A. Meunier, Arachidonic acid potentiates exocytosis and allows neuronal SNARE complex to interact with Munc18a, J. Neurochem. 100 (2007) 1543–1554. https://doi.org/10.1111/j.1471-4159.2006.04286.x.
[32] A.I.P.M. de Kroon, P.J. Rijken, C.H. De Smet, Checks and balances in membrane phospholipid class and acyl chain homeostasis, the yeast perspective, Prog. Lipid Res. 52 (2013) 374–394. https://doi.org/10.1016/j.plipres.2013.04.006.
[33] I. Lager, J.L. Yilmaz, X.-R. Zhou, K. Jasieniecka, M. Kazachkov, P. Wang, J. Zou, R. Weselake, M.A. Smith, S. Bayon, J.M. Dyer, J.M. Shockey, E. Heinz, A. Green, A. Banas, S. Stymne, Plant acyl-CoA:lysophosphatidylcholine acyltransferases (LPCATs) have different specificities in their forward and reverse reactions, J. Biol. Chem. 288 (2013) 36902–36914. https://doi.org/10.1074/jbc.M113.521815.
[34] C. Galli, P. Risé, F. Marangoni, Fate of exogenous arachidonic acid in THP-1 cells: incorporation in cell lipids and conversion to other N-6 fatty acids, Prostagl. Leukot. Essent. Fat. Acids 52 (1995) 103–106. https://doi.org/10.1016/0952-3278(95)90006-3.
[35] D. Caruso, P. Risé, G. Galella, C. Regazzoni, A. Toia, G. Galli, C. Galli, Formation of 22 and 24 carbon 6-desaturated fatty acids from exogenous deuterated arachidonic acid is activated in THP-1 cells at high substrate concentrations, FEBS (Fed. Eur. Biochem. Soc.) Lett. 343 (1994) 195–199. https://doi.org/10.1016/0014-5793(94)80554-7.
[36] T.P. Rogasevskaia, J.R. Coorssen, The role of phospholipase D in regulated exocytosis, J. Biol. Chem. (2015). https://doi.org/10.1074/jbc.M115.681429.
[37] S.S. Vogel, E.A. Leikina, L.V. Chernomordik, Lysophosphatidylcholine reversibly arrests exocytosis and viral fusion at a stage between triggering and membrane merger, J. Biol. Chem. 268 (1993) 25764–25768.
[38] A.R. Brash, Arachidonic acid as a bioactive molecule, J. Clin. Investig. 107 (2001) 1339–1345. https://doi.org/10.1172/JCI13210.
[39] R.H. Butt, J.R. Coorssen, Postfractionation for enhanced proteomic Analyses: routine electrophoretic methods increase the resolution of standard 2d-PAGE, J. Proteome Res. 4 (2005) 982–991. https://doi.org/10.1021/pr050054d.
[40] M.A. Churchward, D.M. Brandman, T. Rogasevskaia, J.R. Coorssen, Copper (II) sulfate charring for high sensitivity on-plate fluorescent detection of lipids and sterols: quantitative analyses of the composition of functional secretory vesicles, J. Chem. Biol. 1 (2008) 79–87. https://doi.org/10.1007/s12154-008-0007-1.
[41] E.G. Bligh, W.J. Dyer, A rapid method of total lipid extraction and purification, Can. J. Biochem. Physiol. 37 (1959) 911–917. https://doi.org/10.1139/o59-099.
[42] M. Murakami, Y. Nakatani, G.I. Atsumi, K. Inoue, I. Kudo, Regulatory functions of phospholipase A2, Crit. Rev. Immunol. 37 (2017) 121–179. https://doi.org/10.1615/CritRevImmunol.v37.i2-6.20.
[43] J.A. Hamilton, Fatty acid transport: difficult or easy? JLR (J. Lipid Res.) 39 (1998) 467–481.
[44] F.X. Contreras, L. Sanchez-Magraner, A. Alonso, F.M. Goni, Transbilayer (flip-flop) lipid motion and lipid scrambling in membranes, FEBS Lett. 584 (2010) 1779–1786. https://doi.org/10.1016/j.febslet.2009.12.049.
[45] J.A. Szule, N.L. Fuller, R.P. Rand, The effects of acyl chain length and saturation of diacylglycerols and phosphatidylcholines on membrane monolayer curvature, Biophys. J. 83 (2002) 977–984. https://doi.org/10.1016/S0006-3495(02)75223-5.
[46] M. Nakano, M. Fukuda, T. Kudo, N. Matsuzaki, T. Azuma, K. Sekine, H. Endo, T. Handa, Flip-flop of phospholipids in vesicles: kinetic analysis with time-resolved small-angle neutron scattering, J. Phys. Chem. B 113 (2009) 6745–6748. https://doi.org/10.1021/jp900913w.
[47] J.M. Boggs, Lipid intermolecular hydrogen bonding: influence on structural organization and membrane function, Biochim. Biophys. Acta Rev. Biomembr. 906 (1987) 353–404. https://doi.org/10.1016/0304-4157(87)90017-7.
[48] J.P. Slotte, The importance of hydrogen bonding in sphingomyelin's membrane interactions with co-lipids, Biochim. Biophys. Acta Biomembr. 1858 (2016) 304–310. https://doi.org/10.1016/j.bbamem.2015.12.008.
[49] A. Ausili, P. Martínez-Valera, A. Torrecillas, V. Gómez-Murcia, A.M. de Godos, S. Corbalán-García, J.A. Teruel, J.C. Gómez Fernández, Anticancer agent edelfosine exhibits a high affinity for cholesterol and disorganizes liquid-ordered membrane structures, Langmuir 34 (2018) 8333–8346. https://doi.org/10.1021/acs.langmuir.8b01539.
[50] M. Mahadeo, S. Nathoo, S. Ganesan, M. Driedger, V. Zaremberg, E.J. Prenner, Disruption of lipid domain organization in monolayers of complex yeast lipid extracts induced by the lysophosphatidylcholine analogue edelfosine in vivo, Chem. Phys. Lipids 191 (2015) 153–162. https://doi.org/10.1016/j.chemphyslip.2015.09.004.

Please cite this article as: D. Dabral, J.R. Coorssen, Arachidonic acid and lysophosphatidylcholine inhibit multiple late steps of regulated exocytosis, Biochemical and Biophysical Research Communications, https://doi.org/10.1016/j.bbrc.2019.05.106

CHAPTER – 4

Phospholipase A_2 activating peptide disturbs native membrane lipid homeostasis, affecting terminal steps of Ca^{2+} triggered exocytosis

(Manuscript in preparation)

Abstract: Melittin activates $sPLA_2$ [1-4] and forms membrane pores, promoting regulated exocytosis [3,5-7]. Using CSC (cell surface complexes) and fully primed release-ready native cortical secretory vesicles (CV) isolated from unfertilized sea urchin eggs, here Phospholipase A_2 activating peptide (PLAP) is shown to reduce endogenous free fatty acid (FFA) levels, increase phosphatidylethanolamine (PE), and inhibit priming/docking steps. This indicates that PLAP altered native lipid homeostasis and impaired priming/docking steps, while CV associated phospholipase D (PLD) and calcium-independent phospholipase A_2 ($iPLA_2$) activities were unaffected. Notably, PLAP also reduced membrane capacitance and the readily releasable pool (RRP) size in chromaffin cells. Overall, studies using well-established model systems – CSC and CV fusion assays, that enable tight coupling of functional and molecular analyses [8,11-17] and membrane capacitance measurement of chromaffin cells [18-20] - indicate that PLAP impaired a common underlying mechanism to block late steps in regulated exocytosis.

---

1. Introduction

Sea urchin eggs and mammalian chromaffin cells carry out the different physiological function, however, in response to increasing $[Ca^{2+}]_{free}$ yield a characteristic sigmoidal dose-response curve [11-13,15-17,21-28]. The exact role(s) of Ca^{2+} during triggering are as yet unclear. Nevertheless, studies suggest that Ca^{2+} may clear *trans* SNARE complexes to allow fusion [13,22,23,29] and induce conformational changes in the putative Ca^{2+} sensor - synaptotagmin [30]. The binding of Ca^{2+} to synaptotagmin is proposed to release its inhibitory effect on membrane merger that occurs due to unfavourable membrane bending [30]. Unfertilized sea urchin eggs arrest at G1 phase during oogenesis [31]. However, during upstream vesicle

trafficking stage(s), cortical secretory vesicles (CV) are translocated to the plasma membrane (PM) where they remain fully primed and release-ready until fertilization. Necessary docking and priming involve, at least in part, formation of *trans* SNARE complexes [13,15,23,32,33]. Therefore, unfertilized sea urchin eggs contain a single CV population at the cortex, compared to at least three distinct secretory vesicle pools near the PM in a chromaffin cell, termed the (i) unprimed pool (UPP); (ii) slowly releasable pool (SRP) and; (iii) readily releasable pool (RRP) [25,34,35]. Those docked vesicles that are fully primed and highly Ca^{2+} sensitive constitute the RRP and their distinct molecular state, is due to mechanisms that occur during their transition from the UPP to the RRP [36]. Such mechanisms involve the combined actions of calcium-dependent activator protein for secretion - 1 and -2 (CAPS-1 and -2) [35,37-39] and mammalian uncoordinated (munc) [35,40]. Nevertheless, the close proximity of RRP to Ca^{2+} channels on the PM may also contribute to their high Ca^{2+} sensitivity [41,42]. Importantly, functional SNAREs maintain the RRP [43,44], as SNAP 25 deletion [23,36,45], blocking SNARE complex formation using antibodies [44] and their cleavage using Botulinum Neurotoxin A [46], significantly reduced RRP size [47,48]. Therefore, the molecular state of RRP in chromaffin cells is, in essence, analogous to the endogenously docked CV on the PM (CSC; cell surface complexes) in an unfertilized sea urchin egg. This is because both vesicle types are fully primed, morphologically docked at the PM utilizing already formed SNARE complexes and immediately undergo membrane merger in response to Ca^{2+} triggering [8,9,11,12,14,17,22-24,27,36,49-51].

Phospholipase A_2 generates free fatty acids (FFA) and lysophospholipids (LPL) that modulate priming/docking and the membrane merger steps of regulated exocytosis, respectively [9,10]. Therefore, to enhance PLA_2 activity [9], melittin homologous polypeptide, phospholipase A_2 activating peptide (PLAP) was used, that has been seen to activate $sPLA_2$ *in vitro* [1-4]. Both melittin and PLAP carry a heptad of the leucine zipper dimerization motif,

characterized by leucine separated by six residues in the sequence KV**L**TTGXPP**L**I (Fig. 1A) [52]. Therefore, both have a tendency to form homo or heterodimers. Melittin monomers also have the ability to adopt a helical conformation that orients parallel to the membrane bilayer [53,54]. Therefore, it may also interact with SNARE complexes (Fig. 1A) to inhibit SNARE 'zippering'. Additionally, melittin is also suggested to form membrane pores, hence promote regulated exocytosis [3,5-7]. Also, melittin inhibits PKC [55,56], calmodulin-sensitive Ca^{2+} dependent protein kinase [56,57], phosphorylase kinase [58], and kappa kinases [59], and promotes secretory phospholipase A_2 ($sPLA_2$) [2,3,6,60-62], PM associated scramblase [63] and phospholipase D (PLD) activities [64]. Among these, PKC phosphorylates SNAP 25 [47,48,65-67], PLA_2 isozymes, and PLD regulates priming/docking [9,68] in the late steps of regulated exocytosis.

Using well-established CV-PM and CV-CV fusion assays and standardized lipid analyses [8,9,11,13,15,17,23,24,68-69], PLAP is shown to inhibit fusion of endogenously docked CV with the PM. This occurs due to impaired molecular reactions associated with priming/docking. As PLAP reduced endogenous FFA and caused a parallel increase in endogenous PE, indicated that a critical level of endogenous lipids maintains priming/docking steps. Furthermore, PLAP caused no change in CV associated PLD and PLA_2 activities, nor formed pores in native membranes as suggested in other studies [3, 5-7, 9,16]. Notably, a significant decrease in overall secretion and RRP size in PLAP (and LY311727) treated chromaffin cells, confirmed that PLAP altered common underlying molecular reactions associated with the priming/docking steps of regulated exocytosis.

2. Materials and Methods

2.1 CV treatment and fusion assays

Native sea urchins (Heliocedaris tuberculata) were maintained at 7-8 °C in the local aquatic facility ([9,10]). CSC and CV were isolated as previously described [8,13-15,22] and suspended in baseline intracellular medium (BIM, 210 mM potassium glutamate, 500 mM glycine, 10 mM NaCl, 10 mM PIPES, 50 μM $CaCl_2$, 1 mM $MgCl_2$, 1 mM EGTA pH 6.7) supplemented with 2.5 mM ATP, 2 mM DTT and 1X protease inhibitors [8,14]. PLAP and 1,1,1,2,2-Pentafluoro-7-phenyl-3-heptanone (FKGK-11) were from Enzo Life Sciences (Farmingdale, NY) and Cayman Chemicals (Ann Arbor, US), respectively, and 3-(3-acetamide-1-benzyl-2-ethylindolyl-5-oxy) propane sulfonic acid (LY311727) and Bromoenol lactone (BEL) were from Sigma Aldrich (St. Louis, US). The changes in optical density (OD) used to assess CV-PM and CV-CV fusion were measured using a POLARstar Omega microplate reader (BMG Labtech, Offenburg, Germany) [9,10,12,17]. Each treatment was tested in quadruplicate and repeated in separate experiments, as indicated (*n*).

2.2 Lipid extraction, normalization and High-Performance Thin Layer Chromatography (HPTLC)

Total CSC or CV lipids and parallel membrane proteins were extracted as previously described [8-10,14,68,70]). The dried lipid samples were dissolved in $CHCl_3$:CH_3OH (2:1; *v*/*v*) and loaded onto pre-conditioned silica gel 60 HPTLC plates [8-10,14,68]. For consistency and optimum detection of the individual lipid species, samples corresponding to 1 μg and 2 μg of membrane protein were used to resolve neutral and phospholipids, respectively [8-10], according to established methods [8,11,14,16]. The resolved lipids were visualized on-plate by heating plates that were homogeneously wetted with 10 % cupric sulfate in 8 % aqueous phosphoric acid at 145°C for 10 min [8,9]. Lipids of interest were quantified via calibration curves of the appropriate standards, resolved in parallel with the sample lipids. Images were captured at 460 nm/605 nm (Ex/Em) using the ImageQuant™ LAS 4000 Biomolecular Imager

(GE Healthcare, Buckinghamshire, UK) and analyzed using MultiGauge *v* 3.0 (Fuji Photo Film Co., Ltd. Tokyo, Japan). All lipids except arachidonic acid (ARA; 20:4) were from Avanti Polar Lipids (Alabaster, AL). ARA was purchased from Matreya LLC (Pennsylvania, US).

2.3 PLD activity assay

CV associated PLD activity was measured using an Amplex Red PLD assay kit (Invitrogen, Eugene, OR) with minor modifications [16]. Briefly, CV suspension in 1 X BIM, pH 6.5 (supplemented with 2.5 mM ATP and 1X protease inhibitors [8,14]) were treated with indicated concentrations of PLAP, LY311727, and BEL at 25°C for 25 min. Then, PLD enzymatic activity was measured as per manufacturer's instruction at 520 nm/584 nm (Ex/Em) using a POLARstar Omega microplate reader. Each condition was measured in triplicate and experiments repeated, as indicated (*n*).

2.4 Chromaffin cell culture and capacitance measurement

Adrenal glands were obtained from newborn wild type C57B6N mice. Chromaffin cells were harvested from the glands and maintained as primary cultures for three days according to an established protocol [65]. Briefly, dissected adrenal glands were placed in Lock's solution (154 mM NaCl, 5.6 mM KCl, 5.0 mM HEPES, 3.6 mM $NaHCO_3$, 5.6 mM Glucose) to carefully remove connective tissue using a pair of tweezers. Glands were then incubated with enzyme solution (20-25 unit/ml papain) in 250 ml Dulbecco's Modified Eagle Medium (DMEM) (without sodium and pyruvate) from Thermo scientific (Oregon, USA), with gentle shaking at 37°C for 25 min. To stop enzyme activity, glands were incubated with inactivation solution (225 ml DMEM containing 625 mg trypsin inhibitor, 25 ml heat-inactivated fetal calf serum, and 625 mg albumin) for 10 min at 37°C. Subsequently, inactivation solution was carefully replaced with fresh DMEM supplemented with 1X penicillin-streptomycin, and Insulin-Transferrin-Selenium from Thermo scientific (Oregon, USA) and glands gently triturated (25-

30 times) using a micropipette until no piece of tissue was visible. A small volume of cell suspension was placed on a sterile coverslip and allowed to adhere at 37°C before overnight incubation with ~ 2 ml of fresh DMEM under 8.5 % CO_2.

Borosilicate patch pipettes (GB150F - 8P) were pulled using a Sutter Instrument Model P-87 (Sutter Instrument, Novato, CA). Pipettes were coated with wax to reduce resistance to <5 Ω. During electrical recording, adherent cells on coverslips were immersed in a bath solution (130 mM NaCl, 4 mM KCl, 10 mM $CaCl_2$, 1mM $MgCl_2$, 10 mM HEPES, 20 mM Glucose); the pipette contained patch solution (135 mM CsOH, 135 mM Glutamate, 8mM NaCl, 0.18 mM $CaCl_2$, 0.28 mM BAPTA, 10 mM HEPES, 2 mM Mg-ATP, 0.5 mM Na_2GTP) without or with either 858.0 pM PLAP or 2 nM LY311727. After breaking the Giga seal, chromaffin cells were held in the voltage-clamp whole-cell configuration for 2 min to ensure diffusion of PLAP and LY311727 into the cytosol before triggering secretion using a train of 200 ms triple depolarizing pulses (from -70 mV to +10 mV). Time delays of 0.1 ms and 20 ms were applied between pulse -1 and -2 and pulse -2 and -3, respectively [18,19]. The changes in membrane capacitance and Ca^{2+} current (I_{ca}) were recorded using an EPC-7 (HEKA, Lambrecht, Germany).

3. Data Analyses

In CSC and CV fusion assays, all conditions were tested in quadruplicate and experiments repeated as indicated (*n*). Raw data were normalized by setting zero % fusion at <0.3 µM $[Ca^{2+}]_{free}$ and 100 % fusion at >100 µM $[Ca^{2+}]_{free}$. Ca^{2+} activity curves were fit using a sigmoidal 4-parameter logistic model (PRISM 7.03, GraphPad, San Diego, US). Capacitance traces from the indicated number (*n*) of chromaffin cells were analyzed using Igor software. Data are reported as mean ± SEM. Two-sample, two-tailed *t*-tests with $P<0.05$ are considered significant.

4. Results

4.1 PLAP blocked late steps in regulated exocytosis

As with previous studies, endogenously docked CV at the PM (CSC) undergo heterotypic fusion upon Ca^{2+} triggering, yielding a characteristic sigmoidal dose-response curve with an EC50 of 33.5 ± 8.0 µM $[Ca^{2+}]_{free}$ (Fig. 1B; *n*=8) [8,12-17,23,24]. Treating CSC (OD 0.64 ± 0.02; *n*=3-9) with 2 µM PLAP and 2 µM PLAP + 200 µM LY311727 reduced fusion extent to ~60 % and ~40 %, respectively (Fig. 1B; *n*=5-8); fusion extent reduced to ~13 % in 200 µM LY311727 treated CSC [9]. Treating CSC with 2 µM PLAP caused no change in endogenous FFA. However, when added with 200 µM LY311727, i.e., in 2 µM PLAP + 200 µM LY311727 treated CSC, endogenous FFA significantly reduced by ~ 67 % (Fig. 1C;

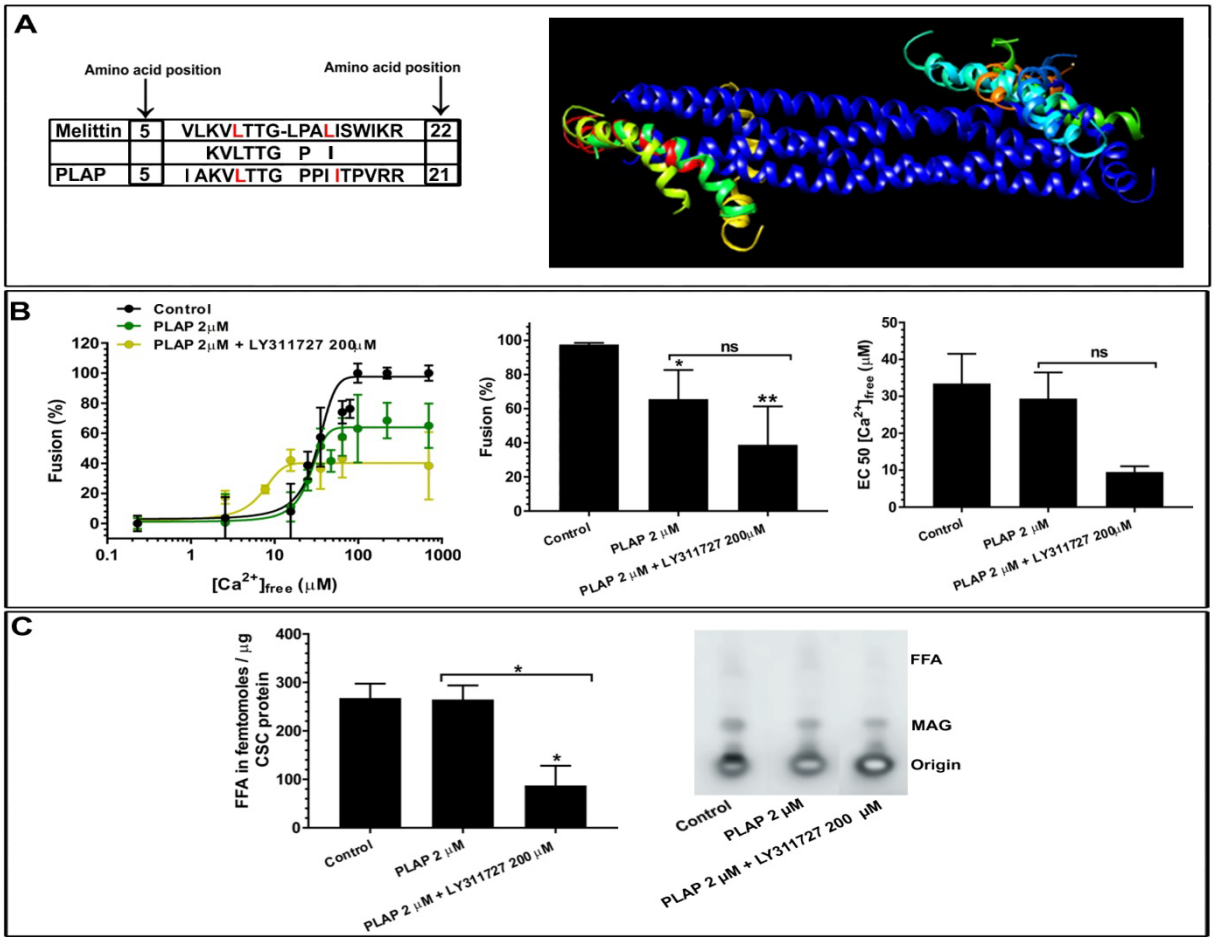

Figure 1: (A) Recombinant melittin (PDB ID 6DST; rainbow ribbon structures) and PLAP are 73 % identical and 72 % similar, and carry a leucine zipper heptad, characterized by leucine (L) separated by six amino acids. Ribbon structures showing interaction between SNARE core complex (PDB ID 1GL2; blue structures) and recombinant melittin. Simulation was carried out using GRAMM-X Protein-Protein Docking Web Server v.1.2.0 and visualized using UCSF Chimera 1.13.1 (B) Effects of PLAP and PLAP + LY311727 on CSC fusion (*n*=3-9). Changes in the Ca^{2+} activity curves, fusion extent and Ca^{2+} sensitivity (EC50); (C) Detection and quantification of endogenous FFA, *n*=3 separate experiments in CSC treated with indicated dose of PLAP and PLAP + LY311727; a representative chromatogram showing changes in endogenous FFA. (p-value, *< 0.05, **=0.006 indicates relative difference to the control and as indicated, ns denotes not-significant) **Note: The sections of the chromatogram shown in B are grouped together from the same HPTLC plate following removal of lanes not associated with this study. A standard neutral lipid protocol was used to resolve the lipids [8-10].**

n=3).We have previously reported a decrease in endogenous FFA by ~ 54 % in 200 µM LY311727 treated CSC [9]. No change in fusion extent nor Ca^{2+} sensitivity occurred in 2 µM PLAP + 200µM LY311727 treated CSC, relative to 200 µM LY311727 treated CSC (not shown).

4.2 PLAP impaired priming/docking, correlating with changes in endogenous lipids

To identify whether blockage of the membrane merger or impairment in the priming/docking steps reduced fusion extent in the PLAP treated CSC, CV (OD 0.96 $\pm$ 0.2; *n*=11) were treated with the indicated concentrations of PLAP and LY311727. The treatment effects were assessed using the standard (Fig. 2A; *n*= 3-11) and settle CV-CV fusion assays

(Fig. 2B; *n*=2-11). In standard assay, only 2 µM PLAP reduced fusion extent to 86.7 ± 4.7 % (Fig. 2A; *n*= 11). Also, a significant decrease in Ca^{2+} sensitivity occurred in 2 µM PLAP + 200 µM LY311727 treated CV, relative to 2 µM PLAP treated CV (Fig. 2A; *n*= 3-11). The Ca^{2+} sensitivity reduced to EC 50 of 89.1 ± 18.1 $[Ca^{2+}]_{free}$ in 2 µM PLAP + 200 µM LY311727 treated CV, relative to control EC50 of 44.7 ± 4.8 $[Ca^{2+}]_{free}$ (Fig. 2A; *n*= 4-11).

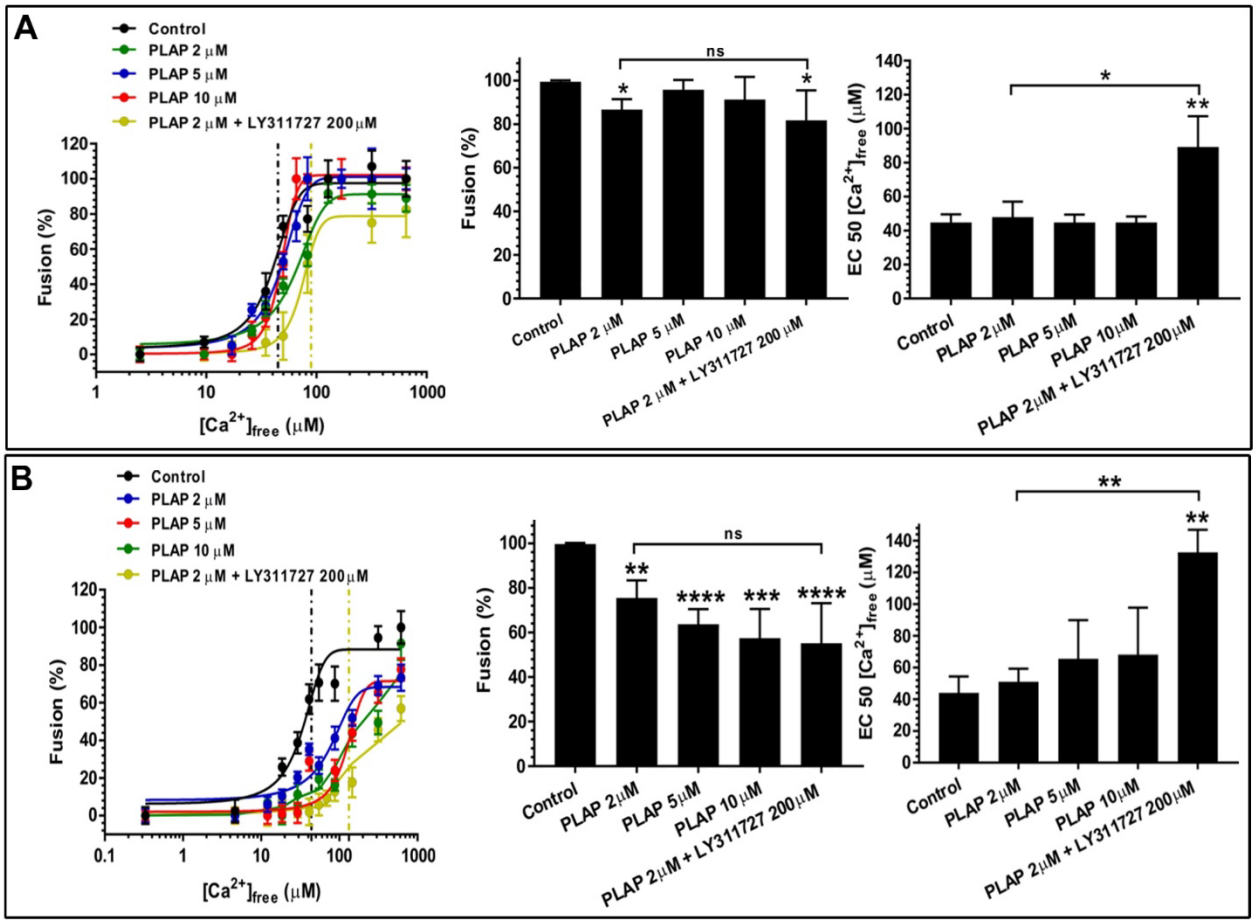

Figure 2: Effects of increasing doses of PLAP and PLAP + LY311727 on CV-CV calcium activity curves, fusion extent and calcium sensitivity (EC50); (A) standard fusion assay, *n*=3-11; (B) settle fusion assay, *n*=2-10. (p-value- *< 0.05, **< 0.0022, ***<0.0002, ****<0.0001, indicates relative difference to the control and as indicated, ns denotes non-significant)

Importantly, a concentration-dependent decrease in fusion extent to 75.4 ± 8.0 %, 63.3 ± 6.8 % and 57.5 ± 13.0 % occurred with 2 µM, 5 µM and 10 µM PLAP, respectively, in the settle fusion assay, clearly indicating PLAP impaired priming/docking steps. As above, no

change in fusion extent but a significant decrease in Ca^{2+} sensitivity occurred in 2 µM PLAP + 200 µM LY311727, relative to 2 µM PLAP treated CV in the settle fusion assay (Fig. 2B; *n*= 3-11). The Ca^{2+} sensitivity was reduced to an EC50 of 132.7 $\pm$ 14.6 $[Ca^{2+}]_{free}$ in 2 µM PLAP + 200 µM LY311727 treated CV, relative to a control EC50 of 44.1 $\pm$ 10.3 $[Ca^{2+}]_{free}$ (Fig. 2B; *n*= 3-11). No significant change in Ca^{2+} sensitivity occurred in 200 µM LY31172 treated CV in either assay [9].

To correlate changes in function with an underlying mechanism, total CV lipids were assessed. Treating CV with 10 µM PLAP and 2 µM PLAP + 200 µM LY311727 reduced endogenous FFA by ~37 % and ~47 %, respectively (Fig. 3; *n*=3-15).

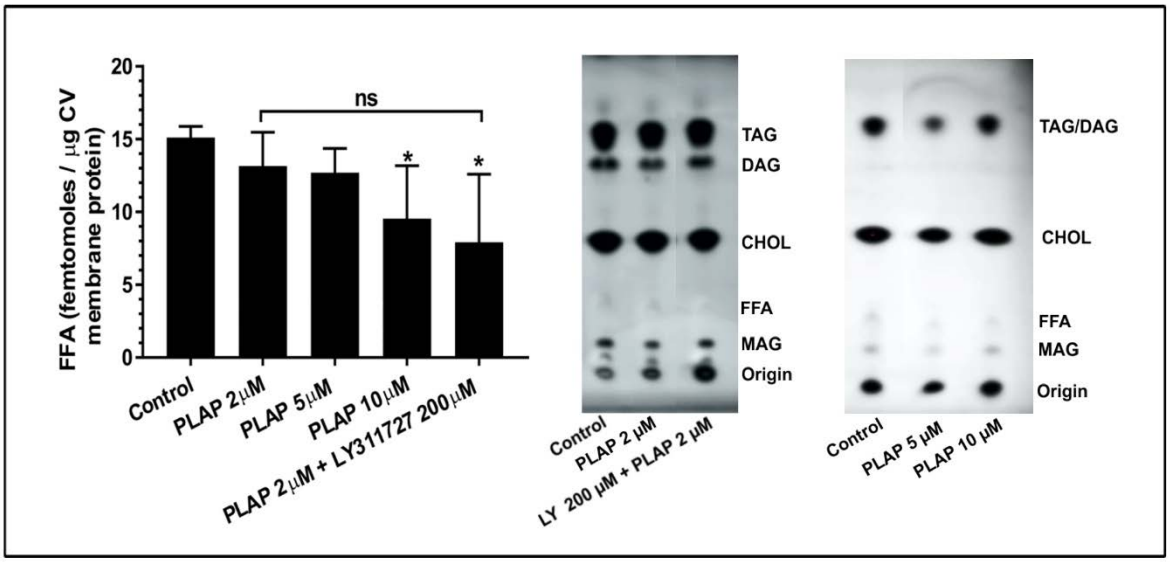

Figure 3: Detection and quantification of endogenous FFA, *n*=3-8 separate experiments in CV treated with increasing concentration of PLAP and PLAP + LY311727; representative chromatogram showing changes in the total CV neutral lipids. (p-value- *< 0.05, indicates relative difference to the control, ns denotes non-significant)

Note: The sections of the chromatogram shown are grouped together from the same HPTLC plate following removal of lanes not associated with this study. A standard neutral lipid protocol was used to resolve the lipids [8-10]

Endogenous FFA decreased by ~27 % in 200 µM LY311727 treated CV [9]. No change in endogenous FFA occurred in CV treated with 2 µM PLAP + 200 µM LY311727, relative to 2 µM PLAP (Fig. 3; *n*=3-15). Beside altering endogenous FFA, treating CV with PLAP also

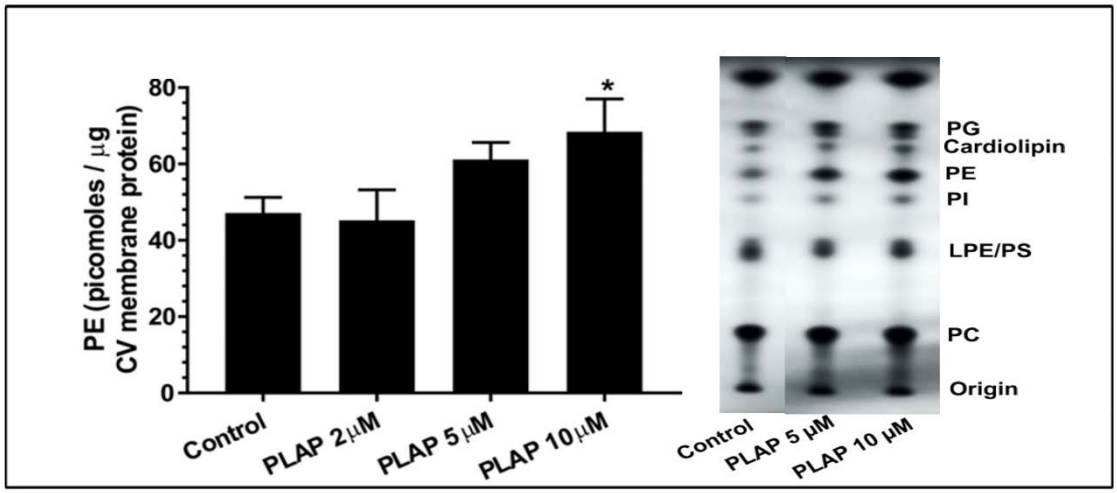

Figure 4: Detection and quantification of endogenous PE in CV treated with increasing concentration of PLAP (*n*=3-17), and representative chromatogram showing changes in the total CV phospholipids. (p-value- *< 0.05, indicates relative difference to the control)

Note: The sections of the chromatogram shown are grouped together from the same HPTLC plate following removal of lanes not associated with this study. A standard phospholipid protocol was used to resolve the lipids [8-10].

caused a concentration-dependent increase in endogenous PE (Fig. 4; *n*=3-17). The endogenous PE significantly increased to 68.5 ± 8.7 pmoles / µg MP in 10 µM PLAP treated CV, relative to 47.0 ± 4.0 pmoles / µg MP in control (Fig. 4; *n*=3-17). No changes in any other lipids were observed (see chromatograms shown in Figs. 3 and 4).

4.3 Cumulative effects of PLAP and PLA_2 inhibitors modulated Ca^{2+} sensitivity

Our previous study established that treating CV with BEL and FKGK-11, selective $iPLA_2$ inhibitors, significantly reduced fusion in both the standard and settle fusion assays [9]. Supplementing BEL with PLAP (i.e., 500 µM BEL + 2 µM PLAP) also reduced fusion extent

to 81.3 ± 9.5 % in the standard fusion assay (Fig. 5A; *n*=6-7) and to 80.1 ± 4.1 % in the settle fusion assay (Fig. 5B; *n*=3-4). Similarly, supplementing FKGK-11 with PLAP reduced fusion extent to 86.0 ± 3.5 % in the standard assay (Fig. 5A; *n*=6-7) and to 78.0 % ± 9.6 in the settle fusion assay (Fig.5B; *n*=3-4). Notably, treating CV with 500 µM BEL + 2 µM PLAP and 200 µM FKGK-11 + 2 µM PLAP, significantly reduced Ca^{2+} sensitivity to an EC50 of 110.9 ± 16.9 µM $[Ca^{2+}]_{free}$ and 74.8 ± 8.0 µM $[Ca^{2+}]_{free}$ respectively, relative to the control EC50 of 50.3 ± 6.2 µM $[Ca^{2+}]_{free}$, in the settle fusion assay (Fig. 5B;*n*=3-7).

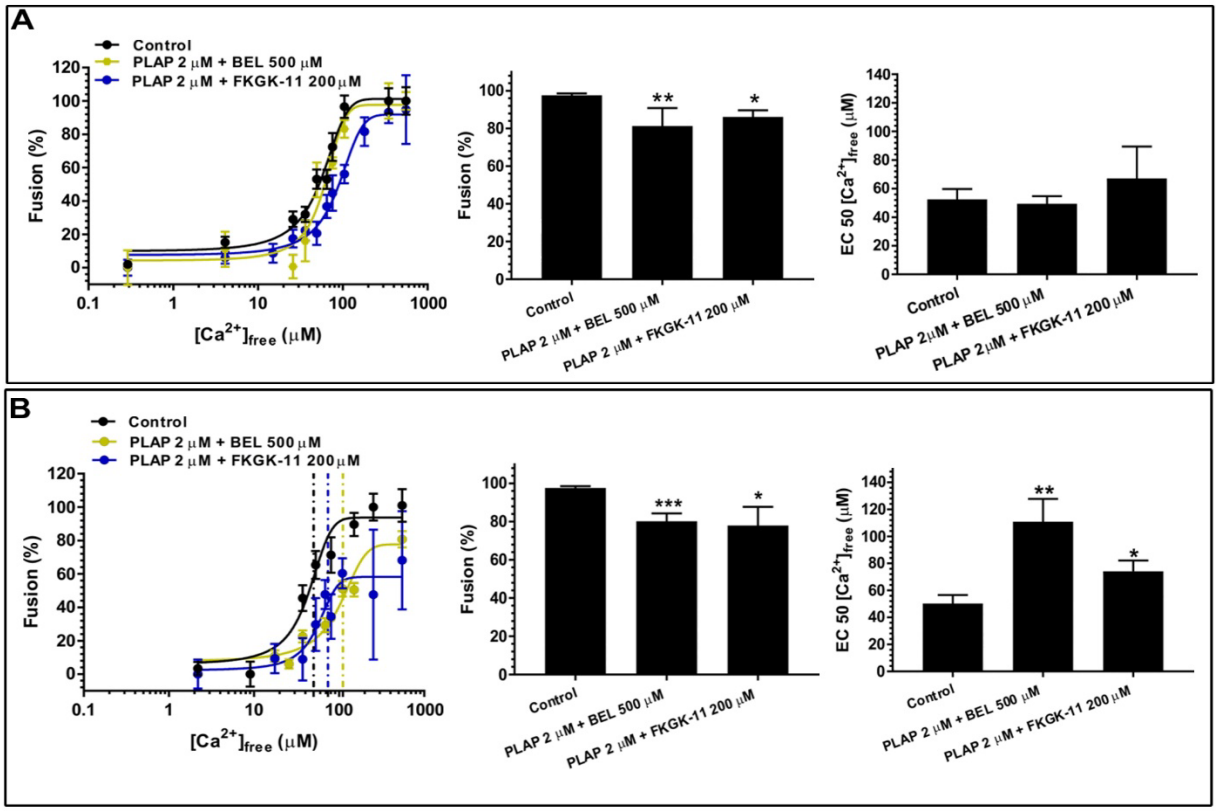

Figure 5: Effects of PLAP + BEL and PLAP + FKGK-11 on CV-CV calcium activity curves, fusion extent and calcium sensitivity (EC50); (A) standard fusion assay, *n*=6-7; (B) settle fusion assay, *n*=3-4. (p-value, *< 0.05, **<0.005, ***=0.0001 indicate relative difference to the control and as indicated).

As above, to correlate functional changes with the molecular targets, lipid analyses were carried out. Treating CV with 500 µM BEL and 200 µM FKGK-11 reduced endogenous FFA by ~ 92 % and 18 %, respectively [9]. Supplementing 2 µM PLAP with inhibitors, i.e., treating CV with 2 µM PLAP + 500 µM BEL and 2 µM PLAP + 200 µM FKGK-11, reduced endogenous FFA below background and by ~14 %, respectively (Fig. 6; *n*=3-4). No change occurred in endogenous FFA levels in CV treated with 500 µM BEL + 2 µM PLAP, relative to 500 µM BEL treated CV and in 2 µM PLAP + 200 µM FKGK-11 treated CV, relative to 200 µM FKGK-11 treated CV. This indicates that PLAP did not alter CV membrane-associated iPLA$_2$ activity (not shown, part of the data is published in [9]).

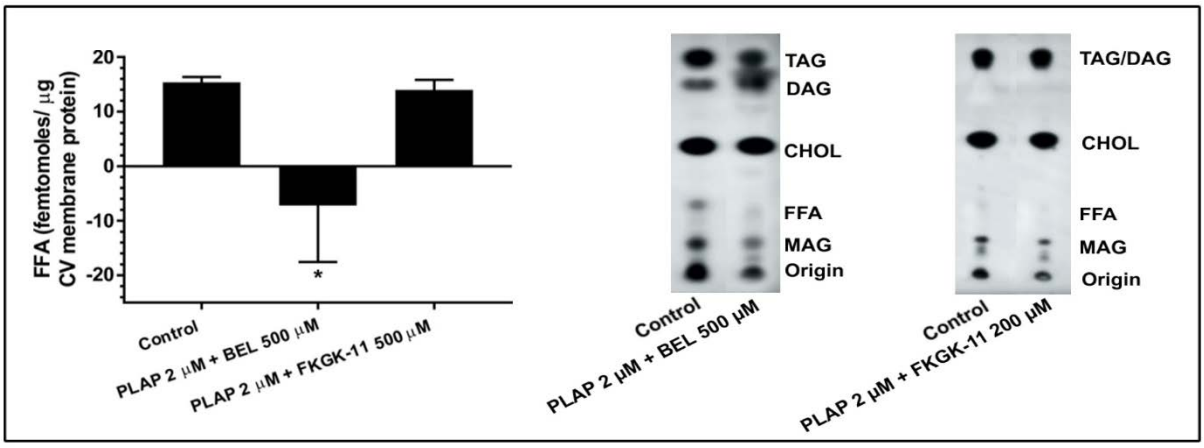

Figure 6: Changes in the endogenous FFA (*n*=3-4) in CV treated with indicated doses of BEL + PLAP and FKGK-11 + PLAP; representative chromatograms showing changes in total CV neutral lipids. (p-value, *< 0.05 indicates relative difference to the control and as indicated).

Note: The sections of the chromatogram shown are grouped together from the same HPTLC plate following removal of lanes not associated with this study. A standard neutral lipid protocol was used to resolve the lipids [8-10]

Additionally, to investigate whether PLAP modulated PLD activity, the enzymatic activity was measured in CV (OD 0.83 $\pm$ 0.01; *n*=3-4) following treatment with the indicated doses of

PLAP, LY311727 and BEL. The estimated PLD activity in an untreated control was 66.7 U/ml which is consistent with our previous study [16]. No change in basal PLD activity occurred in CV treated with the indicated concentrations of PLAP, LY311727, and BEL and also when PLAP was supplemented with LY311727 and BEL (Table-1; *n*=3-4).

	PLD U/ml	SEM	sample size (n)	Student's t- test
Control	66.7	4.4	4	
2 µM PLAP	63.3	3.3	4	0.60
20 µM LY311727	55.8	2.6	4	0.15
200 µM LY311727	33.4	11.9	3	0.06
200 µM LY311727 + 2 µM PLAP	33.9	12.1	3	0.07
100 µM BEL	57.4	5.7	3	0.29
500 µM BEL	53.2	6.3	4	0.17
500 µM BEL + 2 µM PLAP	51.1	6.4	4	0.12

Table -1: No significant change in CV associated PLD activity following treatment with the indicated doses of PLAP, LY311727 and BEL.

4.4 PLAP inhibits regulated secretion by impairing mechanisms that reduced RRP size.

Depolarization of chromaffin cells that were internally dialyzed with 860.0 pM PLAP or 2 nM LY311727, resulted in a significant decrease in exocytosis as indicated by reduced changes in membrane capacitance (Fig. 7A; *n*=4-9); ΔC_{m1}, ΔC_{m2}, and ΔC_{m3} represent change in membrane capacitance triggered by depolarizing pulses -1, -2 and -3, respectively. The

significant decrease in ΔC_{m2} to 23.8 ± 3.8 fF/pF occurred in cells treated with 860.0 pM PLAP, relative to control ΔC_{m2} of 46.9 ± 5.3 fF/pF (Fig. 7A; *n*=7-9). No change in ΔC_{m1} and ΔC_{m3} was observed with 860.0 pM PLAP. Notably, ΔC_{RRP} also reduced to 127.2 ± 21.0 fF in 860.0 pM PLAP treated cells, relative to 272.5 ± 37.8 fF observed in the controls (Fig. 7B; *n*=7-9). Similarly, LY311727 significantly reduced ΔC_{m1} and ΔC_{m3} to 17.12 ± 12.6 fF/pF and 16.5 ± 4.5 fF/pF, respectively (Fig. 7A; *n*=4-9) and also caused a significant decrease in ΔC_{RRP} to 36.0 ± 21.3 fF. No significant change in Ca^{2+} current (I_{ca}) occurred during capacitance measurements.

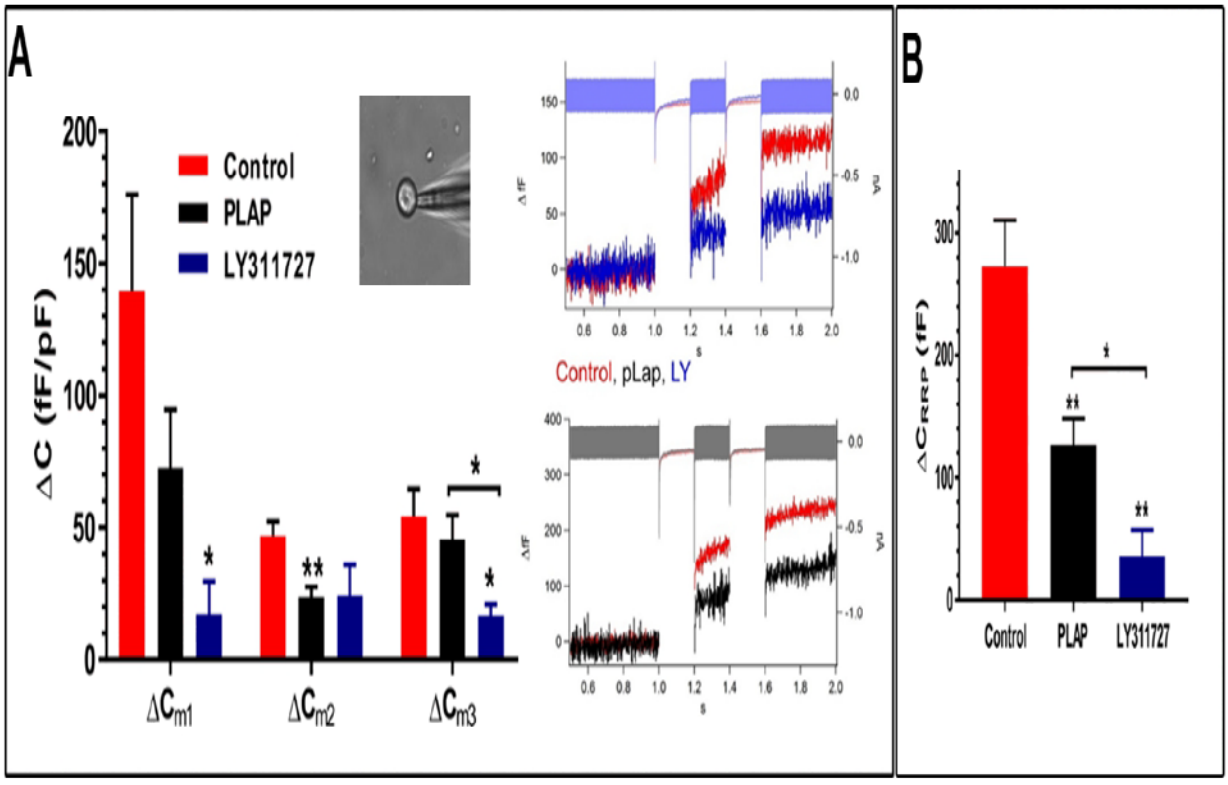

Figure 7: Effect of 860.0 pM PLAP and 2 nM LY311727 on membrane capacitance and RRP size in mouse chromaffin cells (*n*=4-9). (A) Changes in membrane capacitances (denoted as ΔC_{m1}, ΔC_{m2} and ΔC_{m3}) in response to triggering with a train of three depolarizing pulses and; (B) Changes in the size of the release-ready pool (denoted as ΔC_{RRP}). Representative trace showing changes in the capacitance measurement in cells treated with PLAP (black) and LY311727 (blue). (p value, * < 0.05, ** ≤ 0.007 indicate relative difference to the control and as indicated)

5. Discussion

Here, using native CSC and CV, we show for the first time that PLAP reduced fusion of endogenously docked CV with the PM (i.e., exocytosis *in vitro*) (Fig. 1B; *n*=3-9) and a more profound decrease in fusion extent in the settle fusion assay, relative to the standard assay (Fig. 2A, B). This confirmed that PLAP impaired molecular reactions associated with priming/docking. The decrease in function correlated with reduced endogenous FFA (Fig. 3) and increased endogenous PE (Fig. 4) in the PLAP treated CV. Additionally, PLAP reduced Ca^{2+} sensitivity, when supplemented with LY311727, BEL, and FKGK-11 (Fig. 2A, B and; Fig. 5B) but caused no change in the CV associated PLD (Table-1) and $iPLA_2$ activities. The more profound decrease in fusion extent in the settle fusion assay is consistent with a significant decrease in overall secretion and reduced RRP size in PLAP treated chromaffin cells. Overall, the data indicate that PLAP blocked common underlying molecular reactions associated with the late steps of regulated exocytosis in both of these secretory cell types.

5.1 PLAP altered lipid homeostasis in native membranes and impaired priming/docking

PLAP contains a dimerization motif, and thus can potentially form homo or heterodimers, also with the SNARE complexes (Fig. 1A). Such interactions might also block *trans* SNARE complex formation and NH_2 terminus-to-COOH terminus SNARE 'zippering' due to steric hindrance, (also see Discussion, page 65). Treating CSC with 2 µM PLAP caused no significant change in any endogenous lipids, relative to the control. However, a profound decrease in fusion extent to ~61 % was observed (Fig. 1B; *n*=3). We had anticipated an increase in endogenous FFA, relative to the control due to the suggested stimulatory action of PLAP on CV luminal $sPLA_2$ [1,4,61]. Hence, to confirm that luminal $sPLA_2$ was active in the preparation, a potent compound, LY311727 was added with 2 µM PLAP (i.e., treating CSC with 2 µM PLAP + 200 µM LY311727; Fig. 1C). This reduced endogenous FFA levels relative

to CSC treated only with PLAP but nevertheless caused no additional change in the fusion extent nor Ca^{2+} sensitivity (Fig. 1B). Importantly, as CV did not burst in PLAP treatments, which would be indicated by a drastic decrease in absorbance, this indicated that CV luminal $sPLA_2$ was inaccessible. This suggested that PLAP monomers interacted with pre-formed native molecular interactions between CV and PM, possibly including already formed and zippered *trans* SNARE complexes. This would cause steric hindrance to the SNARE action of maintaining priming/docking.

In CSC treatments, PLAP might also have altered those PM (proteins or lipids) constituents that do not play direct roles in the late stages of regulated exocytosis, thus causing 'background' effects. Therefore, it was essential to understand the action of PLAP using isolated CV. Treating isolated CV with 2 µM, 5 µM and 10 µM PLAP reduced fusion extent by ~25%, ~36%, and ~42%, respectively in the settle fusion assay (Fig. 2B) and; 2 µM PLAP also reduced fusion extent by ~13 % % in the standard fusion assay (Fig. 2A). However, the decrease in fusion extent in 2 µM PLAP treated CV was the same in both the standard and settle fusion assays. Therefore, 2 µM PLAP actually reduced priming/docking steps (as measured by the settle fusion assay) as these precede the actual membrane merger steps (measured by the standard fusion assay). This observation is also confirmed by a concentration-dependent decrease in fusion extent in the settle fusion assay. Overall, it appears that PLAP interacted with CV surface proteins, to impair priming/docking steps (Fig. 2), reduce endogenous FFA (Fig. 3) and increase endogenous PE (Fig. 4).

5.2 Ca^{2+} sensing and priming/docking steps are inter-linked.

Treating CSC with 2 µM PLAP + 200 µM LY311727 did not reduce Ca^{2+} sensitivity nor fusion extent, relative to the 2 µM PLAP treated CSC (Fig. 1B). However, treating CV with 2 µM PLAP + 200 µM LY311727 significantly reduced Ca^{2+} sensitivity by ~ 50% and ~ 68%, respectively in the standard and settle fusion assay, relative to 2 µM PLAP treated CV

(Fig. 2). Such a pattern of reduced Ca^{2+} sensitivity also occurred in 500 µM BEL + 2 µM PLAP treated CV and by >100 % in 200 µM FKGK-11 + 2 µM PLAP treated CV in the settle fusion assay (Fig. 5). These data indicated that during isolation of CV from the PM (using lower pH and a chaotropic buffer [22,50]), the pre-formed molecular interactions that maintain priming/docking and Ca^{2+} sensitivity uncouple. Nonetheless, after isolation, such interactions (although inter-vesicular) again form under the conditions of both the standard and settle CV-CV fusion assays, to re-establish priming/docking. PLAP reduced Ca^{2+} sensitivity when supplemented with LY311727, BEL, and FKGK-11 in the CV-CV fusion assays (Figs. 2 and 5) but caused no change in Ca^{2+} sensitivity nor fusion extent in the CSC fusion assays (Fig. 1B). This indicates that cumulative effects of PLAP and inhibitors blocked priming/docking and Ca^{2+} sensing only when new molecular interactions were required to re-establish priming/docking between contacting CV. No such effects of reduced priming/docking or Ca^{2+} sensitivity occurred when native interactions already existed between endogenously docked CV at the PM. This indicated that molecular reactions relating to Ca^{2+} sensing and priming/docking are closely related as a more profound decrease in Ca^{2+} sensitivity was observed in the priming/docking assay, relative to standard fusion assay.

5.3 PLAP caused no change in other CV associated enzymes activities

PLAP is suggested to stimulate $sPLA_2$ *in vitro* [1, 4,61]. In contrast, a concentration-dependent decrease in endogenous FFA in PLAP treated CV (Fig. 3) indicated a decrease in CV associated PLA_2 activities [9,10]. Importantly, PLAP did not form membrane pores which would have resulted in bursting and thus loss of intact CV. Instead, the concentration-dependent decrease in fusion extent with PLAP treatments indicated blockade in the loss of intact CV that occurs due to CV-CV or CV-PM fusion (Fig. 2). Hence, CV luminal $sPLA_2$ also remained inaccessible to PLAP. This was further confirmed in that there was no change in endogenous FFA in 2 µM PLAP + 200 µM LY311727 treated CV, relative to 2 µM PLAP

treated CV (Fig. 3). We have previously shown that 500 µM BEL and 200 µM FKGK-11 inhibit CV membrane-associated iPLA$_2$ [9]. Therefore, to investigate whether PLAP reduced FFA by decreasing CV surface iPLA$_2$ activity, separate aliquots were treated with 2 µM PLAP + 500 µM BEL and 2 µM PLAP + 200 µM FKGK-11 and endogenous FFA measured (Fig. 6). No significant decrease in fusion extent nor endogenous FFA was observed in 500 µM BEL + 2 µM PLAP treated CV, relative to 500 µM BEL treated CV. Similarly, fusion extent and endogenous FFA remain unchanged in 200 µM FKGK-11 + 2 µM PLAP treated CV, relative to 200 µM FKGK-11 treated CV (not shown, part of the data is published in [9]). These observations confirm that PLAP did not modulate CV associated iPLA$_2$ activity. Unaltered TAG levels in PLAP treated CV (see chromatograms shown in Fig. 3), unlike BEL treatments that shifted the lipid homeostasis toward the *de novo* cycle due to blockade of the iPLA$_2$ activity [9,71], was also consistent with these observations. Additionally, no change in PLD activity in CV treated with the indicated doses of PLAP, LY311727 and BEL (Table 1) indicated that PLD possibly acts upstream of PLA$_2$ isozymes in the biochemical pathways underlying the late steps of regulated exocytosis [9,16].

5.4 PLAP blocks regulated exocytosis and reduce RRP size in mammalian cell

Recently, Narayana et al. showed that isolated secretory vesicles maintain basal levels of saturated as well as unsaturated FFA species in the range of 0.0025µM - 5µM per 100 µg of secretory vesicles [72]. These levels also increased significantly following 100 mM Ca^{2+} treatment [72]. This Ca^{2+} dose is of course highly non-physiological and hence worth noting. On checking other references, that are also included in [72], it seems that authors may have mistakenly mentioned 100 mM Ca^{2+} instead of 100 µM Ca^{2+} although there is no indication of whether these are meant to indicate total or $[Ca^{2+}]_{free}$ values. We also note that there are no updated versions of [72], correcting the same. As ARA and DHA are mainly esterified at the sn-2 position in membrane phospholipids, a significant increase in ARA (~50 %) and DHA (~

94 %), after exposing secretory vesicles to 100 mM Ca^{2+} indicated that the vesicles carry a calcium-dependent PLA_2 isozyme(s). These observations are consistent with the basal endogenous FFA levels of ~15 fmoles / µg CV MP in isolated CV and identification of Ca^{2+}-dependent CV luminal $sPLA_2$ [9].

Therefore, to investigate, whether PLAP and LY311727 [9] could also reduce regulated exocytosis in another secretory cell type, both these compounds were internally dialyzed into chromaffin cells via patch pipettes. The cells that were delivered 858.0 pM PLAP had a ΔC_{m2} that was reduced by ~49 % (Fig. 7A). In contrast, cells that were delivered 2 nM LY311727 had a ΔC_{m1} that was reduced by ~88 % and ΔC_{m3} by ~70 % (Fig. 7A). Thus, both test compounds reduced regulated secretion. Importantly, both 858.0 PLAP and 2 nM LY311727 also reduced the RRP by ~53 % and ~87 %, respectively (Fig. 7A). Using a capacitance value of 1.3 fF per vesicle [20], the estimated number of the secretory vesicle in the RRP under control conditions was ~212, consistent with previous studies [20,51]. This number was significantly reduced to ~98 and ~28 in cells treated with 858.0 pM PLAP and 2 nM LY311727, respectively. The decrease in RRP size can also occur due to inhibition in the refilling of vesicles from downstream (SRP) pool, in addition to impaired priming/docking. Notably, recovery of secretory vesicles into the RRP typically occurs in seconds after triggering their release using depolarizing pulse [73,74]. This indicates that due to the $\leq$20 ms delay that was applied between depolarizing pulses, any such impairment in the refilling process had no effect in reducing RRP size [75]. This would be consistent with reduced vesicle numbers in the RRP following treatment with PLAP or LY311727 occurring due to an impaired molecular state of secretory vesicles that constitute the RRP rather than blockade in the refilling process.

6. Conclusion

Overall, using well-established model systems, CSC and CV-CV fusion assays – that enable tight coupling of the functional and molecular analyses [8,11-17] - and membrane capacitance measurements of size in chromaffin cells [18-20,73], the data here confirm that PLAP impaired common underlying mechanisms that disturbed endogenous lipid levels and impaired priming/docking steps. Also, PLAP did not form membrane pores nor modulate CV luminal sPLA$_2$ and PLD activities, contrary to earlier studies. Furthermore, critical interactions between Ca^{2+} sensors and components associated with priming/docking are also indicated.

Abbreviations: CV - cortical vesicles; CSC - cell surface complexes; ΔC_m - change in capacitance; ΔC_{RRP} - change in RRP size; $[Ca^{2+}]_{fee}$ - free calcium concentration; FFA - free fatty acid; PLAP - phospholipase A$_2$ activating peptide; RRP – readily releasable pool

Reference

1. Clark, M.A., et al., *Cloning of a phospholipase A$_2$-activating protein.* Proc Natl Acad Sci U S A, 1991. **88**(12): p. 5418-22.
2. Yunes, R., et al., *Phospholipases: melittin facilitation of bee venom phospholipase A$_2$-catalyzed hydrolysis of unsonicated lecithin liposomes.* Arch Biochem Biophys, 1977. **183**(1): p. 105-12.
3. Yue, H.Y., T. Fujita, and E. Kumamoto, *Phospholipase A$_2$ activation by melittin enhances spontaneous glutamatergic excitatory transmission in rat substantia gelatinosa neurons.* Neuroscience, 2005. **135**(2): p. 485-95.
4. Steiner, M.R., J.S. Bomalaski, and M.A. Clark, *Responses of purified phospholipases A$_2$ to phospholipase A$_2$ activating protein (PLAP) and melittin.* Biochim Biophys Acta, 1993. **1166**(1): p. 124-30.

5. Lee, M.T., F.Y. Chen, and H.W. Huang, *Energetics of pore formation induced by membrane active peptides.* Biochemistry, 2004. **43**(12): p. 3590-9.

6. Vitale, N., D. Thierse, and M.F. Bader, *Melittin promotes exocytosis in neuroendocrine cells through the activation of phospholipase A(2).* Regul Pept, 2010. **165**(1): p. 111-6.

7. van den Bogaart, G., et al., *On the Mechanism of Pore Formation by Melittin.* J Biol Chem, 2008. **283**(49): p. 33854-33857.

8. Churchward, M.A., et al., *Copper (II) sulfate charring for high sensitivity on-plate fluorescent detection of lipids and sterols: quantitative analyses of the composition of functional secretory vesicles.* J Chem Biol, 2008. **1**(1): p. 79-87.

9. Dabral, D. and J.R. Coorssen, *Combined targeted Omic and Functional Assays Identify Phospholipases A2 that Regulate Docking/Priming in Calcium-Triggered Exocytosis.* Cells, 2019. **8**(4): p. 303.

10. Dabral, D. and J.R. Coorssen, *Arachidonic acid and lysophosphatidylcholine inhibit multiple late steps of regulated exocytosis.* Biochem Biophys Res Commun, 2019. **515**(2): p. 261-267.

11. Rogasevskaia, T.P., M.A. Churchward, and J.R. Coorssen, *Anionic lipids in Ca(2+)-triggered fusion.* Cell Calcium, 2012. **52**(3-4): p. 259-69.

12. Abbineni, P. and J. Coorssen, *Application of High-Throughput Assays to Examine Phospho-Modulation of the Late Steps of Regulated Exocytosis.* High-Throughput, 2017. **6**(4): p. 17.

13. Coorssen, J.R., et al., *Biochemical and Functional Studies of Cortical Vesicle Fusion: The SNARE Complex and Ca^{2+} Sensitivity.* J Cell Biol, 1998. **143**(7): p. 1845-1857.

14. Churchward, M.A., et al., *Cholesterol facilitates the native mechanism of Ca^{2+}-triggered membrane fusion.* J Cell Sci, 2005. **118**(20): p. 4833-4848.

15. Coorssen, J.R., et al., *Regulated secretion: SNARE density, vesicle fusion and calcium dependence.* J Cell Sci, 2003. **116**(10): p. 2087-2097.

16. Rogasevskaia, T.P. and J.R. Coorssen, *The role of phospholipase D in regulated exocytosis.* J Biol Chem, 2015. **290**(48): p. 28683-28696.

17. Abbineni, P.S. and J.R. Coorssen, *Sphingolipids modulate docking, Ca^{2+} sensitivity and membrane fusion of native cortical vesicles.* Int J Biochem Cell Biol, 2018. **104**: p. 43-54.

18. Zhao, Y., et al., *Noradrenaline inhibits exocytosis via the G protein βγ subunit and refilling of the readily releasable granule pool via the αi1/2 subunit.* J Physiol, 2010. **588**(18): p. 3485-3498.

19. Lindau, M., *High resolution electrophysiological techniques for the study of calcium-activated exocytosis.* Biochim Biophys Acta, 2012. **1820**(8): p. 1234-1242.

20. Moser, T. and E. Neher, *Estimation of mean exocytic vesicle capacitance in mouse adrenal chromaffin cells.* Proc Natl Acad Sci U S A, 1997. **94**(13): p. 6735-6740.

21. Vogel, S.S., P.S. Blank, and J. Zimmerberg, *Poisson-distributed active fusion complexes underlie the control of the rate and extent of exocytosis by calcium.* J Cell Biol, 1996. **134**(2): p. 329-338.

22. Zimmerberg, J., et al., *A stage-specific preparation to study the Ca^{2+}-triggered fusion steps of exocytosis: Rationale and perspectives.* Biochimie, 2000. **82**(4): p. 303-314.

23. Szule, J.A. and J.R. Coorssen, *Revisiting the role of SNAREs in exocytosis and membrane fusion.* Biochim Biophys Acta, 2003. **1641**(2): p. 121-135.

24. Rogasevskaia, T. and J.R. Coorssen, *Sphingomyelin-enriched microdomains define the efficiency of native Ca^{2+}-triggered membrane fusion.* J Cell Sci, 2006. **119**(13): p. 2688-2694.

25. Heinemann, C., et al., *A two-step model of secretion control in neuroendocrine cells.* Pflügers Archiv, 1993. **424**(2): p. 105-112.

26. Knight, D.E., H. von Grafenstein, and C.M. Athayde, *Calcium-dependent and calcium-independent exocytosis.* Trends Neurosci, 1989. **12**(11): p. 451-458.

27. Dolensek, J., M. Skelin, and M.S. Rupnik, *Calcium dependencies of regulated exocytosis in different endocrine cells.* Physiol Res, 2011. **60 Suppl 1**: p. S29-38.

28. Augustine, G.J. and E. Neher, *Calcium requirements for secretion in bovine chromaffin cells.* J Physiol, 1992. **450**: p. 247-271.

29. Somasundaram, A. and J.W. Taraska, *Local protein dynamics during microvesicle exocytosis in neuroendocrine cells.* Mol Biol Cell, 2018. **29**(15): p. 1891-1903.

30. Brunger, A.T., et al., *Ca(2+)-Triggered Synaptic Vesicle Fusion Initiated by Release of Inhibition.* Trends Cell Biol, 2018. **28**(8): p. 631-645.

31. Aze, A., et al., *Replication origins are already licensed in G1 arrested unfertilized sea urchin eggs.* Dev Biol, 2010. **340**(2): p. 557-70.

32. Bi, G.Q., J.M. Alderton, and R.A. Steinhardt, *Calcium-regulated exocytosis is required for cell membrane resealing.* J Cell Biol, 1995. **131**(6 Pt 2): p. 1747-58.

33. Conner, S., D. Leaf, and G. Wessel, *Members of the SNARE hypothesis are associated with cortical granule exocytosis in the sea urchin egg.* Mol Reprod Dev, 1997. **48**(1): p. 106-18.

34. Voets, T., E. Neher, and T. Moser, *Mechanisms Underlying Phasic and Sustained Secretion in Chromaffin Cells from Mouse Adrenal Slices.* Neuron, 1999. **23**(3): p. 607-615.

35. Neher, E., *Neurosecretion: what can we learn from chromaffin cells.* Pflugers Arch, 2018. **470**(1): p. 7-11.

36. Becherer, U. and J. Rettig, *Vesicle pools, docking, priming, and release.* Cell Tissue Res, 2006. **326**(2): p. 393-407.

37. Jockusch, W.J., et al., *CAPS-1 and CAPS-2 are essential synaptic vesicle priming proteins.* Cell, 2007. **131**(4): p. 796-808.

38. Liu, Y., et al., *Two distinct secretory vesicle-priming steps in adrenal chromaffin cells.* J Cell Biol, 2010. **190**(6): p. 1067-1077.

39. Liu, Y., et al., *CAPS Facilitates Filling of the Rapidly Releasable Pool of Large Dense-Core Vesicles.* J Neurosci, 2008. **28**(21): p. 5594-5601.

40. He, E., et al., *Munc13-1 and Munc18-1 together prevent NSF-dependent de-priming of synaptic vesicles.* Nat Commun, 2017. **8**: p. 15915.

41. Voets, T., E. Neher, and T. Moser, *Mechanisms underlying phasic and sustained secretion in chromaffin cells from mouse adrenal slices.* Neuron, 1999. **23**(3): p. 607-15.

42. Álvarez, Y.D., et al., *The Immediately Releasable Pool of Mouse Chromaffin Cell Vesicles Is Coupled to P/Q-Type Calcium Channels via the Synaptic Protein Interaction Site.* PLOS ONE, 2013. **8**(1): p. e54846.

43. Xu, T. and S.M. Bajjalieh, *SV2 modulates the size of the readily releasable pool of secretory vesicles.* Nat Cell Biol, 2001. **3**: p. 691.

44. Xu, T., et al., *Inhibition of SNARE Complex Assembly Differentially Affects Kinetic Components of Exocytosis.* Cell, 1999. **99**(7): p. 713-722.

45. Duman, J.G. and J.G. Forte, *What is the role of SNARE proteins in membrane fusion?* Am J Physiol Cell Physiol, 2003. **285**(2): p. C237-49.

46. Sorensen, J.B., et al., *Differential control of the releasable vesicle pools by SNAP-25 splice variants and SNAP-23.* Cell, 2003. **114**(1): p. 75-86.

47. Stevens, D.R., et al., *Vesicle pools: lessons from adrenal chromaffin cells.* Front Synaptic Neurosci, 2011. **3**: p. 2.

48. Yang, Y., et al., *A highly Ca^{2+}-sensitive pool of vesicles is regulated by protein kinase C in adrenal chromaffin cells.* Proc Natl Acad Sci U S A, 2002. **99**(26): p. 17060-17065.

49. Zimmerberg, J., et al., *Sea urchin egg preparations as systems for the study of calcium-triggered exocytosis.* J Physiol, 1999. **520 Pt 1**: p. 15-21.

50. Abbineni, P.S., et al., *The Sea Urchin Egg and Cortical Vesicles as Model Systems to Dissect the Fast, Ca^{2+}-Triggered Steps of Regulated Exocytosis*, in *Exocytosis Methods*. 2014. p. 221-241.

51. Stevens, D.R., et al., *Vesicle pools: lessons from adrenal chromaffin cells.* Front Synaptic Neurosci, 2011. **3**: p. 2-2.

52. Asthana, N., S.P. Yadav, and J.K. Ghosh, *Dissection of antibacterial and toxic activity of melittin: a leucine zipper motif plays a crucial role in determining its hemolytic activity but not antibacterial activity.* J Biol Chem, 2004. **279**(53): p. 55042-50.

53. Frey, S. and L.K. Tamm, *Orientation of melittin in phospholipid bilayers. A polarized attenuated total reflection infrared study.* Biophys J, 1991. **60**(4): p. 922-930.

54. Gordon-Grossman, M., et al., *A Combined Pulse EPR and Monte Carlo Simulation Study Provides Molecular Insight on Peptide−Membrane Interactions.* J Phys Chem B, 2009. **113**(38): p. 12687-12695.

55. Gravitt, K.R., N.E. Ward, and C.A. O'Brian, *Inhibition of protein kinase C by melittin: antagonism of binding interactions between melittin and the catalytic domain by active-site binding of MgATP.* Biochem Pharmacol, 1994. **47**(2): p. 425-427.

56. Raynor, R.L., B. Zheng, and J.F. Kuo, *Membrane interactions of amphiphilic polypeptides mastoparan, melittin, polymyxin B, and cardiotoxin. Differential inhibition of protein kinase C, Ca^{2+}/calmodulin-dependent protein kinase II and*

synaptosomal membrane Na,K-ATPase, and Na+ pump and differentiation of HL60 cells. J Biol Chem, 1991. **266**(5): p. 2753-8.

57. Katoh, N., et al., *Inhibition by melittin of phospholipid-sensitive and calmodulin-sensitive Ca^{2+} -dependent protein kinases.* Biochem J, 1982. **202**(1): p. 217-224.

58. Paudel, H.K., et al., *The model calmodulin-binding peptide melittin inhibits phosphorylase kinase by interacting with its catalytic center.* Biochemistry, 1993. **32**(44): p. 11865-11872.

59. Park, H.J., et al., *Melittin inhibits inflammatory target gene expression and mediator generation via interaction with IkappaB kinase.* Biochem Pharmacol, 2007. **73**(2): p. 237-47.

60. Heisler, S., *Phospholipase A_2 activation by melittin causes amylase release from exocrine pancreas.* Can J Physiol Pharmacol, 1989. **67**(5): p. 411-6.

61. Koumanov, K., A. Momchilova, and C. Wolf, *Bimodal regulatory effect of melittin and phospholipase A_2-activating protein on human type II secretory phospholipase A_2.* Cell Biol Int, 2003. **27**(10): p. 871-877.

62. Saini, S.S., J.W. Peterson, and A.K. Chopra, *Melittin Binds to Secretory Phospholipase A_2 and Inhibits Its Enzymatic Activity.* Biochem Biophys Res Commun, 1997. **238**(2): p. 436-442.

63. Sommer, A., et al., *Phosphatidylserine exposure is required for ADAM17 sheddase function.* Nat Commun, 2016. **7**: p. 11523.

64. Saini, S.S., A.K. Chopra, and J.W. Peterson, *Melittin activates endogenous phospholipase D during cytolysis of human monocytic leukemia cells.* Toxicon, 1999. **37**(11): p. 1605-19.

65. Sørensen, J.B., et al., *Differential Control of the Releasable Vesicle Pools by SNAP-25 Splice Variants and SNAP-23.* Cell, 2003. **114**(1): p. 75-86.

66. Hannun, Y.A. and R.M. Bell, *Regulation of protein kinase C by sphingosine and lysosphingolipids.* Clinica Chimica Acta, 1989. **185**(3): p. 333-345.

67. Shu, Y., et al., *Phosphorylation of SNAP-25 at Ser187 mediates enhancement of exocytosis by a phorbol ester in INS-1 cells.* J Neurosci, 2008. **28**(1): p. 21-30.

68. Zimmerberg, J., et al., *Sea urchin egg preparations as systems for the study of calcium-triggered exocytosis.* J Physiol, 1999. **520**(1): p. 15-21.

69. Rogasevskaia, T.P. and J.R. Coorssen, *A new approach to the molecular analysis of docking, priming, and regulated membrane fusion.* J Chem Biol, 2011. **4**(3): p. 117-136.

70. Bligh, E.G. and W.J. Dyer, *A rapid method of total lipid extraction and purification.* Can J Biochem Physiol, 1959. **37**(8): p. 911-7.

71. Dabral, D. and J.R. Coorssen, *Phospholipase A_2: Potential roles in native membrane fusion.* Int J Biochem Cell Biol, 2017. **85**: p. 1-5.

72. Narayana, V.K., et al., *Profiling of Free Fatty Acids Using Stable Isotope Tagging Uncovers a Role for Saturated Fatty Acids in Neuroexocytosis.* Chem Biol, 2015. **22**(11): p. 1552-1561.

73. Moser, T. and E. Neher, *Rapid exocytosis in single chromaffin cells recorded from mouse adrenal slices.* J Neurosci, 1997. **17**(7): p. 2314-23.

74. Voets, T., *Dissection of three Ca^{2+}-dependent steps leading to secretion in chromaffin cells from mouse adrenal slices.* Neuron, 2000. **28**(2): p. 537-45.

75. Smith, C., et al., *Cytosolic Ca^{2+} Acts by Two Separate Pathways to Modulate the Supply of Release-Competent Vesicles in Chromaffin Cells.* Neuron, 1998. **20**(6): p. 1243-1253.

CHAPTER – 5

Discussion and Future Directions

General Discussion and Future Directions

The late steps of Ca^{2+} triggered exocytosis involve Ca^{2+} sensing, docking, priming, and membrane merger. Hence, to understand steps preceding membrane merger, one must consider the basal biochemical state of the system (i.e., unstimulated), and this is true for all potentially active molecular species, including membrane lipids. My working hypothesis states that localized PLA_2 supply FFA (e.g., ARA) and LPL (e.g., LPC) near docking / fusion sites; LPC in the proximal monolayers acts as a molecular fusion 'brake' to block spontaneous membrane merger while ARA aids in SNARE mediated priming/docking [1]. The data presented in **Chapter 2** indicate that catalytically active endogenous vesicle-associated PLA_2 isoforms – $iPLA_2$ on the CV surface and $sPLA_2$ in the CV lumen – carry out these orchestered roles in regulating and maintaining vesicle priming/docking [2]. This resolves a long-standing question in the field as to the possible role(s) of PLA_2 in exocytosis [3-6]. As proteolytic cleavage of CV surface proteins (including SNAREs and $iPLA_2$) significantly reduced priming/docking, this suggested a need to investigate whether SNARE mediated priming/docking requires functional $iPLA_2$ [2]. However, due to time constraints, direct assays of SNARE interactions could not be carried out. To further probe the role(s) of PLA_2, the data presented in **Chapter 3** show that addition of the canonical PLA_2 metabolites ARA and LPC, respectively, inhibit priming/docking and the membrane merger step of regulated exocytosis. That exogenous LPC blocked membrane merger (likely at an initiating step [7-11]) is consistent with the working hypothesis [1] and identification of $iPLA_2$ on the CV surface, that can generate local LPC to block spontaneous membrane merger [2]. However, that exogenous ARA impaired priming/docking is contradictory of the suggested supporting role of PLA_2 generated ARA in promoting SNARE complex formation [1]. This portion of the working hypothesis was proposed based on earlier *in vitro* [12-14] and *in vivo* [15,16] studies suggesting that ARA promoted SNARE complex formation and interacted with SNARE microdomains. However, a

crucial consideration relating to ARA supplementation in whole-cell studies is its rapid metabolism to generate shorter FFA species [17,18], that then reorganize FFA species in the membrane phospholipids [18-20]. Indeed, the data presented in **Chapter 3**, show that even isolated CV carry native enzymes to convert exogenous ARA into endogenous FFA within 10 min; nevertheless, using a non-metabolizable analogue, it was also clear that exogenous ARA directly impaired the priming/docking steps of regulated exocytosis [11]. Does this imply that ARA altered membrane biophysical properties by reorganizing FFA species in membrane phospholipids that reduced priming/docking? Importantly, priming and docking steps are considered as the functional consequence of SNARE complex formation and 'zippering' [2,21-26]. If so, then the ARA induced decrease in priming/docking, and studies suggesting ARA promotes SNARE complex formation are inconsistent. Hence, the claim of ARA promoted SNARE complex formation thus requires more focussed investigation. In this regard, probing changes in individual native SNARE monomers and complex formation in ARA treated CV, relative to control would likely prove useful.

Additionally, data presented in **Chapter 4** showed that PLAP, a melittin homolog, inhibited CSC and CV fusion by impairing priming/docking but caused no change in the CV luminal $sPLA_2$ activity. Melittin is a polypeptide that tends to form α-helical monomers. It can also oligomerize to form dimers or tetramers [27,28], likely via a leucine zipper dimerization motif. Nevertheless, under physiological conditions and a low peptide-to-lipid ratio, melittin exists as a monomer [28]. According to the proposed mechanism of Terwilliger et al., at low concentrations, melittin monomers orient parallel to the outer monolayer, thus increasing the surface area of the outer monolayer [29,30]. This eventually results in the formation of membrane pores when melittin concentrations exceed a critical peptide-to-lipid ratio due to the imbalance in the surface area of the outer monolayer relative to the inner monolayer [29,30]. As PLAP shares high identity and similarity with melittin, including a leucine zipper motif, it

is also expected to form membrane pores, as described above. However, in contrast, PLAP blocked fusion by impairing priming/docking steps. As PLAP did not form membrane pores (which would have resulted in bursting and thus loss of intact CV), CV luminal $sPLA_2$ remained inaccessible, and therefore its activity was unaltered by PLAP; the recognized stimulatory action of PLAP has only been demonstrated on already released $sPLA_2$ [31,32]. This thus indicates that PLAP concentration in the CSC and CV treatments was likely below the critical peptide-to-lipid ratio. Due to this, it would appear that PLAP monomers likely interacted with the molecular entities on the outer CV monolayer, thus blocking inter-membrane contact and/or *trans* SNARE complex formation and 'zippering' due to steric hindrance. Importantly, PLAP impaired priming/docking steps and also altered endogenous PE and FFA levels, indicating that priming/docking, the endogenous lipid composition, and SNARE complex formation or 'zippering' could be inter-related. These are interesting observations that warrant more focussed future studies.

Overall, the findings in **Chapters 2 and 3** are novel and significant as they further contribute to our understanding of how PLA_2 and its metabolites contribute to the fundamental molecular mechanisms that modulate the late steps of regulated exocytosis. Additionally, data presented in **Chapter 4** further highlight the similarity in the molecular state of RRP secretory vesicles in the chromaffin cell and fully primed release-ready CV.

The concentration of non-bilayer forming lipids (e.g., LPC, Cholesterol, ARA), relative to bilayer forming lipids (e.g., PC) in the membrane modulates the progression of membrane merger steps after initial membrane contact [1,8,10,33]. In this regard, all membrane-bound enzymes and those present in the vesicle lumen that can cleave bilayer forming phospholipids to generate non-bilayer forming lipids are critical. These include phospholipases A_1 (PLA_1), phospholipase B (PLB) and phospholipase C (PLC). PLB and PLC cleave membrane phospholipids to generate LPL and FFA, and DAG and inositol triphosphate (IP_3), respectively.

Importantly, isolated secretory vesicles also generate saturated FFA in an unstimulated state, possibly due to the basal activity of vesicle-associated PLA_1 [34]. Therefore, to identify their roles in the late steps of regulated exocytosis, inhibiting PLA_1 isozyme activities using diisopropylfluorophosphate and arachidonyl fluorophosphonate [35] and studying treatment effects using functional assays [2,36,37] would be informative.

Importantly, the data presented in **Chapters 2** and **3** indicate that a dynamic equilibrium among lipid species in the native CV membrane is under tight regulation by the action of endogenous enzymes [2,36,37]. Therefore, outcomes of lipid supplementation should be carefully considered as added lipids also disturb the equilibrium between the lipid species in the biochemical pathways, thus complicating interpretation of the data. Importantly, for some enzymes, Ca^{2+} could be an essential co-factor [38,39], so that these might also be considered to act as Ca^{2+} sensors operating at low $[Ca^{2+}]_{free}$ to regulate docking and priming, as has also been suggested [26,40]. Therefore, identification and characterization of such CV associated Ca^{2+}-binding enzymes can be done using Immobilized Metal Chelate Affinity Chromatography (IMAC) [41,42] and top-down proteomics [2,42,43]. The Ca^{2+} sensing ability of these enzymes can then be confirmed by modulating their activities, as was previously done [2,36,44,45] to study the associated effects in the standard and settle fusion assays [2,22,37,44,46-48]. After identification, characterization, and purification, such membrane attached enzymes that act as Ca^{2+} sensors can also be reconstituted with correct orientation in (PC/PE/PS/PI/cholesterol) giant unilamellar liposomes (GUV) [49] to confirm their role via heterotypic CV-GUV fusion [50]. The orientation of reconstituted proteins in the membrane can be confirmed using trypsin [49], western blotting, and enzyme assays. This approach would also be useful in quantifying the minimum copy number of the target protein required to carry out its role in the GUV-CV fusion assay.

As $iPLA_2$ has been identified on the outer CV monolayer, it would also be interesting to investigate whether Botulinum toxin types B/C/F (BoNT B/C/F) could modulate its activity, in addition to the cleavage of SNAREs [51]. If so, what effects does this then exert on the priming/docking steps and how to dissociate the effects of toxin treatments on SNAREs vs. $iPLA_2$? The BoNT B and F toxins cleave VAMP 2 at peptide bonds after Q^{78} and L^{56}, respectively and BoNT C cleaves both SNAP 25 and syntaxin at peptide bonds after R^{198} and K^{252} [51]. Therefore, carrying out residue-specific reversible modifications or 'bioconjugation' [52] to block BoNT B/C/F cleavage sites on CV SNAREs coupled with standard and settle fusion assays [2,36,37,45,47] would be useful to dissociate the effects of SNAREs and $iPLA_2$ on priming/docking. This would first involve blocking of BoNT B/C/F cleavage sites on the CV SNAREs by modifying their Q, L, and R residues [52], thus allowing toxin-induced modification in the $iPLA_2$ activity during treatments. With this, the selective effects of toxins on $iPLA_2$, and therefore on priming/docking would be confirmed. In the next step, treating CV aliquots (that carry modified Q, L, R residues) with toxins but after unblocking BoNT B/C/F cleavage sites on CV SNAREs [52] would now allow cleavage of the SNAREs during treatments. Effects on the functional assays would now reflect the roles of SNAREs in priming/docking. Nevertheless, while this study looks promising, initial experiments to optimize conditions for efficient and selective amino acid modifications, and to probe any associated 'background' effects of bioconjugation would be essential.

Furthermore, CV luminal $[Ca^{2+}]_{free}$ transients occur in the range of ~1-10 µM due to opening/closing of p-type Ca^{2+} channels [53]. Therefore local $[Ca^{2+}]_{free}$ at the inner CV membrane would likely be higher than the global average in the CV lumen itself [2]. Therefore, to confirm that during Ca^{2+} transients localized Ca^{2+}-dependent CV luminal $sPLA_2$ activity at the inner CV membrane also increases [2], monitoring changes in the PED6 labelled inner monolayer of an intact CV together with luminal $[Ca^{2+}]_{free}$ levels using Indo-1 might be

promising. PED 6 is a selective PLA_2 substrate that has absorption and emission maxima at ~488 nm and ~530 nm, respectively [2]. However, as CV also carry an active surface $iPLA_2$, it would thus be essential to inhibit its activity before PED6 labeling using a selective inhibitor, such as Bromoenol lactone (BEL) [2]. Indo-1 is a high Ca^{2+} affinity ratiometric dye that has an absorption maximum at ~350 nm, and two emission maxima at ~405 nm and ~485 nm, corresponding to the bound and unbound [Ca^{2+}] states, respectively [54]. Given that emission maxima of PED6 and Indo-1 are well-separated (530 nm vs. 405nm), a single (argon) laser would be able to generate well-separated emission spectra from both fluorophores; argon lasers emit 13 wavelengths, including 488nm and 351nm. Using select filters and detectors on the microscope, these spectra would thus produce separate corresponding images, and when superimposed would show co-related spatiotemporal changes in localized $sPLA_2$ activity and $[Ca^{2+}]_{free}$ levels [53,55]. Nevertheless, the biggest technological challenge relating to this study will be the acquisition of super-resolution fluorescent images of isolated CV that have an average diameter of ~1 μM [53,56]. Further, interference due to potential auto-fluorescence from the biological samples upon excitation at 350 nm might also pose an issue.

The molecular definition and distinction between priming/docking are still unknown [57,58]; nevertheless, it has been long known that at least some priming reactions require ATP [59,60], perhaps to phosphorylate SNAP 25 [61,62], synaptotagmin [63], and phosphatidylinositol to generate Phosphatidylinositol 4,5-bisphosphate (PIP_2) [64-66]. The settle fusion assay evaluates the priming/docking capacity of CV by allowing them to freely undergo the biochemical reactions that support inter-membrane attachment. Therefore, molecular targets of the phosphorylation reactions associated with priming/docking, can be measured by assessing changes in ATP [67-69] and total CV lipids (including PIP_2) using top-down lipidomics at the beginning (0 hr), mid-point (30 min) and end of the incubation (1 hr) and co-relating these changes with the outcome of the functional assays carried out at the end

of each incubation. This test can further be extended to assess changes in CV luminal and membrane proteins using top-down proteomics at the end of each incubation to identify protein targets of the phosphorylation reaction.

In conclusion, homotypic CV fusion, as well as heterotypic CV-PM fusion, are excellent stage-specific models which can still teach us a great deal concerning the late steps of regulated exocytosis, including Ca^{2+} sensing, docking, priming, and membrane merger. Using biochemical and molecular assays, targeted omics coupled with functional analyses and single-vesicle super-resolution microscopy, unidentified molecular targets (protein, lipid or both) associated with the above mentioned steps can be identified to further co-relate their biochemical state (e.g., levels of phosphorylation) with priming/docking.

References

1. Dabral, D. and J.R. Coorssen, *Phospholipase A_2: Potential roles in native membrane fusion.* Int J Biochem Cell Biol, 2017. **85**: p. 1-5.
2. Dabral, D. and J.R. Coorssen, *Combined Targeted Omic and Functional Assays Identify Phospholipases A_2 that Regulate Docking/Priming in Calcium-Triggered Exocytosis.* Cells, 2019. **8**(4): p. 303.
3. Coorssen, J.R., *Phospholipase activation and secretion: evidence that PLA_2, PLC, and PLD are not essential to exocytosis.* Am J Physiol, 1996. **270**(4): p. C1153-C1163.
4. Frye, R.A. and R.W. Holz, *Arachidonic acid release and catecholamine secretion from digitonin-treated chromaffin cells: effects of micromolar calcium, phorbol ester, and protein alkylating agents.* J Neurochem, 1985. **44**(1): p. 265-73.
5. Zimmerberg, J. and L.V. Chernomordik, *Synaptic Membranes Bend to the Will of a Neurotoxin.* Science, 2005. **310**(5754): p. 1626-1627.

6. Matsuzawa, A., et al., *Release of secretory phospholipase A_2 from rat neuronal cells and its possible function in the regulation of catecholamine secretion.* Biochem J, 1996. **318**: p. 701-9.

7. Chernomordik, L.V., et al., *Lysolipids reversibly inhibit Ca^{2+}-, GTP- and pH-dependent fusion of biological membranes.* FEBS Lett, 1993. **318**(1): p. 71-76.

8. Chernomordik, L., et al., *The hemifusion intermediate and its conversion to complete fusion: regulation by membrane composition.* Biophys J, 1995. **69**(3): p. 922-9.

9. Chernomordik, L., *Non-bilayer lipids and biological fusion intermediates.* Chem Phys Lipids, 1996. **81**(2): p. 203-13.

10. Chernomordik, L.V. and M.M. Kozlov, *Mechanics of membrane fusion.* Nat Struct Mol Biol, 2008. **15**(7): p. 675-683.

11. Dabral, D. and J.R. Coorssen, *Arachidonic acid and lysophosphatidylcholine inhibit multiple late steps of regulated exocytosis.* Biochem Biophys Res Commun, 2019.

12. Latham, C.F., et al., *Arachidonic acid potentiates exocytosis and allows neuronal SNARE complex to interact with Munc18a.* J Neurochem, 2007. **100**(6): p. 1543-54.

13. Mounier, C.M., et al., *Arachidonic Acid Release from Mammalian Cells Transfected with Human Groups IIA and X Secreted Phospholipase A_2 Occurs Predominantly during the Secretory Process and with the Involvement of Cytosolic Phospholipase A_2-α.* J Biol Chem, 2004. **279**(24): p. 25024-25038.

14. Rickman, C. and B. Davletov, *Arachidonic acid allows SNARE complex formation in the presence of Munc18.* Chem Biol, 2005. **12**(5): p. 545-53.

15. García-Martínez, V., et al., *Lipid Metabolites Enhance Secretion Acting on SNARE Microdomains and Altering the Extent and Kinetics of Single Release Events in Bovine Adrenal Chromaffin Cells.* PLOS ONE, 2013. **8**(9): p. e75845.

16. Darios, F. and B. Davletov, *Omega-3 and omega-6 fatty acids stimulate cell membrane expansion by acting on syntaxin 3.* Nature, 2006. **440**(7085): p. 813-817.

17. Williard, D.E., et al., *Conversion of eicosapentaenoic acid to chain-shortened omega-3 fatty acid metabolites by peroxisomal oxidation.* J Lipid Res, 1998. **39**(5): p. 978-86.

18. Galli, C., P. Rise, and F. Marangoni, *Fate of exogenous arachidonic acid in THP-1 cells: incorporation in cell lipids and conversion to outer N-6 fatty acids.* Prostaglandins Leukot Essent Fatty Acids, 1995. **52**(2-3): p. 103-6.

19. Bolognesi, A., et al., *Membrane Lipidome Reorganization Correlates with the Fate of Neuroblastoma Cells Supplemented with Fatty Acids.* PLOS ONE, 2013. **8**(2): p. e55537.

20. Levental, K.R., et al., *Homeostatic remodeling of mammalian membranes in response to dietary lipids is essential for cellular fitness.* bioRxiv, 2018: p. 342873.

21. Coorssen, J.R., et al., *Biochemical and Functional Studies of Cortical Vesicle Fusion: The SNARE Complex and Ca^{2+} Sensitivity.* J Cell Biol, 1998. **143**(7): p. 1845-1857.

22. Coorssen, J.R., et al., *Regulated secretion: SNARE density, vesicle fusion and calcium dependence.* J Cell Sci, 2003. **116**(10): p. 2087-2097.

23. Szule, J.A., et al., *Calcium-triggered Membrane Fusion Proceeds Independently of Specific Presynaptic Proteins.* J Biol Chem, 2003. **278**(27): p. 24251-24254.

24. Duman, J.G. and J.G. Forte, *What is the role of SNARE proteins in membrane fusion?* Am J Physiol Cell Physiol, 2003. **285**(2): p. C237-C249.

25. Stevens, D., et al., *Vesicle Pools: Lessons from Adrenal Chromaffin Cells.* Front Synaptic Neurosci, 2011. **3**(2).

26. Becherer, U. and J. Rettig, *Vesicle pools, docking, priming, and release.* Cell and Tissue Res, 2006. **326**(2): p. 393-407.

27. Othon, C.M., et al., *Solvation in protein (un)folding of melittin tetramer–monomer transition.* Proc Natl Acad Sci U S A, 2009. **106**(31): p. 12593-12598.

28. Fox, S.J., et al., *Conformational Transitions of Melittin between Aqueous and Lipid Phases: Comparison of Simulations with Experiments.* J Phys Chem B, 2018. **122**(37): p. 8698-8705.

29. Lee, M.-T., et al., *Process of inducing pores in membranes by melittin.* Proc Natl Acad Sci U S A, 2013. **110**(35): p. 14243-14248.

30. Terwilliger, T.C., L. Weissman, and D. Eisenberg, *The structure of melittin in the form I crystals and its implication for melittin's lytic and surface activities.* Biophys J, 1982. **37**(1): p. 353-61.

31. Clark, M.A., et al., *Cloning of a phospholipase A_2-activating protein.* Proc Natl Acad Sci U S A, 1991. **88**(12): p. 5418-5422.

32. Steiner, M.R., J.S. Bomalaski, and M.A. Clark, *Responses of purified phospholipases A_2 to phospholipase A_2 activating protein (PLAP) and melittin.* Biochim Biophys Acta, 1993. **1166**(1): p. 124-30.

33. Chernomordik, L., M.M. Kozlov, and J. Zimmerberg, *Lipids in biological membrane fusion.* J Membr Biol, 1995. **146**(1): p. 1-14.

34. Narayana, Vinod K., et al., *Profiling of Free Fatty Acids Using Stable Isotope Tagging Uncovers a Role for Saturated Fatty Acids in Neuroexocytosis.* Chem Biol, 2015. **22**(11): p. 1552-1561.

35. Inoue, A. and J. Aoki, *Phospholipase A_1: structure, distribution and function.* Future Lipidol, 2006. **1**(6): p. 687-700.

36. Rogasevskaia, T.P. and J.R. Coorssen, *The role of phospholipase D in regulated exocytosis.* J Biol Chem, 2015.

37. Abbineni, P.S. and J.R. Coorssen, *Sphingolipids modulate docking, Ca^{2+} sensitivity and membrane fusion of native cortical vesicles.* Int J Biochem Cell Biol, 2018. **104**: p. 43-54.

38. Soupene, E., H. Fyrst, and F.A. Kuypers, *Mammalian acyl-CoA:lysophosphatidylcholine acyltransferase enzymes.* Proc Natl Acad Sci U S A, 2008. **105**(1): p. 88-93.

39. Mellgren, R.L., *Calcium-dependent proteases: an enzyme system active at cellular membranes?* FASEB J, 1987. **1**(2): p. 110-5.

40. Voets, T., *Dissection of three Ca^{2+}-dependent steps leading to secretion in chromaffin cells from mouse adrenal slices.* Neuron, 2000. **28**(2): p. 537-45.

41. Chaga, G.S., B. Ersson, and J.O. Porath, *Isolation of calcium-binding proteins on selective adsorbents application to purification of bovine calmodulin.* J Chromatogr A, 1996. **732**(2): p. 261-269.

42. Lopez, M.F., et al., *High-throughput profiling of the mitochondrial proteome using affinity fractionation and automation.* Electrophoresis, 2000. **21**(16): p. 3427-3440.

43. Kawashima, A., et al., *CABS1 Is a Novel Calcium-Binding Protein Specifically Expressed in Elongate Spermatids of Mice1*. Biol Reprod, 2009. **80**(6): p. 1293-1304.

44. Rogasevskaia, T. and J.R. Coorssen, *Sphingomyelin-enriched microdomains define the efficiency of native Ca^{2+}-triggered membrane fusion.* J Cell Sci, 2006. **119**(13): p. 2688-2694.

45. Rogasevskaia, T.P., M.A. Churchward, and J.R. Coorssen, *Anionic lipids in Ca(2+)-triggered fusion.* Cell Calcium, 2012. **52**(3-4): p. 259-69.

46. Rogasevskaia, T.P. and J.R. Coorssen, *The role of phospholipase D in regulated exocytosis.* J Biol Chem, 2015(290): p. 28683-28696. .

47. Churchward, M.A., et al., *Specific Lipids Supply Critical Negative Spontaneous Curvature—An Essential Component of Native Ca^{2+}-Triggered Membrane Fusion.* Biophys J, 2008. **94**(10): p. 3976-3986.

48. Churchward, M.A., et al., *Cholesterol facilitates the native mechanism of Ca^{2+}-triggered membrane fusion.* J Cell Sci, 2005. **118**(20): p. 4833-4848.

49. Schuette, C.G., et al., *Determinants of liposome fusion mediated by synaptic SNARE proteins.* Proc Natl Acad Sci U S A, 2004. **101**(9): p. 2858-2863.

50. Chanturiya, A., M. Whitaker, and J. Zimmerberg, *Calcium-induced fusion of sea urchin egg secretory vesicles with planar phospholipid bilayer membranes.* Mol Membr Biol, 1999. **16**(1): p. 89-94.

51. Pirazzini, M., et al., *Botulinum Neurotoxins: Biology, Pharmacology, and Toxicology.* Pharmacol Rev, 2017. **69**(2): p. 200-235.

52. deGruyter, J.N., L.R. Malins, and P.S. Baran, *Residue-Specific Peptide Modification: A Chemist's Guide.* Biochemistry, 2017. **56**(30): p. 3863-3873.

53. Raveh, A., et al., *Observations of calcium dynamics in cortical secretory vesicles.* Cell Calcium, 2012. **52**(3): p. 217-225.

54. Paredes, R.M., et al., *Chemical calcium indicators.* Methods 2008. **46**(3): p. 143-151.

55. Sanderson, M.J., et al., *Fluorescence microscopy.* Cold Spring Harb Protoc, 2014. **2014**(10): p. pdb.top071795-pdb.top071795.

56. Nienhaus, K. and G.U. Nienhaus, *Where Do We Stand with Super-Resolution Optical Microscopy?* J Mol Biol, 2016. **428**(2, Part A): p. 308-322.

57. Siksou, L., et al., *A common molecular basis for membrane docking and functional priming of synaptic vesicles.* Eur J Neurosci, 2009. **30**(1): p. 49-56.

58. Neher, E. and T. Sakaba, *Multiple roles of calcium ions in the regulation of neurotransmitter release.* Neuron, 2008. **59**(6): p. 861-72.

59. Parsons, T.D., et al., *Docked granules, the exocytic burst, and the need for ATP hydrolysis in endocrine cells.* Neuron, 1995. **15**(5): p. 1085-1096.

60. Eliasson, L., et al., *Rapid ATP-dependent priming of secretory granules precedes Ca(2+)-induced exocytosis in mouse pancreatic B-cells.* J Physiol, 1997. **503 (Pt 2)**: p. 399-412.

61. Gao, J., et al., *Differential role of SNAP-25 phosphorylation by protein kinases A and C in the regulation of SNARE complex formation and exocytosis in PC12 cells.* Cell Signal, 2016. **28**(5): p. 425-437.

62. Nagy, G., et al., *Regulation of Releasable Vesicle Pool Sizes by Protein Kinase A-Dependent Phosphorylation of SNAP-25.* Neuron, 2004. **41**(3): p. 417-429.

63. de Jong, A.P.H., et al., *Phosphorylation of synaptotagmin-1 controls a post-priming step in PKC-dependent presynaptic plasticity.* Proc Natl Acad Sci U S A, 2016. **113**(18): p. 5095-5100.

64. Hay, J.C. and T.F. Martin, *Phosphatidylinositol transfer protein required for ATP-dependent priming of Ca(2+)-activated secretion.* Nature, 1993. **366**(6455): p. 572-5.

65. Milosevic, I., et al., *Plasmalemmal phosphatidylinositol-4,5-bisphosphate level regulates the releasable vesicle pool size in chromaffin cells.* J Neurosci, 2005. **25**(10): p. 2557-65.

66. Mayer, A., et al., *Phosphatidylinositol 4,5-Bisphosphate Regulates Two Steps of Homotypic Vacuole Fusion.* Mol Biol Cell, 2000. **11**(3): p. 807-817.

67. Manfredi, G., et al., *Measurements of ATP in mammalian cells.* Methods, 2002. **26**(4): p. 317-326.

68. Khlyntseva, S.V., et al., *Methods for the determination of adenosine triphosphate and other adenine nucleotides.* J Anal Chem, 2009. **64**(7): p. 657-673.

69. Wojnicz, A., et al., *Simultaneous monitoring of monoamines, amino acids, nucleotides and neuropeptides by liquid chromatography-tandem mass spectrometry and its application to neurosecretion in bovine chromaffin cells.* J Mass Spectrom, 2016. **51**(8): p. 651-664.